TURUN
YLIOPISTO
UNIVERSITY
OF TURKU

VASCULAR FUNCTION IN KIDNEY TRANSPLANT RECIPIENTS AND IN PATIENTS WITH RENOVASCULAR DISEASE

Johanna Päivärinta

TURUN YLIOPISTON JULKAISUJA – ANNALES UNIVERSITATIS TURKUENSIS
SARJA – SER. D OSA – TOM. 1579 | MEDICA – ODONTOLOGICA | TURKU 2021

TURUN
YLIOPISTO
UNIVERSITY
OF TURKU

VASCULAR FUNCTION IN KIDNEY TRANSPLANT RECIPIENTS AND IN PATIENTS WITH RENOVASCULAR DISEASE

Johanna Päivärinta

TURUN YLIOPISTON JULKAISUJA – ANNALES UNIVERSITATIS TURKUENSIS
SARJA – SER. D OSA – TOM. 1579 | MEDICA – ODONTOLOGICA | TURKU 2021

University of Turku

Faculty of Medicine
Department of Internal Medicine
Doctoral Programme in Clinical Research
Turku PET-Centre

Supervised by

Docent Kaj Metsärinne, MD, PhD
Kidney Centre
Turku University Hospital and
University of Turku,
Turku, Finland

Docent Niina Koivuviita, MD, PhD
Kidney Centre
Turku University Hospital and
University of Turku,
Turku, Finland

Reviewed by

Professor Marja Hedman, MD, PhD
Heart Center and Clinical Imaging
Center, Kuopio University Hospital
Institute of Clinical Medicine,
University of Eastern Finland,
Kuopio, Finland

Docent Ilkka Helanterä, MD, PhD
Transplantation and Liver Surgery,
Helsinki University Hospital
and University of Helsinki,
Helsinki, Finland

Opponent

Professor Ilkka Pörsti, MD, PhD
Department of Internal Medicine,
Tampere University Hospital
Faculty of Medicine,
University of Tampere,
Tampere, Finland

The originality of this publication has been checked in accordance with the University of Turku quality assurance system using the Turnitin OriginalityCheck service.

ISBN 978-951-29-8586-9 (PRINT)
ISBN 978-951-29-8587-6 (PDF)
ISSN 0355-9483 (Print)
ISSN 2343-3213 (Online)
Painosalama, Turku, Finland 2021

To my Family

UNIVERSITY OF TURKU
Faculty of Medicine
Department of Internal Medicine
JOHANNA PÄIVÄRINTA: Vascular Function in Kidney Transplant Recipients and in Patients with Renovascular Disease
Doctoral Dissertation, 160 pp.
Doctoral Programme in Clinical Research, Turku PET Centre, Turku, Finland
October 2021

ABSTRACT

Cardiovascular mortality is 20 times higher in patients with chronic kidney disease and 3─5 times higher in patients with a kidney transplant than in the age-matched general population, which is partly explained by endothelial dysfunction. Endothelial function is pivotal in the pathogenesis of coronary artery disease, kidney allograft failure and atherosclerotic renovascular disease.

In this study, our aim was to measure the myocardial perfusion reserve of patients with a kidney transplant with positron emission tomography (PET), which is the gold standard for measuring myocardial perfusion. Secondly, the aim was to test PET for evaluation of kidney perfusion in patients with a kidney transplant and to examine if early kidney perfusion predicts renal histology at one year after transplantation. In addition, our aim was to measure renal flow reserve by PET in patients with atherosclerotic renovascular disease. The results were compared to those of the healthy controls.

The myocardial perfusion reserve was similar in patients and in healthy controls after correction for cardiac workload. Renal cortical perfusion was decreased in kidney transplant recipients compared with healthy control subjects. Allograft perfusion assessed early after transplantation did not predict renal fibrosis 12 months after transplantation. The renal flow reserve was small and highly variable both in patients with atherosclerotic renovascular disease and in healthy controls.

The myocardial perfusion reserve is well preserved in patients with a kidney transplant. PET is an adequate method for evaluation of renal perfusion in patients with a kidney transplant, but not for prediction of renal fibrosis one year after transplantation. The decreased renal cortical perfusion in kidney transplant recipients is probably explained by microcircular and endothelial dysfunction of the allograft. The renal flow reserve was modest, which makes the value of this variable questionable for prognosticating the response to revascularisation in renovascular disease.

KEYWORDS: renal perfusion, renal vascular resistance, kidney transplant, atherosclerotic renovascular disease, chronic kidney disease, renal flow reserve, myocardial perfusion reserve, positron emission tomography

TURUN YLIOPISTO
Lääketieteellinen tiedekunta
Sisätautioppi
JOHANNA PÄIVÄRINTA: Vaskulaarifunktio munuaissiirron saaneilla sekä renovaskulaaritautia sairastavilla potilailla
Tohtorin väitöskirja, 160 s.
Turun kliininen tohtoriohjelma, Valtakunnallinen PET-keskus, Turun yliopisto ja Turun yliopistollinen keskussairaala
Lokakuu 2021

TIIVISTELMÄ

Sydän- ja verisuonitautikuolleisuus on 20 kertaa suurempi kroonista munuaisten vajaatoimintaa sairastavilla ja 3-5 kertaa suurempi munuaissiirteen saaneilla potilailla kuin ikävakioidulla muulla väestöllä. Tämän katsotaan selittyvän osin verisuonten sisäkalvon eli endoteelin toiminnan häiriöllä. Endoteelin toiminnalla on keskeinen asema sepelvaltimotaudin, munuaissiirteen toiminnan heikkenemisen ja renovaskulaaritaudin patofysiologiassa.

Tämän tutkimuksen tavoitteena oli määrittää munuaissiirtopotilaiden sepelvaltimoiden virtausreservi kvantitatiivisella positroniemissiotomografialla (PET), joka on sepelvaltimoiden verenvirtauksen eli sepelvaltimoperfuusion arvioinnin kultainen standardi. Tavoitteena oli myös selvittää PET-tutkimuksen toimivuus munuaissiirteen perfuusion mittauksessa. Tutkimuksella pyrittiin lisäksi selvittämään, ennustaako varhainen munuaissiirteen perfuusio munuaissiirteen histologiaa vuoden kohdalla siirrosta. Viimeisenä tavoitteena oli selvittää PET-tutkimuksella munuaisen virtausreservi renovaskulaaritautia sairastavilla potilailla.

Sepelvaltimoiden virtausreservi oli yhtä suuri munuaissiirtopotilailla ja terveillä, kun sydämen työkuorma otettiin huomioon. Sen sijaan munuaisperfuusio oli heikentynyt siirtopotilailla verrattuna terveisiin. Varhain munuaissiirron jälkeen määritetty munuaisperfuusio ei ennustanut siirteen histologiaa vuoden kohdalla siirrosta. Munuaisen virtausreservi oli pieni ja arvot vaihtelevia sekä ateroskleroottista munuaissairautta sairastavilla potilailla että terveillä verrokeilla.

Sepelvaltimoiden virtausreservi on hyvin säilynyt munuaissiirtopotilailla. PET on käypä metodi munuaissiirteen perfuusion mittauksessa, mutta se ei ennusta siirteen fibroosia vuoden kuluttua siirrosta. Munuaisperfuusion väheneminen siirtopotilailla selittynee mikrosirkulaation ja endoteelin toiminnan häiriöllä. Munuaisen virtausreservin pieni koko kyseenalaistaa sen käytön munuaisvaltimoahtauman laajennusvasteen ennustajana.

AVAINSANAT: munuaisperfuusio, munuaisperfuusion vastus, munuaissiirre, renovaskulaaritauti, krooninen munuaisten vajaatoiminta, munuaisen virtausreservi, sepelvaltimoiden virtausreservi, positroniemissiotomografia

Table of Contents

Abbreviations

AAC	Abdoninal aortic calcification
ACE	Angiotensin convertizing enzyme
ARB	Angiotensin receptor blocker
ARVD	Atherosclerotic renovascular disease
ASL	Arterial spin labelling
BNP	Brain natriuretic peptide
BOLD	Blood oxygen level dependent imaging
^{11}C	Carbon-11
CAC	Coronary artery calcification
CAD	Coronary artery disease
CAI	Chronic allograft injury
C4d	Classical pathway complement degradation product
CFV	Coronary flow velocity
CFVR	Coronary flow velocity reserve
CKD	Chronic kidney disease
CKD stage 5D	Chronic kidney disease dependent on dialysis
CMV	Cytomegalovirus
CNI	Calcineurin inhibitor
CrCl	Creatinine clearance
Crea	Creatinine
CT	Computed tomography
CV	Cardiovascular
CVD	Cardiovascular disease
CVR	Coronary vascular resistance
DCE MRI	Dynamic contrast enhanced magnetic resonance imaging
DM	Diabetes mellitus
EBCT	Electron beam computed tomography
EF	Ejection fraction
eGFR	Estimated glomerular filtration rate
ERPF	Effective renal plasma flow
ESRD	End-stage renal disese

^{18}F	Fluorine-18
FMD	Flow-mediated dilation
FFR	Fractional flow reserve
FFR_{REN}	Renal fractional flow reserve
Hb	Hemoglobin
HDL	High density lipoprotein
HfpEF	Heart failure with preserved ejection fraction
^{131}I	Iodine-131
IFTA	Interstitial fibrosis and tubular atrophy
LDL	Low-density lipoprotein
LV	Left ventricle
LVH	Left ventricular hypertrophy
LVM	Left ventricular mass
LVMI	Left ventricular mass index
MAP	Mean arterial pressure
MDCT	Multidetector helical computed tomography
MP	Myocardial perfusion
MP_{corr}	Corrected myocardial perfusion
MPR	Myocardial perfusion reserve
MPR_{corr}	Corrected myocardial perfusion reserve
MRI	Magnetic resonance imaging
^{13}N	Nitrogen-13
NO	Nitric oxide
NODAT	New onset diabetes after transplantation
$[^{15}O]H_2O$	^{15}O-labelled water
PAH	Para-aminohippurate
PC MRI	Phase contrast magnetic resonance imaging
PET	Positron emission tomography
ptc	Peritubular capillaries
PTH	Parathyroid hormone
RAAS	Renin-angiotensin-aldosterone-system
RAS	Renal artery stenosis
^{82}Rb	Rubidium-82
RFR	Renal flow reserve
RI	Resistance index
ROI	Region of interest
RPP	Rate pressure product
RVR	Renal vascular resistance
SD	Standard deviation
SPECT	Single-photon emission computed tomography

SV40	Simian virus 40
TAC	Time-activity curve
^{99m}Tc	Technetium- 99m
TnT	Troponin T
TTDE	Transthoracic Doppler echocardiography
^{133}Xe	Xenon-133

List of Original Publications

This dissertation is based on the following original publications, which are referred to in the text by their Roman numerals I–IV:

I Päivärinta J., Koivuviita N., Oikonen V., Iida H., Liukko K., Manner I., Löyttyniemi E., Nuutila P. & Metsärinne K. The renal blood flow reserve in healthy humans and patients with atherosclerotic renovascular disease measured by positron emission tomography using [^{15}O]H_2O. *EJNMMIR*, 2018; 8(1): 45–51. <https://doi.org/10.1186/s13550-018-0395-3>

II Päivärinta J., Metsärinne K., Löyttyniemi E., Teuho J., Tolvanen T., Knuuti J. & Koivuviita N. Myocardial perfusion reserve of kidney transplant patients is well preserved. *EJNMMIR*, 2020; 10(1): 9–16. <https://doi.org/10.1186/s13550-020-0606-6>

III Päivärinta J., Oikonen V., Räisänen-Sokolowski A., Tolvanen T., Löyttyniemi E., Iida H., Nuutila P., Metsärinne K. & Koivuviita N. Renal vascular resistance is increased in patients with kidney transplant. *BMC Nephrol*, 2019; 20(1): 437–445. <https://doi.org/10.1186/s12882-019-1617-2>

IV Päivärinta J., Koivuviita N., Oikonen V., Räisänen-Sokolowski A., Tolvanen T., Löyttyniemi E., Iida H., Nuutila P. & Metsärinne K. Renal vascular resistance decreases during the first year after kidney transplantation: a follow up study with [^{15}O]H_2O PET. *Manuscript.*

1 Introduction

The prevalence of cardiovascular (CV) mortality is 20 times higher in patients with chronic kidney disease (CKD) than that in the general population (Foley et al., 1998). Although kidney transplantation reduces CV mortality in end stage renal disease (ESRD), CV mortality is still 3–5 times higher in kidney transplant recipients than in controls of the general population matched for age and sex (Foley et al., 1998; Meier-Kriesche et al., 2004). Endothelial dysfunction is probably one of the factors contributing to the increased CV mortality in CKD. The endothelial response to flow-mediated vasodilation (FMD) of the brachial artery decreases in parallel with decreased kidney function (Yilmaz et al., 2006) and reflects the CV risk in patients with CKD (Yilmaz et al., 2011). Endothelial function in peripheral arteries seems to improve but not to normalize after renal transplantation (Passauer et al., 2003; Oflaz et al., 2006).

Peripheral endothelial function assessed by FMD has been shown to correlate with coronary artery endothelial function (Anderson et al., 1995). Myocardial perfusion reserve (MPR) is the ratio of hyperemic to baseline myocardial perfusion (MP) and reflects the function of coronary microcirculation and endothelium. MPR can be measured non-invasively (Camici et al., 2015). Reduced MPR has been associated with a poor CV prognosis (Taqueti & Di Carli, 2018; Charytan et al., 2018). There have been conflicting results regarding the value of MPR in patients with CKD studied by positron emission tomography (PET) (Koivuviita et al., 2009; Charytan et al., 2010; Charytan et al., 2018) ─ which is considered the golden standard for the measuring MPR ─ and by other methods (Chade et al., 2006; Niizuma et al., 2008). There are no studies on MPR by quantitative imaging methods.

As in the heart, there is perfusion/flow reserve in kidney, although it is significantly smaller than of the heart (van Brussel et al., 2017). The renal flow reserve (RFR), which reflects renal endothelial function, might serve as a functional predictor of the response to dilatation in renal artery stenosis (RAS). Large studies with patients with atherosclerotic renovascular disease (ARVD) did not find any benefit of renal artery stenting (Wheatley et al, 2009; Bax et al., 2009; Cooper et al., 2014), but in these studies the RAS grade was evaluated only anatomically. ARVD seems to involve a transition from a hemodynamic condition to a profibrotic disease

with microvascular rarefaction, the major determinant of the response to RAS revascularisation (Eirin et al., 2019). However, there have been no studies with quantitative methods to measure RFR in patients with ARVD.

The loss of capillary network seems to be crucial for the development of fibrosis in patients with a kidney transplant (Ishii et al., 2005; Steegh et al., 2011). Some imaging studies on renal perfusion have documented a correlation between renal cortical fibrosis and perfusion in patients with chronic allograft injury (CAI) (Nankivell et al., 2002; Pereira et al., 2010; Wang et al., 2019).

Kidney transplant dysfunction is present in 90% of kidney transplant recipients and it is associated with a poor CV prognosis in these patients (Meier-Kriesche et al., 2003). The most effective way to decrease cardiovascular disease (CVD) in kidney transplant recipients is preservation of good kidney allograft function (Jardine et al., 2011), which underlies the importance of early diagnostics of kidney deterioration. Biopsy of the kidney is the golden standard of kidney pathology; however, it is an invasive method.

Measurement of kidney allograft perfusion might provide a non-invasive method to evaluate allograft function. PET imaging is a compelling method to evaluate kidney transplant perfusion ─ PET provides quantitative and regional one-kidney perfusion data without the need for radiocontrast agent (Green, 2011). Thus far, however, PET has been used only to study patients with CKD (Alpert et al., 2002; Juillard et al., 2002; Koivuviita et al., 2012), not patients with renal allografts.

In this study, our aim was to evaluate the 15O-labelled water ($[^{15}O]H_2O$) PET method for assessment of renal cortical perfusion in patients with a kidney allograft and to establish whether early renal cortical perfusion predicts renal fibrosis at one year after kidney transplantation. A further aim was to compare the MPR of kidney transplant recipients with the MPR of healthy control subjects by means of $[^{15}O]H_2O$ PET. We also studied the feasibility of measuring quantitatively enalapril-stimulated RFR in patients with ARVD by means of $[^{15}O]H_2O$ PET.

2 Review of the Literature

2.1 Cardiovascular disease and kidney impairment

2.1.1 Cardiovascular morbidity and mortality in patients with chronic kidney disease and with a kidney transplant

Patients with CKD have a high risk for CV events, substantial already at the early stages of CKD (Go et al., 2004). CKD patients dependent on dialysis (CKD stage 5D), have a 20-fold prevalence of CV mortality compared to the general population (Foley et al., 1998). Kidney transplantation improves patient survival in ESRD (Meier-Kriesche et al., 2004; Pilmore et al., 2010); especially CV mortality decreases after kidney transplantation (Pilmore et al., 2010). The 5-year survival in Finland was as high as 91% in 2002 among deceased-donor kidney recipients (Salmela & Kyllönen, 2004).

Meier-Kriesche et al. analyzed 60141 patients with a kidney transplant registered in the United States Renal Data System from 1995 to 2000 with regard to the primary endpoint of CV death by transplant vintage. The results were compared to 66813 patients in the kidney wait list by waitlisting vintage during the same period (Meier-Kriesche et al., 2004). The CV death rates among the patients on the wait list increased progressively by waitlisting vintage, whereas CV death rates decreased constantly by transplant vintage starting 3 months from the transplantation (Meier-Kriesche et al., 2004) (**Figure 1**).

However, cardiovascular disease (CVD) is the most common cause of death also in renal transplant recipients accounting for 30–40% of all deaths after the first-year post-transplant (Pilmore et al., 2010). CV mortality is 3–5 times higher in kidney transplant recipients than in the age- and sex matched members of general population (Foley et al., 1998).

Recently, some evidence has emerged that CV mortality is decreasing in kidney transplant recipients (Pilmore et al., 2010). This phenomenon is probably explained by improved primary and secondary prevention of CVD as well as by increased CV screening and interventions of potential transplant recipients (Bottomley & Harden, 2013). Still, patient survival has not improved significantly since the early 1990´s (Matas et al., 2015). Increasing age of kidney donors and recipients as well as the

increasing prevalence of malignancies may explain why the prognosis of kidney transplant recipients is plateauing (Pilmore et al., 2010; Bottomley & Harden, 2013).

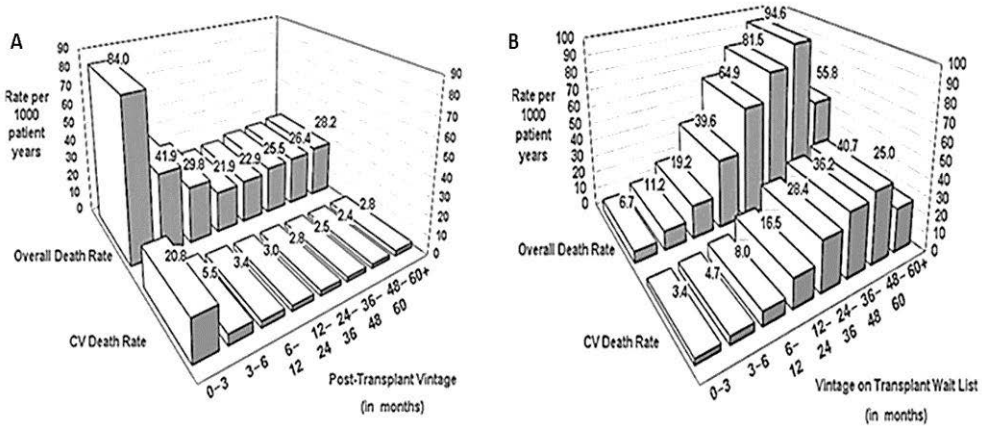

Figure 1 **A** Overall and cardiovascular death rates by wait list vintage 1995-2000 (censored at transplant. **B** Overall and cardiovascular death rates by post-transplant vintage for deceased donor transplant recipients 1995-2000 (censored at graft loss) (Meier-Kriesche et al., 2004). Reproduced by permission of John Wiley and Sons.

2.1.2 Pathophysiology of cardiovascular disease in patients with chronic kidney disease

In patients with CKD, the CVD phenotype differs from that of the general population: there is a disproportionate level of sudden cardiac death, arrhythmia, and heart failure rather than myocardial infarction. Non-atherosclerotic mechanisms, like arteriosclerosis, abnormalities of cardiac structure, and arterial stiffening seem to account for most of the increased CV risk (Gansevoort et al., 2013).

The traditional risk factors, like dyslipidemia and diabetes mellitus (DM), which are highly prevalent among patients with CKD, seem to explain only partly the increased CV risk. In the advanced stages of CKD, the benefits of risk factor management may be attenuated (Gansevoort et al., 2013). Two large trials with patients with CKD stage 5D, showed no benefit of statin use with respect to CV outcome (Wanner et al., 2005; Fellström et al., 2009). On the other hand, the Study of Heart and Renal Protection (SHARP) showed a reduction in the occurrence of major atherosclerotic events in a wide range of patients with advanced CKD, including patients with CKD stage 5D (Baigent et al., 2011).

A reverse epidemiological phenomenon ─ that the body mass index and hypertension correlate inversely with mortality ─ is well known for patients with CKD stage 5D and this naturally complicates CVD risk assessment (Nanayakkara & Gaillard, 2010). Non-traditional risk factors, *e.g.*, anemia,

oxidative stress, inflammation, vascular calcification, endothelial dysfunction, and sympathetic overactivation, appear also to play an important role in the pathogenesis of atherosclerosis in patients with CKD (Stenvinkel et al., 2008; Nanayakkara & Gaillard, 2010).

2.1.3 Pathophysiology of cardiovascular disease in patients with a kidney transplant

The CVD of kidney transplant recipients represents an amalgamation of traditional and non-traditional risk factors, risk factors related to CKD and the era of dialysis and risk factors associated with the transplantation (Bottomley & Harden, 2013) (**Figure 2**).

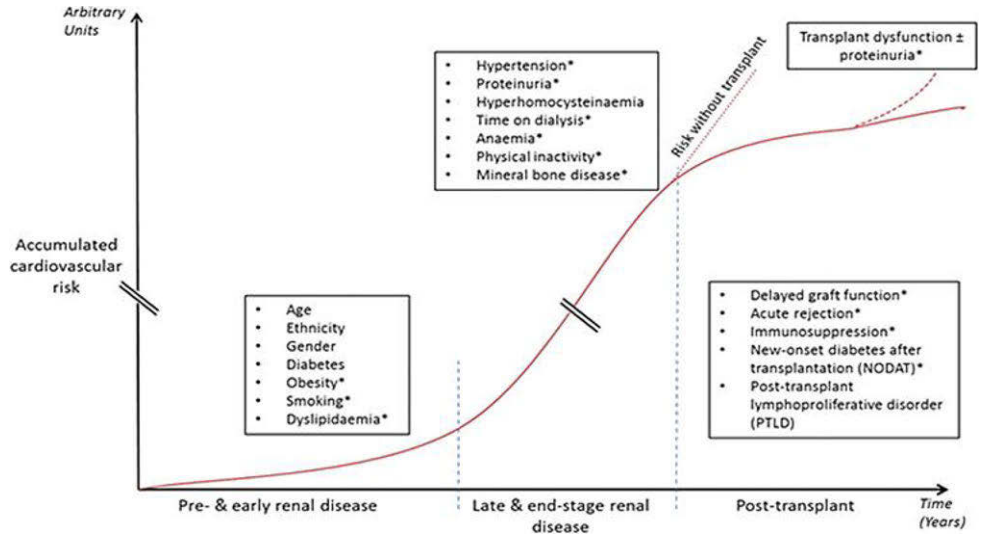

Figure 2. The accumulation of risk factors for cardiovascular disease in the transplant recipient. Each box corresponds to the approximate time the risk factor begins to contribute to risk. Asterisk indicates potentially modifiable factors (Bottomley & Harden, 2013). Reproduced with the permission of Oxford University Press.

Traditional and non-traditional risk factors

Patients who have undergone renal transplantation exhibit a high prevalence of traditional risk factors, like dyslipidemia (50%), smoking (25%), hypertension (40–90%), and DM (20–40%) (Rangaswami et al., 2019). Posttransplantation DM is present in up to 50% of patients with kidney transplant 5 years after transplantation (Van Loon et al., 2020a). After transplantation, the relationship between risk factors and CV events seems to revert towards the general population.

However, the Framingham Heart Study score underestimates the CV risk for patients with a kidney transplant, suggesting that other factors may be involved (Jardine et al., 2011). The multicentre, randomised, double-blind, placebo-controlled trial Assesment of Lescol in Renal Transplantation (ALERT) did not show any reduction in the occurrence of primary endpoints (non-fatal myocardial infarction, cardiac death, or coronary intervention procedure) despite a significant reduction of 32% of the concentration of plasma low-density lipoprotein (LDL) in the fluvastatin group (Holdaas et al., 2003). A study extension and an increase of fluvastatin dose to 80 mg did, nevertheless, demonstrate a reduced rate of CV events according to a post-hoc analysis (Holdaas et al., 2005).

Anemia, homocysteinemia, hyperparathyroidism, and hyperphosphatemia have been proposed as non-traditional CV risk factors for kidney transplant recipients (Jardine et al., 2011). Extensive vascular calcification is firmly associated with CKD-related disorders of mineral metabolism, in which the homeostasis of serum fibroblast growth factor 23, phosphorus, calcium, parathyroid hormone, and vitamin D sterol levels are altered. In a meta-analysis which summarised 13 studies on vascular calcification in patients with a kidney transplant, progression of coronary artery calcification (CAC) slowed down but was not halted after kidney transplantation (Cianciolo et al., 2014).

Sympathetic overactivation is discussed in section 2.1.4 (Sympathetic nervous system and the cardiovascular pathophysiology in patients with chronic kidney disease and with a kidney transplant). Endothelial dysfunction, oxidative stress, and inflammation are discussed in section 2.1.5 (Endothelial function and cardiovascular disease/Endothelial dysfunction).

Dialysis vintage

CV death rates increase by dialysis vintage due to accelerated CVD progression (Meier-Kriesche et al., 2004), and dialysis vintage pretransplant, *i.e.*, waiting time on dialysis, is a strong risk factor for CV death after kidney transplantation (Meier-Kriesche et al., 2000; Meier-Kriesche et al., 2004; Helanterä et al., 2014). Relative to pre-emptive kidney transplantation, a waiting time of 12–24 months is associated with a 72% increase in the risk of mortality after transplantation (Meier-Kriesche et al., 2000).

Kidney transplantation related factors

Kidney transplant dysfunction is present in 90% of kidney transplant recipients, and 60% of the recipients have CKD stage 3 (Karthikeyan et al., 2004). In the study of Meier-Kriesche et al., there was a significant and progressive increase in the risk of

CV death when the serum creatinine value was above 133 µmol/l at 1 year after kidney transplantation (Meier-Kriesche et al., 2003). The most effective way to decrease CV disease in patients with a kidney transplant is to achieve and maintain good kidney graft function.

Immunosuppressive medication is associated with an increased CV risk by affecting other CV risk factors (Jardine et al., 2011). Calcineurin inhibitors (CNI) induce hypertension via systemic and renal vasoconstriction as well as via renal sodium retention, which are probably mediated by the renin-angiotensin-aldosterone system (RAAS) and the sympathetic nervous system. In addition to vascular dysfunction, CNI's induce chronic nephrotoxicity with irreversible damage to the renal interstitial, glomerular, and vascular architecture and this impairs the function of the kidney transplant and contributes to blood pressure increase (Naesens et al., 2009).

2.1.4 Sympathetic nervous system and the cardiovascular pathophysiology in patients with renal disease

The first observations of increased sympathetic nerve activity in patients with CKD came from studies which showed elevated plasma levels of norepinephrine (Ishii et al., 1983). Grassi et al. demonstrated sympathetic overactivation early in CKD by measuring sympathetic nerve activity in muscles; microelectrodes were placed on skeletal muscle tissue to record action potentials in postganglionic sympathetic nerves (Grassi et al., 2011). The sympathetic nerve activity in muscles correlated inversely with kidney function.

Sympathetic overactivation is associated with hypertension and increased left ventricular mass (LVM), and it is an independent risk factor for increased CV mortality in patients with CKD. Exaggerated sympathetic nerve activity has shown to contribute to the progression of kidney disease in animal studies (Schlaich et al., 2009).

Renal sympathetic activation leads to volume retention through activation of the RAAS and sodium reabsorption. Angiotensin II potentiates norepinephrine release from peripheral sympathetic nerves and from the brainstem. There seems to be disproportionately increased concentrations of renin in relation to the state of sodium-volume balance in patients with CKD (Schlaich et al., 2009). Renal afferent nerves from an injured kidney increase sympathetic outflow from the brain (Schlaich et al., 2009).

Kidney transplantation reduces sympathetic dysfunction in non-diabetic patients as judged by heart rate variability and baroreflex function testing (Agarwal et al., 1991; Yildiz et al., 1998; Rubinger et al., 2009). Recovery from autonomic dysfunction has been seen as early as 4–6 months after transplantation (Agarwal et

al., 1991; Yildiz et al., 1998), and the beneficial response persists (Rubinger et al., 2009).

Despite excellent graft function after kidney transplantation, increased muscle sympathetic nerve activity comparable to that of patients with CKD stage 5D has been reported (Hausberg et al., 2002). However, removal of diseased native kidneys reduced the muscle sympathetic nerve activity of kidney transplant recipients to the level of healthy controls. The increased sympathetic nerve activity seems to be mediated by afferent signals arising in the injured native kidneys in patients with CKD stage 5D (Hausberg et al., 2002).

Sympathetic nervous system and renal perfusion are discussed in section 2.3.2 (Sympathetic innervation of the kidney and renal perfusion) and 2.6.2 (Sympathetic nervous system and perfusion of kidney transplant).

2.1.5 Endothelial function and cardiovascular disease

Function of normal endothelium and methods to study endothelial function

The healthy endothelium is the largest organ in the body and the key regulator of vascular tone. It can sense physical signals, *e.g.*, pressure and shear stress, and chemical signals, *e.g.*, vasoactive mediators. In response, it releases vasoactive molecules which relax or constrict the vessel. This endothelial regulation of vessel diameter and tone is pivotal for the balance of the metabolic demand and oxygen supply of tissues. The endothelium also regulates smooth muscle cell proliferation, hemostasis, angiogenesis, vascular permeability, and vessel wall inflammation (Deanfield et al., 2007).

The endothelium-derived relaxing factor, nitric oxide (NO), is generated from L-arginine by endothelial NO synthase (Furchgott & Zawadzki, 1980). NO that diffuses to the surrounding vascular smooth muscle cells mediates vasodilatation. Shear stress is the main activator of endothelial NO synthase (Deanfield et al., 2007).

The golden standard method to study endothelial function is *quantitative coronary angiography associated with intravascular sonography*. However, it is a highly invasive method which limits its use. Quantitative coronary angiography has been used to image vasomotor responses of epicardial coronary arteries to intracoronary endothelium-dependent vasodilators, like acetylcholine. Blood volume quantification is based on changes in epicardial artery diameters and blood flow velocity. Ludmer et al. (Ludmer et al., 1986) were the first to show *in vivo* the association between endothelial dysfunction and CAD. Their study demonstrated that acetylcholine causes a dose-dependent dilation of coronaries in subjects without CAD and, paradoxically, vasoconstriction in subjects with CAD.

Flow-mediated vasodilation (FMD) of the brachial artery is a non-invasive and widely used technique to evaluate peripheral endothelial function. The technique measures the dilatation of the brachial artery during reactive hyperemia after brief occlusion of the brachial artery with a blood pressure cuff (Deanfield et al., 2007). The dilatation response is mainly NO-mediated and based on shear-stress which activates NO synthase in the endothelium of the artery. Importantly, peripheral endothelial function assessed by FMD correlates with coronary artery endothelial function (Anderson et al., 1995).

Several alternative non-invasive methods have been developed to evaluate endothelial function in the peripheral circulation including *venous occlusion plethysmography, applanation tonometry,* and *laser Doppler flowmetry* (Deanfield et al., 2007).

Endothelial dysfunction

Endothelial dysfunction has been associated with CAD, smoking, dyslipidemia, DM, and arterial hypertension (Brunner et al., 2005).

In patients with CKD, there are many endothelial mechanisms which could cause generally reduced bioavailability of NO, *e.g.*, lack of arginine, inhibition of endothelial NO synthase, and increased degradation of NO (Baylis, 2008). The FMD response decreases in parallel with kidney function impairment (Yilmaz et al., 2006), which, again, has been associated with an increased CV risk in patients with CKD 1–5 (Yilmaz et al., 2011). In contrast to peripheral arteries, there seems to be no reduction in acetylcholine response in the coronary arteries according to the results of a study with patients with CKD stage 5D, although adenosine-stimulated coronary stress perfusion was decreased (Nelson et al., 2019).

Surrogate markers of endothelial dysfunction, *e.g.*, vascular cell adhesion molecule-1 and albuminuria, predict a poor outcome in patients with CKD. Also detached circulating endothelial cells may serve as potential markers of endothelial damage in patients with CKD (Stenvinkel et al., 2008). Plasma levels of inflammatory markers like interleukin-6 and C-reactive protein, and asymmetric dimethylarginine, an endogenous antagonist of endothelial NO synthase, are all increased in patients with CKD and are associated with a poor CV prognosis (Stenvinkel et al., 2008).

In patients with a kidney transplant, endothelial function assessed through venous occlusion plethysmography and FMD has shown to be improved but not normalised after renal transplantation (Passauer et al., 2003; Oflaz et al., 2006).

2.2 Myocardial perfusion and cardiac microvascular function

2.2.1 Regulation of cardiac blood flow

At rest, roughly 60–80% of the oxygen is extracted by the myocardium from the arterial blood. Consequently, increases in myocardial O_2 needs are mainly met through proportional increases in myocardial perfusion (MP). There is a complex control of coronary perfusion involving shear-mediated neurohormonal regulation, metabolic regulation, and pressure-dependent myogenic control (Camici et al., 2015). Under normal hemodynamic conditions, resting MP increases 4–5 fold during vasodilation (Duncker et al., 2014).

Epicardial coronaries (diameter 0.5–5 mm) are conduit arteries, which represent approximately 5% of the coronary flow resistance when there is no obstructive stenosis. Coronary arterial resistance vessels, *i.e.*, vessels of cardiac microcirculation, comprise prearterioles (diameter 100–500 μm), which respond to changes in wall shear stress (flow-mediated response) and transmural pressure (myogenic response), and arterioles (diameter < 100 μm), which sense changes in local tissue metabolism and control perfusion of the coronary capillary bed. The total resistance of the coronary circulation decreases by approximately 70% during hyperemia.

Coronary resistance vessels are innervated with adrenergic (sympathetic) and cholinergic (parasympathetic) neurons. Parasympathetic nerves release acetylcholine, which exerts a direct vasodilatory action via muscarine receptors. The effects of sympathetic activation (via norepinephrine) on coronary resistance vessel tone are complex and depend on the net effect of β_1-, β_2- and α_1-receptor stimulation. Sympathetic tone in the heart and in the coronary vessels at rest is negligible (Duncker et al., 2014).

2.2.2 Methods to study coronary microvascular function

Unlike epicardial arteries, prearterioles and arterioles are below the resolution of current angiographic systems and remain thus invisible (Camici et al., 2015). Considering that atherosclerotic disease is a continuum, it is obvious that also patients with angiograms perceived as normal have, in fact, preclinical CAD that affects coronary microcirculation.

Myocardial perfusion reserve (MPR) reflects the function of coronary microcirculation. MPR is defined as the ratio of hyperemic to baseline *myocardial perfusion (MP)*. MPR is an integrated measure of blood flow through both the epicardial arteries and the coronary microcirculation. However, discrimination

between the effects of microcirculation and epicardial arteries on MP is difficult because dysfunction of these two often coexist (Camici et al., 2015).

Maximal hyperemia is usually induced with intracoronary or intravenous infusion of adenosine or dipyridamole or an intravenous bolus of regadenoson. Dipyridamole inhibits adenosine deaminase, which catabolises adenosine. Adenosine vasodilatates coronary microvessels < 150 μm in diameter leading to an increase in myocardial blood flow with little effect on systemic blood pressure. Inhibition of endogenous NO synthesis attenuates myocardial perfusion during adenosine-induced hyperemia, indicating that coronary vasodilatation is partly dependent on the endothelium (Buus et al., 2001).

MPR can be measured by intracoronary Doppler ultrasound or thermodilution during coronary catheterisation (Camici et al., 2015). The thermodilution method with a single pressure-temperature sensor-tipped coronary wire has enabled simultaneous measurement of MPR and *fractional flow reserve (FFR)*. In addition, the *index of microcirculatory resistance*, the minimal resistance during hyperemic flow induced by intracoronary administration of adenosine, is obtained by the thermodilution method. The microcirculatory resistance index is a relative index and its validity is limited to the same patient in the same myocardial territory (Camici et al., 2015).

Angiographic methods are invasive and therefore justified only in patients who may have CAD. The non-invasive methods to study microvascular coronary function include transthoracic Doppler echocardiography (TTDE), cardiac magnetic resonance imaging (MRI), dynamic myocardial perfusion computed tomography (CT), single photon emission computed tomography (SPECT) and PET.

SPECT is not a quantitative method, nor is *coronary flow velocity (CFV)* based TTDE, which gives the *coronary flow velocity reserve (CFVR)*. Cardiac MRI provides a quantitative method to assess MPR, but requires gadolinium contrast, which is problematic in patients with CKD due to the risk of nephrogenic fibrosis. CT requires a radiocontrast agent, as well. A gadolinium-free stress cardiac MRI method has been recently introduced for the diagnosis of myocardial ischemia (Taqueti & Di Carli, 2018). Thus, PET is the golden standard method for quantitatively defining MPR so far. It is especially useful in patients with CKD since no radiocontrast agent is needed. The measures of coronary circulation are explained in **Table 1**.

Table 1. Definitions of variables used in evaluation of coronary circulation

Myocardial perfusion, MP	Quantitative measure of myocardial blood flow at rest or during vasodilatation Expressed as $ml \cdot g^{(-1)} \cdot min^{(-1)}$
Myocardial perfusion reserve, MPR	Hyperemic MP divided by resting MP Expressed as a ratio
Coronary flow velocity, CFV	Non-quantitative measure of myocardial blood flow at rest or during vasodilatation Expressed as unit of distance/unit of time
Coronary flow velocity reserve, CFVR	Hyperemic CFV divided by resting CFV Expressed as a ratio
Coronary vascular resistance, CVR	Arterial mean pressure divided by MP or CFV
Fractional flow reserve, FFR	Ratio of mean coronary artery pressure after stenosis to mean aortic pressure during maximal hyperemia
Index of microcirculatory resistance	Ratio of distal coronary pressure and hyperemic average peak flow velocity

2.2.3 Myocardial perfusion and microvascular function assessment with PET

General principles of PET method in the evaluation of myocardial perfusion

PET offers better image quality than SPECT due to enhanced spatial resolution and high count rates, in addition to the routine availability of attenuation correction. PET tracers also permit lower radiation exposure and track perfusion better at high MP values than technetium-99m (^{99m}Tc)-labelled SPECT tracers (Feher & Sinusas, 2017).

The radiotracers used in myocardial perfusion PET are 15O-labelled water ([^{15}O]H_2O), nitrogen-13 (^{13}N)-ammonia, rubidium-82 (^{82}Rb) and carbon-11 (^{11}C)-acetate. Fluorine-18 (^{18}F)-flurpiridaz is not yet available for routine clinical use. [^{15}O]H_2O and ^{13}N-ammonia are the most often used MP tracers currently and they require an onsite cyclotron for production, because the half-lives of these readionuclides are short (2 min and 10 min, respectively). [^{15}O]H_2O has almost 100% first-pass extraction and is freely diffusible without metabolic intervention, which makes it an ideal agent for dynamic perfusion imaging. The short half-life of [^{15}O]H_2O permits rapid serial imaging (Feher & Sinusas, 2017). On the other hand, due to the rapid clearance and the short half-life, [^{15}O]H_2O images cannot be used for visual analysis.

In myocardial perfusion studies with [^{15}O]H_2O PET the input function is derived from the left ventricle (LV) time-activity curve (TAC). The myocardial TAC is fitted with a one-chamber kinetic model (Iida et al., 1988; Feher & Sinusas, 2017).

Normal values of myocardial perfusion reserve by PET

Resting MP has a linear relationship with cardiac work and is influenced by blood pressure, heart rate, metabolic demand, and duration of the diastolic phase. Thus, the rate-pressure product (RPP), defined as the product of systolic blood pressure and heart rate, must be considered when calculating resting MP (Camici et al., 2015). Basal MP increases with age, mainly due to increased systolic blood pressure (Czernin et al., 1993; Uren et al., 1995). Anemia seems to increase both basal and stress MP (Abendschein et al., 1982). Normal resting MP ranges from 0.6 ml $g^{(-1)}\cdot min^{(-1)}$ to 1.2 $ml\cdot g^{(-1)}\cdot min^{(-1)}$ (Sdringola et al., 2011).

A recent review that summarises data from over 250 publications on MP quantification with PET arrived at an MPR-value of 3.6 and stress MP-value of 2.9 $ml\cdot g^{(-1)}\cdot min^{(-1)}$ in healthy subjects (Gould et al., 2013). After age 70 years, there is a physiological decrease in stress MP (Uren et al., 1995). MP values may vary depending on the tracers used (Camici et al., 2015).

Coronary artery disease and coronary microvascular dysfunction by PET

Coronary artery stenosis attenuates hyperemic flow progressively when the degree of coronary artery stenosis exceeds 40%. When the degree of stenosis is 80% or greater, hyperemic flow approaches unity with basal flow (Uren et al., 1994). Cutoff values of 2.3 $ml\cdot g^{(-1)}\cdot min^{(-1)}$ and 2.5 for normal stress MP and MPR, respectively, were reported by Danad et al. who used [^{15}O]H_2O PET in patients with symptoms suggestive of CAD (Danad et al., 2014). In that study, stenosis > 90% and/or fractional flow reserve (FFR) ≤ 0.80 was considered obstructive; stenosis < 30% and/or FFR > 0.80 was non-obstructive.

Abnormalities of coronary vasodilatation and coronary microvascular function have been demonstrated in patients with non-obstructive CAD, in patients with traditional risk factors like hypertension and DM, and in patients with inflammatory diseases (Camici et al., 2015). Symptomatic patients with no flow-limiting CAD-reduced MPR have a poor CV outcome. There is emerging data that patients at high risk for major adverse CV events can be identified by means of MPR measured with PET, independently of angiographic disease severity (Taqueti & Di Carli, 2018).

2.2.4 Myocardial perfusion in patients with chronic kidney disease

2.2.4.1 Methods to study coronary artery disease in patients with chronic kidney disease

Most of the existing data on non-invasive coronary stress tests in patients with CKD are derived from studies of kidney transplant candidates in more advanced stages of CKD. Non-invasive coronary stress tests have poor accuracy in detecting CAD in advanced stages of CKD, but they do seem to be useful for risk stratification. In a meta-analysis, which compared the ability of SPECT, dobutamine stress echocardiography, and coronary angiography to predict CV events and mortality in kidney transplant candidates, non-invasive tests were as good as coronary angiography (Wang et al., 2015). SPECT has shown to be a prognostic tool also for patients with milder stages of CKD. In a retrospective study with patients with mild to moderate CKD, the risk of cardiac death rose with the severity of perfusion defects, regardless of CKD or DM (Hakeem et al., 2010).

Coronary CT angiography and CAC score have emerged as new and promising methods to study coronary arteries. In the study of Winther et al. involving kidney transplant candidates, a CAC-score < 400 combined with coronary CT angiography provided a sensitivity of 80% and a specificity of 80% for detecting coronary artery stenosis ≥ 50%, while a CAC-score <400 combined with SPECT yielded a sensitivity of only 60%, although specificity was the same 80% (Winther et al., 2016). Diagnostic findings in coronary CT angiography and a high CAC score are associated with an increased risk for major adverse CV events and death in patients queuing for a kidney transplant (Winther et al., 2018).

Abdominal aortic calcification (AAC) score > 15 in patients with CKD stage 5D is associated with a 9-fold risk of mortality and non-fatal CV events compared with patients with an AAC score ≤ 4 (Verbeke et al., 2014).

2.2.4.2 Myocardial perfusion and perfusion reserve in patients with chronic kidney disease

The next section presents clinical cardiac studies of patients with CKD by different methods. The impact of CAD and left ventricular hypertrophy (LVH) on stress MP (or CFV) and of RPP on basal MP (or CFV) are discussed with regard to the impact of plain microvascular function on MPR (or CFVR) in patients with CKD.

Studies using an intracoronary Doppler guide wire (obstructive epicardial CAD excluded by coronary angiography) for evaluating of CFVR in patients with CKD

Chade et al. used an intracoronary Doppler guide wire to study patients with CKD stage 3, and found that CFVR was reduced compared to controls, but the difference was largely explained by sex, gender, and hypertension (Chade et al., 2006). Ragosta et al. studied patients with DM type II with or without ESRD (Ragosta et al., 2004). Patients with ESRD had a reduced CFVR based on increased basal CFV compared to patients with DM without ESRD. However, correction for cardiac workload was not made for basal CFV. Nelson et al. demonstrated that the baseline CFV in patients with ESRD was the same as for controls, but stress CFV was impaired (Nelson et al., 2018). In that study the presence of LVH, which reduces stress MP (Olsen et. al., 2004), was not reported.

Studies using transthoracic Doppler echocardiography for evaluating CFVR in patients with CKD

In two TTDE-based studies CFVR was shown to be reduced among hypertensive patients with CKD stage 2 (Fujii et al., 2008; Bezante et al., 2009). In the study of Fujii et al., basal and stress CFV were not reported (Fujii et al., 2008). In the study of Bezante et al., stress CFV was decreased, but coronary angiography was not performed and thus obstructive CAD was not excluded (Bezante et al., 2009).

Four TTDE-based studies on patients with CKD stage 5D have demonstrated reduced CFVR (Tok et al., 2005; Bozbas et al., 2008; Caliskan et al., 2008; Niizuma et al., 2008). In these studies, the reduction of CFVR was based on decreased stress CFV, except in the study of Niizuma et al. (Niizuma et al., 2008), which reported increased basal CFV, but no correction for cardiac workload was made. In the studies of Caliskan et al. and Bozbas et al. on patients with CKD stage 5D and decreased stress CFV, obstructive CAD was excluded only on clinical grounds, *i.e.*, without coronary angiography (Caliskan et al., 2008; Bozbas et al., 2008). LVH was more prevalent in patients than in controls in the studies of Bozbas et al. and Caliskan et al., which may have affected the values of stress CFV. The only TTDE-based study in which CAD was excluded by coronary angiography and the impact of left ventricular mass index (LVMI) was considered, is the study of Tok et al., who demonstrated decreased stress CFV and CFVR in patients with CKD stage 5D (Tok et al., 2005).

Studies using PET for evaluation of MPR in patients with CKD

Charytan et al. studied patients with CKD stage 2–3 by means of ^{13}N-ammonia PET and did not find any statistically significant correlation between renal function and MPR (Charytan et al., 2010). Instead, they demonstrated that baseline creatinine clearance (CrCl) was a strong and independent predictor of a higher rate of change in MPR during one year of follow-up. There was a loss of 0.11 MPR units for each 10 ml/min drop in baseline CrCl (Charytan et al., 2010).

Koivuviita et al. studied MPR with the [^{15}O]H_2O PET method in patients with CKD stage 3–5 (Koivuviita et al., 2009). A statistically significant negative linear correlation was demonstrated between eGFR and basal MP after correction for cardiac workload. Stress MP was similar in healthy controls and in patients with CKD. MPR tended to decrease in parallel with the decrease of eGFR, but not statistically significantly so (Koivuviita et al., 2009). Pointing to the same direction, Fukushima et al. showed in patients with CKD stage 3 a statistically significant correlation between ^{82}Rb PET-based basal MP and MPR and eGFR after correction for cardiac workload (Fukushima et al., 2012). In the [^{15}O]H_2O PET-study of Koivuviita et al. in patients with ARVD and CKD stage 3, most patients had impaired MPR and reduced stress MP probably due to subclinical CAD (Koivuviita et al., 2011).

In a large retrospective ^{13}N-ammonia and ^{82}Rb based PET study of 3946 patients with CKD stage 1–5D and with a high prevalence of CAD, MPR decreased in parallel with eGFR reduction in patients with CKD stage 1–3. However, MPR did not differ among patients with CKD stage 4, 5 and 5D (Charytan et al., 2018). The reduction of MPR was mainly due to reduced stress MP. In the same study the risk of mortality decreased by 65% for each tertile increase in MPR. Impaired MPR in patients with CKD has been associated with an increased risk for CV events and death also in other PET studies (Murthy et al., 2012; Shah et al., 2016; Wenning et al., 2020). In the study of Murthy et al., MPR below the median (< 1.5) was associated with a 2.1-fold increase in the risk of cardiac death in patients with CKD stage 3–5D (Murthy et al., 2012). Similarly, Shah et al. showed in patients with CKD stage 5D increased CV and all-cause mortality risk among patients who had MPR < 1.4 (Shah et al., 2016).

In conclusion, the methodology as well as the results of MPR studies of patients with CKD are heterogenous. Many studies have neither corrected MP and MPR for cardiac workload nor reported basal and stress MP separately. In addition, many studies have not excluded angiographically epicardial CAD, which reduces stress MP. Furthermore, the presence of LVH, which is associated with decreased stress MP (Olsen et al., 2004) has not always been reported in the studies.

2.2.5 Myocardial perfusion in patients with kidney transplant

Studies with transthoracic Doppler echocardiography

In three different studies of patients with a kidney allograft and mild kidney impairment and without clinical CAD, stress CFV was shown to be reduced with decreasing CFVR compared with control subjects (Bozbas et al., 2008; Caliskan et al., 2008; Turiel et al., 2008). Obstructive CAD was excluded on clinical grounds in these studies. In the studies of Bozbas et al. and Caliskan et al., LVH was more prevalent among patients with a kidney transplant than control subjects which might have impaired stress MP (Bozbas et al., 2008; Caliskan et al., 2008). Dialysis vintage before transplantation correlated negatively with CFVR (Caliskan et al., 2008; Bozbas et al., 2008; Turiel et al., 2008).

Bozbas et al. and Caliskan et al. also compared the CFVR of patients with a kidney transplant and of patients with CKD stage 5D in two cross-sectional studies (Caliskan et al., 2008; Bozbas et al., 2008). In both studies, CFVR and stress CFV were better in patients with a kidney transplant than in patients with CKD stage 5D (Caliskan et al., 2008; Bozbas et al., 2008). There was no difference in the prevalence of LVH between patients with CKD stage 5D and patients with a kidney transplant in either study. Dialysis vintage prior to kidney transplantation in patients with a kidney transplant was shorter than in patients with CKD stage 5D (Caliskan et al., 2008; Bozbas et al., 2008).

Viganò et al. studied 25 young males with a kidney transplant and mild CKD and found that their mean CFVR was 2.8; half of the patients had abnormal CFVR < 2.7 (Viganò et al., 2007). Dialysis vintage prior to transplantation was associated with low CFVR.

MRI studies

Semiquantitative MRI and magnetic resonance coronary angiography were performed in 20 patients with a renal transplant with CKD stage 2 but no known CAD, in 15 liver transplant patients with CKD stage 2 but no known CAD, and in 10 hypertensive controls with normal eGFR (Parnham et al., 2015). The MPR index was lower in both transplant groups than among the hypertensive controls. There was a discrepancy between magnetic resonance coronary angiography and the MPR index, implying that the mechanism of MPR index reduction was related to small vessel disease (Parnham et al., 2015).

2.2.6 Uremic cardiomyopathy and myocardial perfusion

Vascular changes, *e.g.*, decreased left ventricular capillary density and myocyte-capillary mismatch, are associated with uremic cardiomyopathy. The thickness of the tunica media of vascular walls is increased, due to both hyperplasia and hypertrophy of vascular smooth muscle cells. Coronary calcification occurs in the tunica media and tunica intima of vascular walls (Amann et al., 1998).

Uremic cardiomyopathy is characterised by LVH and diastolic as well as systolic ventricular dysfunction. The microscopic findings associated with uremic cardiomyopathy are focal scarring and diffuse myocardial interstitial fibrosis (Radhakrishnan et al., 2019). LVH, the prevalence of which is approximately 75% in patients with CKD stage 5D (Foley et al., 1998), is associated with reduced stress MP and MPR (Olsen et al., 2004).

The prevalence of heart failure with preserved ejection fraction (HFpEF) has been reported to be no less than 32% in patients with CKD stage 3–5D (Hensen et al., 2018). Reduced global longitudinal strain, the main index of HFpEF and the early feature of uremic cardiomyopathy, is associated with an increased risk for all-cause mortality and for hospitalisation due to heart failure of patients with CKD (Hensen et al., 2018). There seems to be an association between MPR and diastolic and systolic indices of LV in patients with CKD (Bajaj et al., 2020). It is not clear if coronary microvascular dysfunction is a cause or a consequence of uremic cardiomyopathy. The relationship between CMD and myocardial fibrosis may be reciprocal. CMD and fibrosis exacerbate each other; this leads to progressive ischemia and myocardial dysfunction (Radhakrishnan et al., 2019) (**Figure 3**).

The prevalence of LVH is approximately 50–70% in patients with a kidney transplant (Foley et al., 1998). In some studies, kidney transplantation has been associated with improvement of the structural changes caused by uremic cardiomyopathy. Kidney transplantation is also associated with improvement of global longitudinal strain (Hewing et al., 2016).

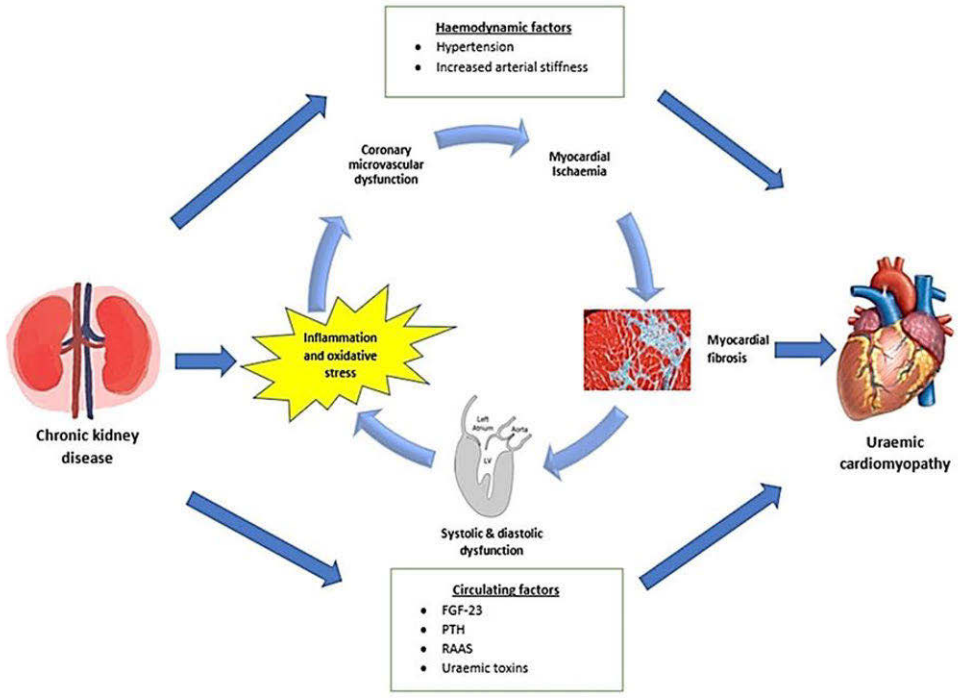

Figure 3. Proposed mechanism of uremic cardiomyopathy. FGF-23, fibroblast growth factor-23; PTH, parathyroid hormone; RAAS, renin-angiotensin-aldosterone system (Radhakrishnan et al., 2019). Reproduced under permission of BMJ Publishing Group LTD.

2.3 Renal perfusion

2.3.1 Renal vasculature

Renal blood flow per minute is approximately 1.2–1.3 litres (= 4 ml $g^{(-1)}$ $min^{(-1)}$) in an adult weighing 70 kg and with 300 g of kidney mass, and accounts for 20% of the cardiac output in the resting adult. The ratio between O_2 consumption and O_2 delivery is approximately 10% (Evans et al., 2008) in the kidney which is low compared to the ratio in the heart, where 70–80% of the delivered oxygen is extracted into the myocardium at rest. Renal microvascular anatomy is presented in **Figure 4**.

2.3.2 Renal sympathetic innervation and renal perfusion

The sympathetic nerves innervate blood vessels, tubules, and the juxtaglomerular apparatuses. Increased renal sympathetic nerve activity reduces renal blood flow, GFR, and sodium and water excretion. The effects are mediated by a contraction of the afferent and efferent arteriole and by an increase of sodium reabsorption, and

through renin release from the juxtaglomerular apparatus. There are no parasympathetic nerves in the kidney (Sata et al., 2018).

Activation of the renal sympathetic nervous system reduces renal cortical perfusion (Haddock et al., 2018). In the normal state, the basal renal sympathetic nerve activity is low. Under such circumstances, the renal functional responses to renal denervation consist of an increase in urinary sodium excretion and a decrease in renin secretion rate with no change in renal blood flow or GFR. However, in the states of renal vasoconstriction induced by renal sympathetic nerves, *e.g.* in hypertension or congestive heart failure, renal denervation increases basal renal blood flow (DiBona & Sawin, 2004).

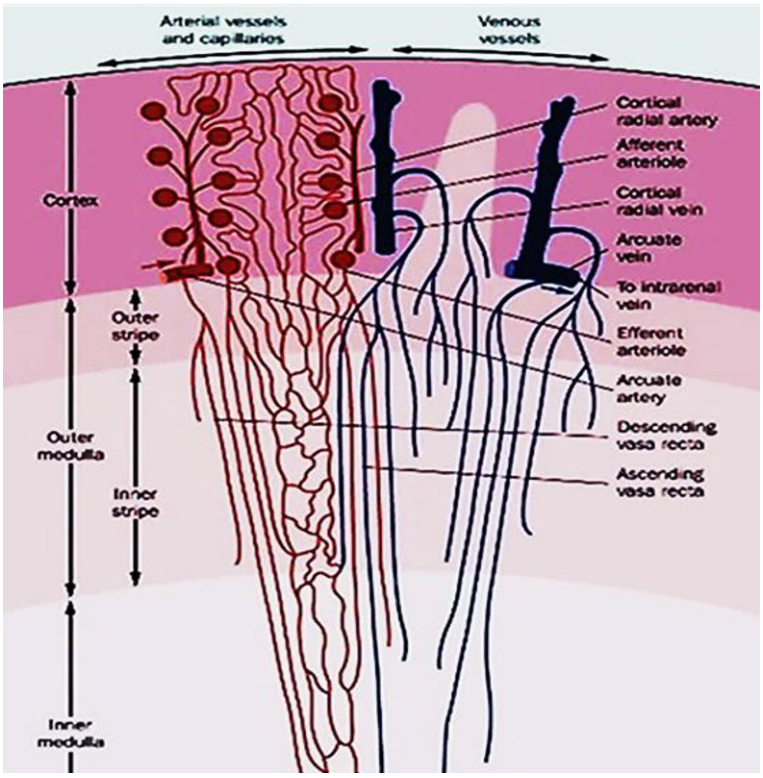

Figure 4. The microvasculature of the kidney. Afferent arterioles supply the glomeruli and efferent arterioles leave the glomeruli and divide into the descending vasa recta, which, together with the ascending vasa recta, form the vascular bundles of the renal medulla. The vasa recta ascending from the inner medulla all traverse the inner stripe within the vascular bundles, whereas most of the vasa recta from the inner stripe of the outer medulla ascend outside the bundles. Both types traverse the outer stripe as wide, tortuous channels. This figure was published in the book of Comprehensive 2nd edition Clinical Nephrology by authors Richard J Johnson and John Feehally. Copyright Elsevier (2003).

2.3.3 Dysfunction of the renal microcirculation and the endothelium

According to the chronic hypoxia hypothesis, renal tissue hypoxia is the unifying pathway in the progression of CKD, irrespective of its cause (Fine & Norman, 2008). Peritubular capillary (ptc) loss correlates with renal interstitial fibrosis and kidney function in animal and human studies (Bohle et al., 1996; Kang et al., 2002). Loss of ptc:s increases postglomerular resistance, leading to further glomerular and ptc injury. More direct support for a causal role for hypoxia in CKD comes from animal studies which show that renal hypoxia precedes matrix accumulation and fibrosis in kidney (Fine & Norman, 2008).

Hypoxia, reactive oxygen species, and NO deficiency induce renal fibrosis, increased endothelial to mesenchymal differentiation, vasoconstriction, inflammation, vascular rarefaction, and tissue damage, which in turn further reduce NO-availability (Chade, 2017). Despite the increased expression of hypoxia inducible factor-1α, the amount of vascular endothelial growth factor, a proangiogenic cytokine, is reduced, and the amounts of antiangiogenic substances, like endostatin and angiostatin, are increased. Endothelial cell apoptosis contributes to microvascular rarefaction (Chade, 2017).

2.3.4 Methods for studying renal perfusion

Quantitative renal perfusion refers to the blood volume that passes through a unit mass of renal tissue in a given time ($ml \cdot g^{(-1)} \cdot min^{(-1)}$ of tissue). Measurement of quantitative parameters requires signal intensity changes within the abdominal aorta, *i.e.*, an arterial input function. The measurement of semi-quantitative parameters requires only signal intensity changes within the kidney (Grenier et al., 2013).

Semi-quantitative methods to measure kidney perfusion

Renal plasma flow can be measured by means of *para-aminohippurate (PAH)*, which is almost completely removed from the plasma by the kidneys. Because part of the renal blood flow does not contribute to PAH-secretion (extranephronic perfusion), the renal plasma flow determined by PAH clearance is termed the effective renal plasma flow (ERPF). The PAH clearance is approximately 10% lower than the true renal plasma flow. The accuracy of the PAH-method decreases in CKD due to impaired tubular secretion of PAH and this will result in underestimation of ERPF. The mean value of ERPF in the healthy adults is about 600 ml/min per 1.73 m^2 (Fisher et al., 1999). Renal blood flow is derived from PAH-clearance by dividing PAH-clearance by (1-blood hematocrit). Ureteral catheterisation is needed for assessment of single-kidney ERPF.

Renal scintigraphy (renography) is a radionuclide technique which does not provide proper tissue attenuation correction. Thus, quantification of tissue perfusion is prone to errors, image quality is suboptimal, and no information on intrarenal flow distribution is obtained. An injection of a radiolabelled tracer is administered and the radiation is captured by an external gamma camera. When iodine-131 (^{131}I) coupled to orthoiodohippurate is used, renal blood flow can be measured, but ^{99m}Tc-mercapto-acetylglycyl-glycyl-glycine is currently the tracer of choice for this purpose. Alternatively, renal perfusion may be measured by assessment of plasma clearance of radioactive ^{131}I-hippuran or ^{99m}Tc-mercapto-acetylglycyl-glycyl-glycine which are administered as a single injection (Miyamori et al., 1986; Schneider et al., 2013).

Doppler ultrasound of the kidneys is a non-invasive and low-cost method to evaluate renal blood flow velocity. However, regular Doppler sonography is not a quantitative method and it is largely operator dependent. The resistive index (RI) and pulsatility index are calculated from blood flow velocity values in arcuate or interlobar arteries during the cardiac cycle; these variables reflect renovascular resistance and compliance. The normal value of the resistive index is 0.5–0.7 (Tublin et al., 2003). Velocities of renal artery blood flow can also be measured invasively by a Doppler guidewire technique (Manoharan et al., 2006).

Doppler imaging with more advanced properties to evaluate renal perfusion has been introduced in recent years. In real-time contrast-enhanced sonography the perfusion is performed by injecting microbubbles into a peripheral vein (Schneider et al., 2012). In dynamic tissue perfusion Doppler sonography the software determines a colour pixel area and flow velocity inside a region of interest of a video sequence (Scholbach et al., 2005). Renal blood flow is expressed as perfusion indexes in both modalities.

Quantitative methods to measure kidney perfusion

The xenon washout technique is a highly invasive method to evaluate kidney perfusion. After infusion of ^{133}Xe into the renal artery, the washout of ^{133}Xe is recorded with a scintillation counter at the kidney level. The xenon technique provides a quantitative measurement of overall renal blood flow, but its capability to estimate regional blood flow is limited (Aukland, 1980).

CT, especially *multidetector helical CT (MDCT) angiography,* offers the advantages of excellent spatial resolution, fast image acquisition, and numerous postprocessing capabilities. *Electron-beam computed tomography (EBCT)* uses an electron gun instead of regular x-rays and allows also accurate and non-invasive quantification of the volume and perfusion of each kidney separately

(Flickiger et al., 1996). The drawbacks of CT imaging are the need for ionising radiation and for iodinated contrast agents which are nephrotoxic.

Renal perfusion can be assessed noninvasively and quantitatively by *dynamic contrast enhanced (DCE) MRI*. Gadolinium is used for radiocontrast in DCE MRI and is cleared almost completely by glomerular filtration and thus it does not remain in the blood circulation complicating perfusion evaluation. The association between high doses of gadolinium contrast in patients with CKD and nephrogenic systemic fibrosis mandates judicious use of gadolidium, although new gadolinium agents seem to be safer than previous ones (Woolen et al., 2020). The development of MRI techniques not requiring gadolinium enhancement is ongoing.

Ultrasmall superparamagnetic iron oxide particles have been introduced as contrast agents. Ferumosytol, which is used intravascularly for iron supplementation therapy, seems to be feasible in patients with impaired renal function. Unlike gadolinium derivatives, ferumosytol resides in the blood pool and does not diffuse out into the extracellular fluid space (Toth et al., 2017).

Phase-contrast MRI (PC-MRI) provides a contrast-agent free MRI technique for determining blood flow velocity and volume in a vessel during the cardiac cycle (Villa et al., 2020). Blood flow must be corrected for kidney volume to yield quantitative kidney perfusion. Regional blood flow cannot be determined.

Arterial spin labelling (ASL) MRI exploits the water in blood as a freely diffusible tracer to measure quantitatively and non-invasively renal regional perfusion; no contrast agent is needed. The spatial resolution of ASL is relatively low and prone to movement artifacts. A positive correlation between renal cortical perfusion and eGFR has been shown by means of ASL MRI (Odudu et al., 2018; Buchanan et al., 2019).

Blood oxygen level dependent imaging (BOLD-MRI) does not directly measure kidney perfusion but reflects kidney metabolism, *i.e.*, the balance between tissue oxygen consumption and delivery. BOLD-MRI utilizes the paramagnetic properties of deoxyhemoglobin to assess tissue oxygenation. The higher the local deoxyhemoglobin level is, the lower is the tissue oxygen content, assuming that blood O_2 pressure is in equilibrium with tissue O_2 pressure (Pruijm et al., 2018). The difficulties to establish correlations between the renal oxygenation obtained by BOLD-MRI and renal perfusion and GFR are related to the fact that BOLD-MRI cannot be translated directly to an absolute quantitative measure of oxygenation. It cannot differentiate between oxygen delivery, oxygen consumption, and efficiency of arteriovenous oxygen diffusion.

2.3.5 PET and renal perfusion.

The PET-technique provides non-invasively and without contrast agent quantitative and regional data on the perfusion of each kidney separately. The radiopharmaceutical should show complete and perfusion-rate-independent extraction from arterial blood during its first pass transit through the renal capillaries. Since the extravascular space is large compared with the capillary volume, an inert and freely diffusible tracer is ideal (Green & Hutchins, 2011).

$[^{15}O]H_2O$ is an inert and freely diffusible tracer and has been used by several PET-based studies to evaluate renal perfusion. The kinetic model of $[^{15}O]H_2O$-PET assumes that the kidney parenchyme excretes all activity rapidly and that tubular transport has not yet started. Inaba et al. were the first to quantify renal perfusion in humans by means of PET using $[^{15}O]H_2O$ as a tracer (Inaba et al., 1989). Since then, the $[^{15}O]H_2O$-PET method has been validated in porcine studies against the microsphere reference method (Juillard et al., 2000). The linear relationship between $[^{15}O]H_2O$-PET based and PAH-clearance based kidney perfusion has been documented in healthy humans and in patients with CKD (Juillard et al., 2000; Alpert et al., 2000) and a correlation between renal cortical perfusion and eGFR has been demonstrated by means of $[^{15}O]H_2O$-PET (Rebelos et al., 2019).

^{13}N-ammonia is neither freely diffusible nor inert, and its extraction fraction varies with the rate of perfusion. However, the 10-minute half-life of ^{13}N-ammonia and its prolonged retention in the kidney allow extended image acquisition periods which improves image and data quality (Green & Hutchins, 2011). Nitzsche et al. demonstrated in healthy humans that estimates of renal cortical perfusion by $[^{15}O]H_2O$ correlate linearly with results obtained by ^{13}N-ammonia-PET (Nitzsche et al., 1993).

^{11}C-acetate, a tracer of oxidative metabolism, can also be used with PET to evaluate kidney perfusion and kidney oxygen consumption in humans (Normand et al., 2019).

2.3.6 Renal cortical perfusion in healthy subjects

Quantitative cortical perfusion values of kidney in healthy subjects are presented in **Table 2**.

Table 2. Quantitative values of perfusion in the renal cortex of healthy subjects with different imaging techniques

Method	Cortex (ml $g^{(-1)}min^{(-1)}$)	Reference
^{133}Xe washout	3.0–5.4	Hollenberg et al., 1981; Hollenberg et al., 1989
Dynamic MDCT	4.7	Miles et al., 1994
EBCT	3.6–3.9	Flickiger et al., 1996
PET ([^{15}O]H_2O)	1.6–4.7	Nitzsche et al., 1993; Middlekauff et al., 2001; Alpert et al., 2002; Kudomi et al., 2009; Damkjær et al., 2010; Damkjær et al., 2012; Koivuviita et al., 2012; Assersen et al., 2019; Rebelos et al., 2019
PET (^{13}N-ammonia)	4.6	Nitzsche et al., 1993
ASL	1.4–4.3	Odudu et al., 2018; Buchanan et al., 2019
DCE-MRI	2.2	Vallée et al., 2000

^{133}Xe, Xenon-133; MDCT, multidetector computed tomography; EBCT, electron-beam computed tomography; PET, positron emission tomography; ASL, arterial spin labelling; DCE-MRI, dynamic contrast enhanced magnetic resonance imaging

2.3.7 Renal cortical perfusion in patients with chronic kidney disease

A consistent finding from several studies with different methods has been that renal cortical perfusion is reduced in patients with CKD compared with healthy subjects.

ERPF based on PAH-clearance is higher in subjects with normal kidney function than in patients with moderate to severe CKD (750 ml/min, 280 ml/min and 200 ml/min, respectively) (Alpert et al., 2002). In the ASL-study of Buchanan et al. renal cortical perfusion was 2.0 $ml \cdot g^{(-1)} \cdot min^{(-1)}$ and 0.5 $ml \cdot g^{(-1)} \cdot min^{(1)}$ of tissue when eGFR was 92 and 34 ml/min, respectively (Buchanan et al., 2019). In the same study, PC-MRI yielded a value for total renal artery blood of 490 ml/min for the patients with CKD and 860 ml/min for the healthy subjects.

[^{15}O]H_2O-PET studies in patients with CKD have yielded renal cortical perfusion values of 2.2 (CKD stage 3) (Juillard et al., 2002), 2.1 (CKD stage 3–4) (Alpert et al., 2002), and 1.3 $ml \cdot g^{(-1)} \cdot min^{(-1)}$ (CKD stage 4–5) (Koivuviita et al., 2012). Alpert et al. and Koivuviita et al. also reported renal cortical perfusion values of healthy controls, which were higher than those of patients with CKD (3.2 and 1.8 $ml \cdot g^{(-1)} \cdot min^{(-1)}$, respectively) (Alpert et al., 2002; Koivuviita et al., 2012).

2.4 Atherosclerotic renovascular disease

Atherosclerosis accounts for over 90% of all cases of renal artery stenosis (RAS). Approximately 25% of patients with atherosclerotic renovascular disease (ARVD) present with at least one renal artery totally occluded and approximately 30% of patients have bilateral lesions. Angiographically documented RAS exceeding 70% is considered to be significant or severe, and a stenosis of 50–70% is considered to be moderately severe and its hemodynamic significance is uncertain (Prince et al., 2019).

2.4.1 Prevalence and prognosis of atherosclerotic renovascular disease

The prevalence of hemodynamically significant RAS (> 60% stenosis in Doppler echo) in the general elderly population is approximately 7% (Hansen et al., 2002). Patients with ARVD have often other associated risk factors, like DM type II, hypertension, and hypercholesterolemia. In these risk groups the prevalence of hemodynamically significant RAS is even higher.

ARVD reflects widespread CVD and implies involvement of other vascular regions, as well. The annual mortality rate of patients with ARVD in the Revascularisation versus medical therapy for renal-artery stenosis (ASTRAL)-study was 8% (Wheatley et al., 2009).

2.4.2 Clinical presentations of atherosclerotic renovascular disease

2.4.2.1 Renovascular hypertension

More than 90% of patients with ARVD have hypertension which is often treatment resistant. Studies using latex casts have shown that hemodynamic effects emerge above an approximate threshold value of 75–85% of luminal occlusion of the renal artery (Herrmann & Textor, 2019). A decrease in renal perfusion pressure activates the RAAS, which releases renin and angiotensin II. De Bruyne et al. used an expanded balloon to induce gradual RAS in human volunteer subjects and found that renin release increased after a pressure drop of 10–20% distal to the balloon placed in the renal artery (De Bruyne et al., 2006).

There is a complex set of pressor signals, including activation of the RAAS, sympathoadrenergic activation, and recruitment of oxidative stress pathways which all contribute to renovascular hypertension (Textor & Lerman, 2019). The essence of angiotensin in RAS has been demonstrated in an angiotensin II subtype 1A

receptor knockout mouse model of 2-kidney-1-clip Goldblatt hypertension (Cervenka et al., 2002). In a similar animal model renovascular hypertension was prevented by blocking the RAAS with the angiotensin convertizing enzyme (ACE) inhibitor captopril (DeForrest et al., 1982).

The role of the RAAS in ARVD depends partially on whether the RAS is unilateral or bilateral. Unilateral RAS in humans is analogous to the 2-kidney-1-clip Goldblatt animal model in which hypertension is renin-dependent and peripheral vascular resistance is increased. The contralateral kidney responds to the increased blood pressure by increasing natriuresis and by reducing sodium retention and volume overload. Consequently, the perfusion pressure in the kidney supplied by a stenotic renal artery decreases and this leads to continuous release of renin (Herrmann & Textor, 2019), albeit usually transiently.

Angiotensin II mediated vasoconstriction affects mainly the efferent arterioles and is crucial in maintaining glomerular filtration pressure distal to the stenosis in bilateral and in solitary kidney RAS (Herrmann & Textor, 2019). Blockade of the RAAS may lead to an abrupt fall in blood pressure and glomerular filtration. In the 1-kidney-1-clip Goldblatt animal model (which is analogous to bilateral or unilateral kidney RAS in humans) the blood pressure drop after inhibition of angiotensin II was greater in hypertensive, sodium-depleted animals than in sodium-replete animals (Gavras et al., 1973). Thus, in the 1-kidney-1-clip model, blood pressure is more dependent on volume than renin.

2.4.2.2 Ischemic nephropathy

The exact degree of RAS that threatens oxygenation and renal function leading to ischemic nephropathy is a matter of debate. Kidney tissue oxygen levels are regulated by a triad of factors including oxygen consumption (primarily associated with tubular solute transport), afferent arteriolar blood flow and arteriovenous shunting of kidney (Evans, 2008).

Renal perfusion is maintained quite stable due to autoregulation until cross-sectional area of the renal artery lumen falls by 70–80% (Textor&Lerman, 2019). Gloviczki et al. studied hypertensive patients with and without RAS with BOLD-MRI and found that despite reduced blood flow in the kidney at 70% RAS, kidney oxygenation was preserved (Gloviczki et al., 2010). However, in patients with severe vascular occlusion (stenosis grade approximately more than 80%), decreased renal blood flow overwhelmed the autoregulatory capacity of the kidney leading to reduced renal tissue oxygenation (Gloviczki et al., 2011).

2.4.3 Renal perfusion in atherosclerotic renovascular disease

Renography (a scintigraphic method) can be used to evaluate the proportion of perfusion to each kidney. Although some studies of unilateral RAS scintigraphy have shown a decreased uptake of the radioactive agent in stenosed kidney, sensitivity and specificity of the method are poor (Mann et al., 1991). Split renal ^{131}I-iodohippurate scintigraphy was used in the study of Miyamori et al. (Miyamori et al., 1986), who found that, in patients with unilateral RAS, ERPF was 117 ml/min in the stenosed kidney and 265 ml/min in the contralateral kidney. In patients with bilateral RAS, ERPF was 109–128 ml/min, depending on the side of the kidney (Miyamori et al., 1986).

Gloviczki et al. compared renal cortical perfusion with EBCT between patients with unilateral 70% RAS and patients with essential hypertension (Gloviczki et al., 2010). The renal cortical perfusion was 2.7 $ml \cdot g^{(-1)} \cdot min^{(-1)}$ of tissue in stenosed kidneys and 2.9 $ml \cdot g^{(-1)} \cdot min^{(-1)}$ in contralateral kidneys of patients with RAS. In patients with essential hypertension, renal cortical perfusion was 3.5 ml $g^{(-1)} \cdot min^{(-1)}$ of tissue (Gloviczki et al., 2010).

There are several MRI techniques which have been used in the evaluation of renal cortical perfusion in patients with ARVD, including gadolinium enhanced MRI, ASL, and BOLD. Vallée et al. used gadolinium enhanced MRI and found that renal cortical perfusion was 1.1 $ml \cdot g^{(-1)} \cdot min^{(-1)}$ in stenosed kidneys of patients with ARVD, 0.5 $ml \cdot g^{(-1)} \cdot min^{(-1)}$ in patients with severe CKD, and 2.2 $ml \cdot g^{(-1)} \cdot min^{(-1)}$ in patients with normal kidney function (Vallée et al., 2000). In the ASL-based study of Fenchel et al. renal cortical perfusion was 2.4 $ml \cdot g^{(-1)} \cdot min^{(-1)}$ in patients with no or mild RAS and 1.5 $ml \cdot g^{(-1)} \cdot min^{(-1)}$ in patients with severe RAS (Fenchel et al., 2006).

The reduction in renal cortical perfusion characterising RAS makes BOLD-MRI suitable for assessing tissue oxygenation in post-stenotic kidneys (Pruijm et al., 2018). However, it should be emphasised that physiological changes in renal work may limit the ability of BOLD MRI to detect changes in kidney oxygenation. The lack of solute transport and glomerular filtration in subjects with severe RAS may lead to normal oxygenation values in the renal cortex and medulla.

[$^{15}H_2O$]PET was used to evaluate renal cortical perfusion in patients with RAS in the study of Koivuviita et al. (Koivuviita et al., 2012). Renal cortical perfusion correlated inversely with the degree of RAS. In patients with unilateral RAS, the mean cortical perfusion in stenosed kidneys was 1.5 $ml \cdot g^{(-1)} \cdot min^{(-1)}$ of tissue and in the contralateral kidneys 1.8 $ml \cdot g^{(-1)} \cdot min^{(-1)}$ of tissue (Koivuviita et al., 2012).

2.4.4 Anatomical evaluation of atherosclerotic renovascular disease

Renal Doppler sonography is an appropriate initial method to estimate the severity of ARVD. A peak systolic velocity of > 200 cm/s is associated with 95% sensitivity and 90% specificity for > 50% stenosis (Prince et al., 2019). If renal Doppler sonography cannot confirm the hemodynamic severity of RAS, then cross-sectional imaging with CT angiography or magnetic resonance angiography are the next choices. The sensitivity and specificity of CT- and magnetic resonance angiography are over 90% for stenosis > 50% (Prince et al., 2019). However, in patients with CKD, CT angiography predisposes to contrast-induced nephropathy and magnetic resonance angiography to gadolinium associated nephrogenic systemic fibrosis which needs to be taken into consideration.

PC-MRI provides a contrast-agent free MRI technique for determining blood flow velocity and volume in a vessel during the cardiac cycle. The combined approach of morphologic 3-dimension gadolinium-enhanced magnetic resonance angiography and functional PC-MRI offers reliable and reproducible grading of RAS which is comparable with digital subtraction angiography (Villa et al., 2020).

2.4.5 Functional evaluation of atherosclerotic renovascular disease

The selection of renal arteries suitable for intervention is currently based on anatomic grading of the stenosis rather than on functional assessment under hyperemia (van Brussel et al., 2017). The assessment of functional flow indexes in combination with anatomic stenosis grade in the evaluation of coronary artery stenosis is associated with improved selection of patients for coronary stenting and improved clinical outcome. Especially, the combination of coronary pressure-derived myocardial FFR and MPR provide additional value for identifying hemodynamically significant coronary stenosis. In this setting, FFR provides information on the functional severity of focal coronary artery stenosis, whereas MPR provides information on the functional properties of both focal and diffuse CAD and microvascular function (Danad et al., 2014; van Brussel et al., 2017). Translating these principles to ARVD might improve the selection of patients for renal artery stenting.

2.4.5.1 Renal fractional flow reserve and translesional gradient

A resting or hyperemic translesional gradient (the difference between pressure proximal to stenosis and pressure distal to stenosis during systole) ≥ 20 mmHg and renal fractional flow reserve (FFR_{REN}) (the ratio of renal artery pressure distal to

stenosis to renal artery pressure proximal to stenosis during hyperemic conditions) ≤ 0.8, have been considered to indicate hemodynamically severe RAS. However, most studies have shown a poor correlation between the grade of RAS and these hemodynamic parameters (van Brussel et al., 2017).

There is some evidence that resting or hyperemic translesional pressure gradient in the renal artery predicts blood pressure improvement after RAS stenting in patients with moderate to severe RAS (van Brussel et al., 2017). In a small prospective study of 17 patients with moderate to severe ARVD, the effect of RAS stenting measured by the blood pressure response was better in the patients with impaired FFR_{REN} (< 0.8) than in patients with a normal FFR_{REN} (Mitchell et al., 2007). The translesional gradient did not differentiate responders from non-responders. However, in another small prospective study of patients with moderate to severe ARVD, FFR_{REN} did not predict the blood pressure response after RAS stenting (Kądziela et al., 2013).

2.4.5.2 Renal flow reserve

Renal flow reserve in subjects without RAS

The vasodilator properties of the kidney are modest compared with the heart. Renal perfusion increases 1–2-fold whereas MP increases usually 3- or even 5-fold in response to vasodilatation. The renal perfusion reserve (RFR) seems to depend on the imaging method as well as on the vasoactive medicine used.

Intra-arterial Doppler studies have demonstrated RFR of 1.5–2 (= 50–100%) in normotensive and hypertensive patients (Beregi et al., 2000; Manoharan et al., 2006). In these Doppler studies, intrarenal papaverine, dopamine, and fenoldopam were used as vasodilators. ACE-inhibitors have been used to achieve renal hyperemia in renographic, PAH and xenon studies. In healthy normotensive men, ACE-inhibitor-induced RFR has varied between 6% and 38% (1.06–1.38) (Hollenberg et al., 1981; Hollenberg et al., 1989; Fisher et al., 1999). In a $[^{15}O]H_2O$ PET study, quinalaprilat induced RFR was 26% (1.26) in hypertensive patients with CKD stage 3 (Juillard et al., 2002). In the only $[^{15}O]H_2O$ PET study on RFR in healthy subjects, there was a mild decrease of renal cortical perfusion after enalapril administration (Kudomi et al., 2009).

Renal flow reserve in patients with RAS

There are only a few studies on RFR in patients with RAS. RFR in patients with unilateral RAS was evaluated in an intra-arterial Doppler study in which hyperemic renal flow was induced by administration of papaverine (Mounier-Vehier et al.,

2004). The RFR of stenosed kidneys and of non-stenosed kidneys was 1.1 (10%) and 1.6 (60%), respectively.

Data on the effect of ACE inhibitors on renal perfusion in RAS is mainly based on animal studies or on renographic human studies – results have been conflicting (Miyamori et al., 1986; Tamaki et al., 1988; Peters et al., 1990). Tamaki et al. used ^{82}Rb PET and captopril to study RFR in dogs with unilateral RAS (Tamaki et al., 1988). Renal perfusion did not change in the affected kidney and increased in the contralateral kidney after captopril. Similarly, in the renographic study of Miyamori et al., captopril did not induce any change in renal perfusion on the stenotic side in patients with unilateral RAS, but it caused a slight but signifcant increase in renal perfusion on the non-stenotic side (Miyamori et al., 1986). Patients with bilateral RAS had no change in renal perfusion after captopril. In the renographic study of Peters et al., renal perfusion increased following ACE inhibition in unilaterally stenosed kidneys by 24% and by 18% in contralateral kidneys in patients with ARVD (Peters et al., 1990). In patients with bilateral RAS, renal perfusion increased by 24% after ACE inhibition. RFR did not correlate with clinical outcome after RAS stenting (Peters et al., 1990).

2.4.6 Treatment of atherosclerotic renovascular disease

2.4.6.1 Revascularisation of renal artery stenosis

Large studies (STAR, ASTRAL and CORAL) with patients with ARVD and moderate to severe CKD, in which RAS grading was only anatomically evaluated, demonstrated no benefit of renal artery stenting (Wheatley et al., 2009; Bax et al., 2009; Cooper et al., 2014). These studies have been criticised for entering patients too late for potential benefit of RAS stenting. Furthermore, the studies may have enrolled patients with non-significant stenosis and excluded patients with high-risk clinical manifestations (Prince et al., 2019).

There is emerging evidence that the natural history of ARVD involves transition from a hemodynamic condition to proinflammatory and profibrotic disease with microvascular remodelling and mitochondrial damage (the major determinants of the response to revascularisation), which would accelerate renal injury (Eirin et al., 2019). Experimental studies have shown that after successful RAS stenting renal function is not fully recovered and that microvascular rarefaction and renal fibrosis persist (Chade, 2018).

2.4.6.2 Other therapies for atherosclerotic renovascular disease

Pharmacotherapy for atherosclerotic renovascular disease

Use of both ACE-inhibitors and angiotensin receptor blockers (ARB) is associated with a long-term survival benefit compared with other antihypertensives in ARVD (Chrysochou et al., 2012). ARB:s decrease oxidative stress and improve microvascular density and renal hemodynamics in animal studies (Chade, 2017). Simvastatin has been shown to ameliorate microvascular remodelling, independently of lipid-lowering (Eirin et al., 2019).

Novel therapies for atherosclerotic renovascular disease

In experimental studies, interventions have been developed to ameliorate renal microvascular remodelling, inflammation, and mitochondrial injury to restore perfusion and reverse injury of the post-stenotic kidney (Eirin et al., 2019). Some of such interventions are feasible also in humans.

Experimental studies show that mesenchymal stem cells possess immunomodulatory and anti-inflammatory properties and contribute to the repair of poststenotic renal microcirculation (Eirin et al., 2019). Saad et al. confirmed these findings in humans by infusing into the renal artery autologous adipose tissue-derived mesenchymal stem cells in non-revascularised patients with unilateral atherosclerotic RAS (Saad et al., 2017). Three months after the infusion, CT studies showed that renal cortical perfusion had increased in the stenosed kidneys from a baseline value of 2.0 $ml \cdot g^{(-1)} \cdot min^{(-1)}$ to 2.4 $ml \cdot g^{(-1)} \cdot min^{(-1)}$ and in contralateral kidneys from 2.3 $ml \cdot g^{(-1)} \cdot min^{(-1)}$ to 2.8 $ml \cdot g^{(-1)} \cdot min^{(-1)}$. Hypoxia of the stenosed kidneys measured by BOLD-MRI had decreased, while the single-kidney GFR had remained stable (Saad et al., 2017).

Kidney ischemia induces disruptions to the function of mitochondria and to adenosine triphosphate generation. In addition, renal revascularisation per se can amplify tissue injury by upregulating inflammation and fragmentation of the mitochondria. The mitoprotective drug elamipretide is effective also in humans (Eirin et al., 2019). Intrarenal delivery of vascular endothelial growth factor and endothelial progenitor cells restore the microcirculation of post-stenotic kidneys, according to animal studies (Eirin et al., 2019).

2.5 Chronic kidney allograft injury

2.5.1 Prognosis of kidney transplant

Although first-year survival of kidney allografts has improved tremendously, long-term attrition rates have improved only slightly during the last decades. The yearly graft attrition rate has been approximately 5% in recipients of a deceased-donor transplant in the United States between 1989 and 2009 (Lamb et al., 2011). A large European registry study recently showed for the first time that the short-term improvement in graft survival has decreased since 2000, while long-term improvement has remainded stable (Coemans et al., 2018).

In Finland, graft survival has improved since the 1980's. In a study of 2445 patients with a deceased-donor kidney transplant and taking cyclosporine-based triple immunosuppression, 5-year death-censored graft survival improved from 74% to 94% from 1984 to 2002 (Salmela & Kyllönen, 2004). During the same period, the graft half-life-estimate of 1-year survivors improved from 7.6 to 21.8 years (Salmela & Kyllönen, 2004) (**Figure 5**).

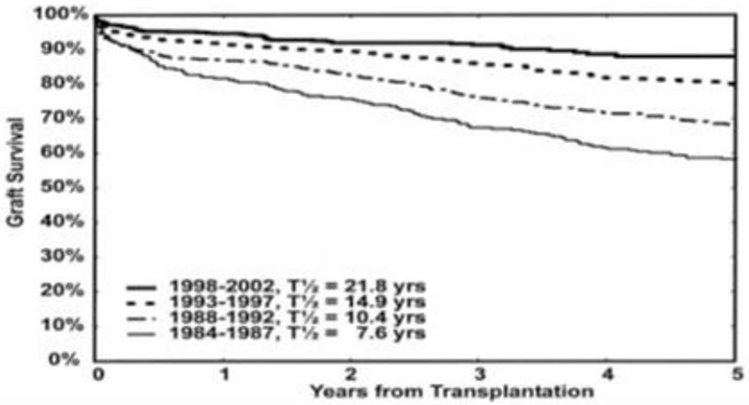

Figure 5. Graft survival and the graft half-life estimates (T1⁄2) for 1-year survivors in each period in 2445 cadaveric kidney transplantations on CsA triple immunosuppression in Helsinki, 1984 to 2002 (Salmela & Kyllönen, 2004). Reproduced with the permission of Elsevier.

2.5.2 Ethiology of chronic kidney allograft injury

Chronic allograft injury (CAI) is a condition characterised clinically by progressive renal dysfunction often associated with hypertension and proteinuria. Histologically, CAI is characterised with interstitial fibrosis and tubular atrophy (IFTA), which was earlier thought to be associated mainly with cyclosporine toxicity (Nankivell et al., 2003).

Our understanding of late graft failure has changed dramatically in recent years. IFTA is a non-specific lesion; it represents a common final pathway of several types of injury, *e.g.*, acute and chronic rejection, and non-immune factors, *e.g.*, recurrent glomerular disease, allograft polyoma virus infection, ischemia-reperfusion injury, and CNI nephrotoxicity (Nankivell & Kuypers, 2011; Stegall et al., 2015). IFTA and other causes of late allograft failure often co-exist. In a recent study of Van Loon et al. there were both active diseases (antibody- and T-cell-mediated rejection, polyoma virus-associated nephropathy, glomerulonephritits) and chronic diseases (IFTA or transplant glomerulopathy) in the failing transplant 1–10 years after transplantation in more than 30% of kidney biopsies (Van Loon et al., 2020b).

Rejection seems to play an important role especially in the progression of CAI (El-Zoghby et al., 2009; Sellarés et al., 2012). In a large retrospective study, which evaluated surveillance and indication biopsies of 1317 patients with a kidney transplant, 330 (25%) grafts were lost during the mean follow-up time of 50 months (El-Zoghby et al., 2009). Approximately half of the losses was due to patient death and the other half due to graft failure sensored for death. The four main causes for graft failure were glomerular disease (38%), moderate to severe IFTA (32%), medical/surgical conditions (12%), and acute rejection (12%). Nearly half of the glomerular diseases were due to alloimmune transplant glomerulopathy. Most cases of IFTA (81%) could be attributed to a specific cause. Chronic cellular or antibody-mediated rejection was the main cause of IFTA (28%) (El-Zoghby et al., 2009). Thus, almost 40% of all graft failures were due to an alloimmune process. Similarly, in the prospective study of Sellarés et al., 56% of late graft losses were due to mixed or antibody-mediated rejection with evidence for donor specific antibodies or panel reactive antibodies at the time of biopsy or allograft failure (Sellarés et al., 2012).

Risk factors for chronic kidney allograft injury

Non-immunological recipient-related factors, like hypertension, DM, hyperlipidemia, smoking, obesity, age, anemia, and dialysis vintage are associated with graft survival (Nankivell & Kuypers, 2011; Rangaswami et al., 2019; Van Loon et al., 2020a). Compared to pre-emptive transplantation, a waiting time of 1–2 years on dialysis increases the risk of death-censored kidney allograft loss by 55% (Meier-Kriesche et al., 2000).

Donor-related factors, like donor age, living donor source, donor kidney quality and size, and donor CV morbidity, are associated with kidney allograft survival. Factors related to the transplant procedure, like ischemia-reperfusion injury, cold ischemia time, and delayed graft function, affect graft survival as well (Nankivell & Kuypers, 2011; Rangaswami et al., 2019; Van Loon et al., 2020a).

Immunological factors, *e.g.*, panel reactive antibody level, C4d staining of the kidney allograft, human leucocyte antigen mismatch, and donor specific antibodies play an important role in graft survival. Kidney allograft failure due to acute rejection during the first year after transplantation has been associated with poor graft outcome in historical studies. However, despite a decrease is the occurrence of acute rejections, long-time allograft survival has not significantly improved during the last decades (Stegall et al., 2015). The causes and risk factors related to deterioration of renal function are presented in **Figure 6**.

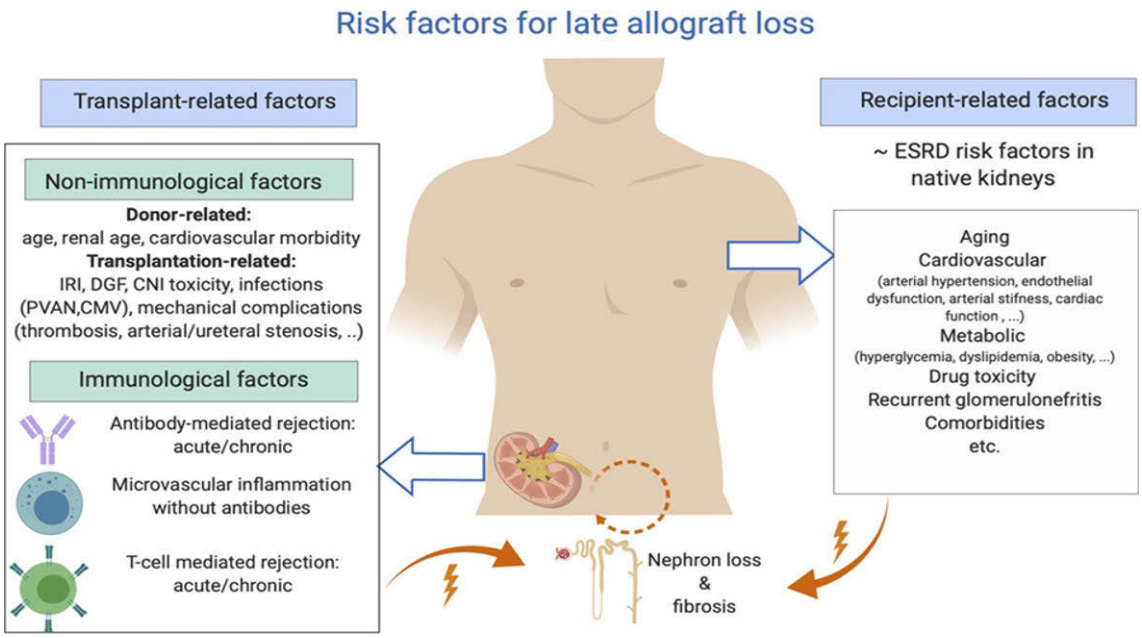

Figure 6. Schematic overview of risk factors for allograft loss, distinguishing recipient-related factors (analogous to risk factors in native kidneys) from transplant-related factors that can be nonimmunological and immunological. All these factors can contribute to allograft injury with nephron loss, further initiating a vicious circle of harmful hyperfiltration of the remnant nephrons, resulting in accelerated nephron loss and fibrosis. CMV, cytomegalovirus; CNI, calcineurin inhibitor; DGF, delayed graft function; ESRD, end-stage renal disease; IRI, ischemia-reperfusion injury; PVAN, polyomavirus-associated nephropathy (Van Loon et al., 2020). Reproduced with the permission of Wolters Kluwer.

2.5.3 Fibrosis and chronic allograft injury

2.5.3.1 Definition of interstitial fibrosis and tubular atrophy

In the Banff classification of renal allograft histology, the individual chronic lesions are IF (ci), TA (ct), arterial fibrous intimal thickening (cv), arteriolar hyalinosis (ah),

mesangial matrix increase (mm), and transplant glomerulopathy (cg) (Racusen et al., 1999; Loupy et al., 2017; Haas et al., 2018; Roufosse et al., 2018). IF and TA usually occur together and are considered as the single parameter IFTA. Since the tubulointerstitium comprises a large part of renal cortical area, IFTA is the most important manifestation of structural allograft deterioration (Vanhove et al., 2017).

In the Banff classification of kidney allografts, IFTA changes are graded in 3 classes: grade I with mild IFTA covering less than 25% of the cortical area, grade II with moderate IFTA covering 26–50% of the cortical area, and grade III with severe IFTA covering more than 50% of the cortical area (Loupy et al., 2017; Haas et al., 2018). The grade of IFTA correlates with GFR (Nankivell et al., 2003).

2.5.3.2 Prevalence and prognostic value of kidney allograft fibrosis

The incidence and severity of allograft fibrosis have decreased in the last 3 decades among allograft recipients probably reflecting advances in immunosuppressive therapy and transplantation procedure (better matching and preservation techniques) (Vanhove et al., 2017). Nankivell et al. reported in a prospective study during the cyclosporine era moderate to severe IFTA in 25%, 66%, and 90% of kidney grafts at 1, 5 and 10 years after transplantation, respectively (Nankivell et al., 2003). In patients using tacrolimus based immunosuppression, moderate to severe IFTA was present in only 13% and 17% of allograft protocol biopsies at 1 year and 5 years after transplantation, respectively (Stegall et al., 2015).

IFTA is an independent risk factor for late graft dysfunction and graft loss, irrespective of its cause (Nankivell et al., 2003; Servais et al., 2011; Naesens et al., 2013, Loupy et al., 2019). It has been shown that the total burden of chronic histological damage correlates better with graft survival than each of the chronic lesions separately in the first year after transplantation (Naesens et al., 2013; Vanhove et al., 2017). Loupy et al. developed recently a risk prediction score of kidney allograft failure where immunological, functional, and histological allograft parameters were combined and human leucocyte antibody profiling was included (Loupy et al., 2019). The score seems to predict quite accurately the risk of long term kidney allograft failure. IFTA was one important prognostic factor in the score.

2.5.3.3 Pathophysiology of kidney allograft fibrosis

Renal fibrosis develops often during the first year after transplantation (Servais et al., 2011; Vanhove et al., 2017) but it is generally mild. It is likely that early accumulation of fibrosis results from self-limiting inflammation related to implantation stress. However, there seems to be a “point of no return” of structural

injury beyond which fibrosis progresses locally, regardless of persisting injury (Vanhove et al., 2017).

Inflammation seems to be pivotal for progression of allograft fibrosis. The inflammatory cascade involves macrophage activation and recruitment of immune cells, which produce profibrotic mediators. Myofibroblasts, fibroblasts, fibrocytes, cells of hematopoietic origin, and tubular epithelial and endothelial cells, synthesise increasing amounts of extracellular matrix (Vanhove et al., 2017).

2.5.3.4 Microcirculation and fibrosis in kidney allograft

There is emerging evidence that the tubulointerstitial microvasculature plays an important role in the progression of CAI as it does in the progression of CKD. In case of persisting allograft injury, interstitial fibrosis and microvascular rarefaction coexist (Vanhove et al., 2017).

Ishii et al. studied retrospectively 79 graft biopsies obtained from patients with unexplained deterioration of kidney graft function or proteinuria 3–11 years after transplantation (Ishii et al., 2005). The amount of ptc:s and glomerular capillaries were counted immunohistochemically after staining for CD34 antibody, which reacts with the surface of endothelial cells. IFTA was present in all biopsies regardless of inflammation, C4d-positivity, or chronic humoral rejection, and correlated with the amount of ptc:s and serum creatinine. Similarly, the number of CD34-positive glomerular capillaries correlated with the degree of glomerular sclerosis. However, the loss of glomerular capillaries did not correlate with graft dysfunction. These findings suggest that the loss of ptc:s is crucial for the development of IFTA (Ishii et al., 2005).

In the retrospective study of Steegh et al., ptc loss mainly occurred in the first 3 months after kidney transplantation and it was associated with inflammation, fibrosis, and eGFR at 1 year after transplantation (Steegh et al., 2011). In addition, peritubular capillaritis at 3 months was associated with IFTA at 12 months in the study.

2.5.3.5 Methods to study kidney allograft fibrosis

Renal biopsy is the gold standard to assess and quantify renal fibrosis in allografts. Trichrome or Picrosirius Red staining are used to assess collagen content in the interstitium. Quantification of fibrosis is assessed either visually or by computer-based morphometry techniques. Renal biopsy tissue can be used for immunohistochemical detection of CD44 (transmembrane glycoprotein) and vimentin (mesenchymal cell marker) which both are involved in renal fibrosis (Boor & Floege, 2015).

Factors involved in fibrogenesis can be measured in blood or in urine when evaluating allograft fibrosis. Analyses of the ribonucleic acid of factors involved in fibrogenesis in biopsy tissue or in urine could be another diagnostic approach. Ultrasound and MRI based measurements of tissue elasticity (elastography) have not been successful methods for evaluation of kidney allograft fibrosis (Boor & Floege, 2015). The most promising imaging method so far is diffusion weighted imaging MRI.

2.6 Perfusion of kidney allograft

2.6.1 Quantification of kidney transplant perfusion

Techniques based on MRI

Cortical perfusion of kidney allografts studied with renal ASL MRI correlates moderately with eGFR (Odudu et al., 2018). In the study of Heusch et al., cortical perfusion of kidney transplants measured with ASL was compared between patients with eGFR > 30 ml/min and patients with eGFR < 30ml/min (Heusch et al., 2014). Renal cortical perfusion amounted to 2.8 $ml \cdot g^{(-1)} \cdot min^{(-1)}$ and 1.8 $ml \cdot g^{(-1)} \cdot min^{(-1)}$, respectively. For comparison, renal cortical perfusion in healthy control subjects assessed with ASL is 1.4–4.3 $ml \cdot g^{(-1)} \cdot min^{(-1)}$ (Odudu et al., 2018; Buchanan et al., 2019).

Djamali et al. used BOLD-MRI to evaluate renal cortical oxygenation in patients with a kidney transplant and CKD stage 3 (Djamali et al., 2007). Renal medullary and cortical oxyhemoglobin concentrations were increased. Moreover, there was an association between serum and urine biomarkers of oxidative stress and renal oxygenation values. The authors proposed that the study findings were due to increased oxidative stress, tubular injury, and, consequently, reduced sodium reabsorption and oxygen consumption (Djamali et al., 2007).

Techniques based on Doppler echo

Renal cortical perfusion measured semiquantitatively with contrast-enhanced sonography during the first year after transplantation predicts kidney function at 3 years after transplantation (Jiménez et al., 2016). Scholbach et al. demonstrated a positive correlation between kidney function and renal cortical perfusion measured by semiquantitative dynamic tissue perfusion Doppler in patients with a kidney allograft (Scholbach et al. 2005).

There was disagreement between two large studies as to the usefulness of Doppler RI in patients with a kidney transplant. In the study of Radermacher et al. the risks of graft loss and death among patients with a RI of 0.8 or higher were enhanced compared to patients with a RI of less than 0.8. They found a weak correlation between kidney transplant histology and RI (Radermacher et al., 2003). RI was the most powerful independent predictor of death and graft loss, although there was also a statistically significant correlation between RI and hemodynamic factors and recipient age (Radermacher et al., 2003). However, according to the results in the prospective study of Naesens et al., RI reflected recipient age and central hemodynamic factors rather than intrarenal processes and was associated with recipient survival but not with graft survival (Naesens et al., 2013).

Renal scintigraphy and effective renal plasma flow

Radionuclide scintigraphy of the kidney transplant was decades ago an important method to monitor graft function and perfusion in the early posttransplant period. The quantification of perfusion was based on mathematical models, but none of them provided enough diagnostic power for specific diagnoses of graft dysfunction (El Maghraby et al., 1998).

ERPF of patients with kidney transplant with CKD stage 3 was measured by means of PAH clearance at 4–8 months after transplantation in the study of Hetzel et al. (Hetzel et al., 2005). They reported that ERPF was 187 ml/min, and renal vascular resistance (RVR) was increased compared to values of kidney donors with one kidney. During losartan treatment ERPF increased and RVR decreased, although the changes were not statistically significant (Hetzel et al., 2005).

2.6.2 Sympathetic nervous system and perfusion of kidney transplant

Although renal transplantation assures total denervation of the kidney, the functional capacity of renal grafts does not seem to change significantly neither experimentally nor clinically. However, there may be an impaired ability of the denervated or transplanted kidney to normally conserve sodium and increase plasma renin activity in response to a reduction in dietary sodium intake (DiBona, 1987). Results of studies on the effects of renal denervation on renal perfusion have been controversial (Barrett et al., 2001). Plasma renin values were rather low in kidney transplant recipients on cyclosporine, which might be due to expansion of the extracellular fluid volume (Mourad et al., 1993).

Both animal and human studies have demonstrated regeneration of sympathetic nerves after renal denervation and after reimplantation of the kidney graft

(Booth et al., 2015; Shannon et al., 1998). In the study of Booth et al. on sheep, there was a normal anatomic distribution of afferent and efferent renal nerves and a normal response to electric stimulation at 11 months after denervation (Booth et al., 2015). A human study with histological specimens from kidney transplant arteries and parenchymas at different time points after transplantation showed that renal nerves do regenerate to some degree (Shannon et al., 1998).

Renal transplantation may alter vascular responses to sympathomimetics, which play a role in maintaining renal perfusion after renal transplantation. As an example, dopamine, which causes a long-lasting increase in renal perfusion after initial short vasoconstriction in the healthy, causes enhancement of initial renal vasoconstriction and attenuation of the vasodilatation phase in patients with a kidney transplant (Morita et al., 1999). Furthermore, phenylephrine (α-receptor blocker) produces a gradual increase in renal perfusion in the native kidney, but produces a sudden reduction in renal perfusion in transplanted kidneys (Morita et al., 1999).

2.6.3 Kidney transplant perfusion and biopsy

The protocol for taking a biopsy of a kidney transplant is both sensitive and specific for assessing the histopathology of the allograft. The disadvantage of taking a biopsy of the allograft is its invasiveness. On the other hand, functional biomarkers, such as serum creatinine or eGFR cannot predict early enough emerging histopathological changes (Yilmaz et al., 2007).

The perfusion of kidney allografts is, according to some studies, related to renal histological findings. Kidney allograft perfusion might serve as a non-invasive surrogate for allograft biopsy in certain circumstances.

Perfusion of kidney allografts by MRI and kidney allograft biopsy

In the study of Pereira et al. kidney biopsies of 10 patients with CAI [serum creatinine 119+/-90 umol/l] were estimated by the Chronic Allograft Damage Index which combines six histologic parameters (interstitial fibrosis, interstitial inflammation, glomerular sclerosis, mesangial matrix increase, fibrous intimal thickening, and tubular atrophy) (Pereira et al., 2010). There was a statistically significant correlation between cortical perfusion of renal allograft measured quantitatively by means of contrast enhanced MRI and the Chronic Allograft Damage Index score.

Wang et al. demonstrated a statistically significant correlation, on the one hand, between renal cortical perfusion measured with the ASL technique and, on the other hand, peritubular capillary density and grade of fibrosis of the allograft approximately 1.5 years after transplantation in patients with a kidney transplant

with CKD stage 3 (Wang et al., 2019). They also showed that renal cortical perfusion measured with ASL reveals subclinical renal pathology in kidney transplants despite stable kidney function (CKD stage 2) (Wang et al., 2020).

Recently, Yu et al. demonstrated in a prospective study with 83 kidney transplant recipients that renal cortical perfusion by ASL and eGFR at baseline predicted kidney function 3 years later (Yu et al., 2021).

Perfusion of kidney allograft assessed with Doppler sonography and kidney allograft biopsy

Scholbach et al. studied patients with a kidney allograft (mean time from transplantation 3.7 years) and found a statistically significant correlation between renal cortical perfusion measured with dynamic tissue perfusion Doppler and peritubular capillaritis (Scholbach et al., 2013). Schwenger et al. studied renal cortical perfusion in patients with a kidney allograft with CKD stage 2–3 with contrast-enhanced Doppler sonography on average 2.5 years after transplantation (Schwenger et al., 2006). In patients with CAI evidenced by biopsy, renal cortical perfusion was lower than in patients without CAI. The renal cortical perfusion correlated with the serum creatinine concentration.

Renal cortical perfusion was estimated in patients with a kidney allograft and CKD stage 2–3 by means of Doppler sonography (semiquantitative maximal fractional area index) 2.5 years after transplantation in a prospective study by Nankivell et al. (Nankivell et al., 2002). A biopsy of the transplant was taken either as a routine protocol biopsy or as indicated for assessing the etiology of slowly detereorating kidney function. CAI was defined as the presence of chronic interstitial fibrosis, tubular atrophy, and glomerulosclerosis, and histologic parameters were graded by severity using the Banff schema. CAI grade was shown to correlate with the maximal fractional area index and with radionuclide GFR (Nankivell et al., 2002).

3 Aims of the study

I to measure quantitatively the RFR with PET in patients with ARVD (I).

II to measure the MPR of patients with a kidney transplant with the use of $[^{15}O]H_2O$ and to compare it with that of healthy control subjects (II).

III to evaluate the $[^{15}O]H_2O$ PET method for measuring the renal cortical perfusion and to compare renal cortical histopathology and perfusion of patients with a kidney transplant (III).

IV to examine if renal cortical perfusion 3 months after kidney transplantation predicts renal cortical histology 12 months after the transplantation (IV).

4 Patients, Materials, and Methods

4.1 Study subjects

Study subjects in *study I* were the same as in the study of Koivuviita et al. (Koivuviita et al., 2012). Patients in *studies II, III, and IV* were recruited from the nephrology outpatient clinic and dialysis unit of the Turku University Hospital during 2017─2019. All the study subjects gave written informed consent. The study was approved by the Ethics Committee of the Turku University Central Hospital and it was conducted in accordance with the Declaration of Helsinki as revised in 1996.

The study included a total of 67 subjects of whom 17 patients had ARVD (I), 32 had a kidney transplant (II, III and IV) and 18 were healthy control subjects. The 10 healthy controls were the same in studies II, III and IV. The characteristics of the patients and controls are summarized in **Table 3**.

Table 3. Characteristics of the study groups

Study	N	Group	Age (y)	Sex (F/M)
I	17 8	Patients with ARVD Healthy controls	66 (52–85) 60 (48–75)	10/7 3/5
II and III	19 10	Patients with Tx Healthy controls	52 (23–70) 56 (48–64)	10 /9 7/3
IV	13 10	Patients with Tx Healthy controls	54 (34–65) 56 (48–64)	7/6 7/3

Age is expressed as median (min-max). Sex is expressed as counts. Tx, kidney transplant; ARVD, atherosclerotic renovascular disease; N, number of subjects; F, female; M, male; y, year

Study I

Study I included 17 patients with ARVD (8 patients had unilateral RAS and 9 patients had bilateral RAS) and 8 healthy control subjects. ARVD was defined as a stenosis of more than 60% of the renal artery as determined by digital subtraction angiography. The indication for revascularisation in all patients was refractory or treatment-resistant hypertension. All patients were on antihypertensive medication. Healthy control subjects were normotensive, and none of them used any medication. The characteristics of the subjects are shown in **Table 4**.

Table 4. Baseline characteristics of the study subjects in study I

	ARVD (N=17)	Unilateral RAS (N=8)	Bilateral RAS (N=9)	Healthy (N=8)
RAS severity (22 kidneys)				
60-80%	15	4	11	0
>80%	7	3	4	0
eGFR (ml/min)	56 (23)	62 (24)	54 (21)	75 (6)
DM (all type II) (N/%)	9/53	2/25%	7/78%	0
Coronary heart disease (N/%)	6/35	1/13	5/56	0
Peripheral vascular disease (N/%)	4/24	1/13	3/33	0
Cerebrovascular disease (N/%)	5/29	1/13	4/44	0
Smoking (N/%)	4/24	1/13	3/33	0

eGFR is reported as mean (SD). ARVD, atherosclerotic renovascular disease; RAS, renal artery stenosis; eGFR, estimated glomerular filtration rate; N, number of subjects. Modified from Päivärinta et al., 2018 (I).

Studies II, III and IV

Because the aim was to study microvascular function, the exclusion criteria in studies II, III, and IV were AAC-score > 8/24 and clinical signs of atherosclerotic disease (CAD, cerebrovascular disease, peripheral artery disease). Patients with eGFR < 30ml/min were also excluded.

Control subjects were healthy and did not use any medication. The baseline characteristics of the study subjects in the studies II, III, and IV are presented in **Table 5**. eGFR (3 and 12 months after kidney transplantation) of patients in study IV is presented in the results section in **Table 15**. The same healthy controls were used in the studies II, III and IV, and the same patients in the studies II and III.

Studies II and III

The causes for CKD before kidney transplantation were as follows: 6 IgA nephropathy, 4 type I diabetic nephropathy, 1 lupus nephritis, 4 autosomal dominant polycystic kidney disease, 2 medullary cystic kidney disease, 1 focal segmental glomerulosclerosis, and 1 kidney disease without a specific diagnosis. 1 of the patients had received a kidney-pancreas transplantation. 5 patients were on hemodialysis and 14 patients on peritoneal dialysis before kidney transplantation.

All patients with a kidney transplant were on antihypertensive medication. Immunosuppressive medication was as follows: 4 patients used a combination of tacrolimus, mycophenolate, and corticosteroid for immunosuppression; 7 patients

used cyclosporine, mycophenolate, and corticosteroid; 4 patients used cyclosporine and mycophenolate; 4 patients used tacrolimus and mycophenolate.

Table 5. Baseline characteristics of the study subjects in the studies II, III and IV

	Patients with kidney transplant (N=19) (Study II,III)	Controls (N=10)	Patients with kidney transplant (N=13) (study IV)
BMI (kg/m^2)	28 (24–32)	25 (23–27)	24 (23–27)
Hypertension (N)	19	0	12
DM I/II	4/0	0	1/0*
Smoking (N)	0	0	0
Time on dialysis (months)	15 (12–27)	0	23 (18–33)
Age of kidney transplant (months)	33 (17–54)	0	12 (12–12)
eGFR (ml/min)	55 (47–69)	82 (79–87)	

Values are median (Q1-Q3). DM is expressed as counts. N, number of subjects; BMI, body mass index; eGFR, estimated glomerular filtration rate; ***,** posttransplantation DM II in 2 patients

Study IV

The causes for CKD before kidney transplantation in study IV were: 5 autosomal dominant polycystic kidney disease, 1 medullary cystic disease, 4 tubulointerstitial nephropathy of unknown origin, 1 tubulointerstitial nephropathy associated with Sjögren´s syndrome, 1 IgA nephropathy, 1 nephrosclerosis, and 1 type I diabetic nephropathy and IgA nephropathy.

All patients with a kidney transplant, except one, were on antihypertensive medication. The number of antihypertensive drugs increased by 1 in 3 patients and decreased by 1 in 2 patients between the study time points 3 and 12 months after kidney transplantation. 9 patients used a combination of tacrolimus, mycophenolate, and corticosteroid for immunosuppression and 4 patients used a combination of cyclosporine, mycophenolate, and corticosteroid.

4.2 General study design

The general outline of the PET imaging is presented in **Figure 7**. The PET studies were performed after a 10-h overnight fast. Alcohol and caffeine were prohibited for 1─3 days before assessment. Subjects with symptoms of acute infections within a week prior to or during the study were excluded from the analysis.

All patients were instructed to interrupt their antihypertensive medication on the study day and ACE inhibitor or ARB 3 days before the study day in study I. In studies

II, III, and IV, patients were instructed to take their medication as usual at the study day except ACE inhibitors and ARBs, which were discontinued 3 days before imaging.

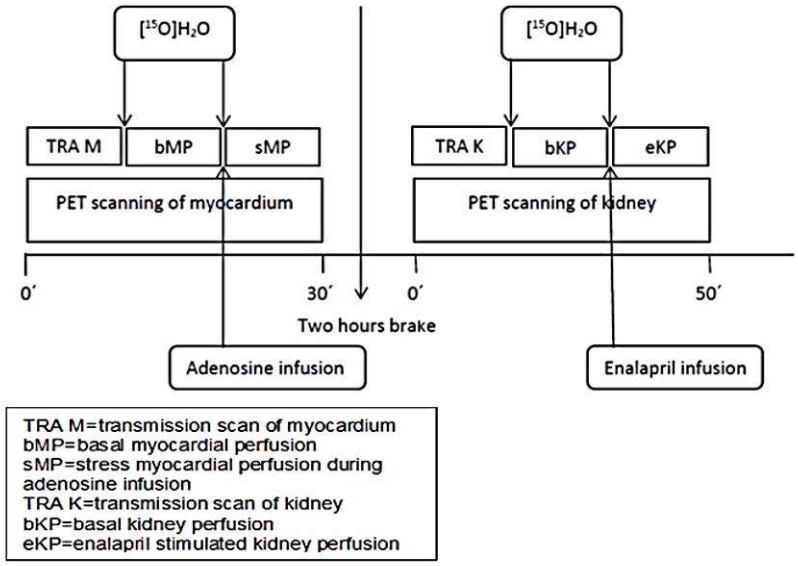

Figure 7. General study outline

Study I

An infusion of 1 mg of enalapril infusion was administered 5 min after the first PET-scan. The 2nd scan was taken at 20, 40, and 60 min after the enalapril infusion. Renal perfusion was maximal 40 min after the infusion and that value was chosen for analysis. The examinees were urged to remain immobile in the supine position between the scans. Blood pressure and heart rate were monitored throughout the study.

Studies II and III

Basal and stress MP were measured with PET, the subjects lying supine inside the scanner. Electrocardiogram, heart rate, and blood pressure were monitored continuously during the studies (study II). After MP imaging, renal perfusion was measured with PET (study III). Blood samples were taken on the day of the PET-study.

Study II: The AAC score was determined from a lateral lumbar radiography, which had been taken before the transplantation. Ejection fraction (EF) and LVMI were derived from echocardiography which had also been performed before the transplantation while the patients were in predialysis follow-up or having dialysis treatment.

Study III: Ambulatory 24 h blood pressure monitoring was assessed within 1 month after PET imaging during normal medication. RI was measured by Doppler sonography as a part of clinical routine follow up 1 to 6 months before or after PET. Histopathology of the kidney transplants was obtained from a kidney biopsy 1 year after transplantation.

Study IV

Renal transplant perfusion of patients with kidney transplant was measured with PET at 3 and 12 months after transplantation. Laboratory samples were taken at both time points. Ambulatory 24 h blood pressure monitoring, measurement of Doppler based RI of the kidney transplant and kidney biopsy were performed at 1 year after transplantation.

4.3 Methods

4.3.1 Production of $[^{15}O]H_2O$

For production of ^{15}O (T1/2─123 s), a low-energy deuteron accelator Cyclone 3 was used (Ion Beam Application Inc. Louvain-la-Neuve, Belgium). $[^{15}O]H_2O$ was produced using a dialysis technique in a continuously working water module (Radiowater Generator, Hidex Oy, Finland).

PET image data acquisition

In *study I*, PET imaging was carried out using a GE Advance PET scanner (General Electric Medical Systems, Milwaukee, WI, USA) with 35 slices of 4.25 mm thickness. Correct positioning of the subject was ascertained on a rectilinear transmission scan followed by a five-minute transmission scan using two rotating rod sources containing 68Ge/68Ga. Renal perfusion was measured with an intravenous bolus of $[^{15}O]H_2O$ (900–1400 MBq); dynamic emission scanning was started simultaneously with data acquisition for a 6-min (frames: 15x4, 4x10, 4x20 and 3x60 s).

In *studies II, III and IV,* PET scanning was carried out using PET/CT scanner (Discovery 690, GE Medical Systems, Waukesha, Wisconsin, USA). A low dose

helical CT scan with automatic dose modulation (120 kVp, 10–80 mAs, noise index 30, pitch of 1.375, rotation time of 0.5 s) was acquired while the patient breathed normally before the PET scan to correct for photon scatter and attenuation.

In the cardiac study (*study II*), an average dose of 470 MBq of $[^{15}O]H_2O$ was infused, and simultaneously dynamic PET data acquisition for 4 min 40 sec (frames: 14x5, 3x10, 3x20, and 4x 30 s) was started. Adenosine administration was started 2 min before the stress scan for maximal coronary vasodilation at a dose of 140 µg/kg/min.

In the renal studies (*studies III and IV*), an average dose of 700 MBq of $[^{15}O]H_2O$ was given, and PET scanning with 47 slices was conducted. The frames used were the same as in study I.

PET image reconstruction

The PET images were reconstructed and all quantitative corrections were applied to the reconstructed images, including attenuation, scatter, decay, and random corrections. In *study I*, images with a matrix size of 128 x 128 were produced using the MRP OSEM reconstruction algorithm. In *study II*, PET data were reconstructed using 3D ordered subset expectation maximization (vendor name: VUE Point HD) with point spread function modelling (vendor name: SharpIR) with a 128 x 128 matrix in size. In *studies III and IV*, PET images were reconstructed using OSEM (VUE Point FX) with matrix size 256 x 256.

Calculation of myocardial perfusion

For the myocardium PET study (study II), Carimas software was used to analyse MP (Nesterov et al., 2009). Parametric MP images were generated with a single-tissue compartment model corrected for a perfusable tissue fraction (Iida et al., 1988). An LV cavity region of interest (ROI) was drawn and used as input function for determination of the LV time-activity curve (Iida et al., 1992).

MPR was calculated as the ratio of stress to rest MP. Because basal MP is related to RPP, basal MP values were corrected for RPP by the equation: corrected basal MP (basal MP_{corr}) = basal MP/individual RPP x average RPP of the healthy controls (Czernin et al., 1993). The average RPP of the healthy controls was used to make comparisons of perfusion values between the patients and the controls easier. Corrected MPR (MPR_{corr}) was defined as the ratio of hyperemic MP divided by basal MP_{corr}.

Coronary vascular resistance (CVR) was calculated as mean arterial pressure (MAP) divided by global MP. MAP after adenosine administration was calculated

as mean of the 3- and 6-min MAP. Stress MP > 2.3 ml·g$^{(-1)}$·min$^{(-1)}$, and MPR > 2.5 were considered normal based on previous validation (Danad et al., 2014).

Calculation of renal cortical perfusion

In studies I, III, and IV, ROIs were drawn for the whole cortical region of the kidney on a summed reconstructed image on an average of six coronal planes using Carimas software. In study I, ROIs of the basal kidney images were copied to the images obtained after enalapril administration.

For calculation of renal cortical perfusion from the PET study in the healthy and in the patients with ARVD, the input function was estimated using the average time-activity curve (TAC) from ROIs drawn over the cavity of the descending aorta (Juillard et al., 2002) on average in six planes. In patients with a kidney transplant, the TAC was taken from the external iliac artery, because the aorta was not included undivided in the scanning field of the kidney transplant.

Renal cortical perfusion was estimated using a single-tissue compartmental model with 4 parameters including k1, k2, Va, and delay, where k1 and k2 are the unidirectional transport rates of [^{15}O]H_2O into and from tissue, Va is the vascular volume fraction, and the delay parameter accounts for the difference of radioactivity appearance times between the blood and tissue curves (Kudomi et al., 2009). Renal cortical perfusion was represented by the clearance rate (k2) multiplied by the physiological partition coefficient (p_{phys}) 0.94ml/g.

Renal vascular resistance (RVR) was calculated according to formula: MAP/renal cortical perfusion. RFR was calculated according to formula: [(enalapril stimulated renal cortical flow - basal renal cortical flow)/basal renal cortical flow]x100%.

4.3.2 Ultrasound studies

Echocardiography

For echocardiography an Acuson SC 2000, Acuson TM 512, Acuson Sequoia C 512 (Siemens, USA) or Vivid E9 (GE, USA) was used. Calculation of LVMI was based on the Devereux equation (Devereux & Reichek, 1977), and normal values of LVMI on the American Society of Echocardiography convention (Lang et al., 2015). According to the American Society of Echocardiography convention, the reference range of LVMI for males is 49–115 g/m^2 and for females 43–95 g/m^2.

Doppler sonography of renal artery and resistance index

Doppler sonography of kidney transplants was assessed by the Acuson S2000 (Siemens, USA) or Logiq E9 (GE, USA) device. Doppler RI was calculated according to formula: (peak systolic velocity - end diastolic velocity)/peak systolic velocity (Tublin et al., 2003).

4.3.3 Kidney biopsy

Kidney transplant biopsy was taken under sonographic guidance (UST-9123 Ultrasound Transducer, Hitachi-Aloka, USA) with the core biopsy instrument Bard Magnum MG 1522 (Becton, Dickinson and Company, USA). UltraCore™ Biopsy Needles 16 G were used (Argon, USA).

The paraffin block was stained with hematoxylin-eosin, periodic acid-Schiff, trichrome-elastic, and methenamine silver. C4d and simian virus (SV) 40 were assessed. The kidney transplant biopsy was evaluated by an experienced nephropathologist following the Banff classification in studies III (Racusen et al., 1999; Loupy et al., 2017; Haas et al., 2018) and IV (Roufosse et al., 2018).

In *study III*, a modified Banff´s fibrosis score (Becker et al., 2015) was calculated as the sum of gs+ci+ct from the biopsy report. Gs corresponded to the degree of glomerulosclerosis (0, no gs; 1, up to 25% gs; 2, 26–50% gs; 3, > 50% gs) and ci and ct corresponded to interstitial fibrosis and tubular atrophy as classified in Banff (Loupy et al., 2017; Haas et al., 2018). Fibrous intimal thickening (cv) was not added to the sum due to lack of cv. Thus, the maximum score was 9. Due to minor sclerotic changes in kidney biopsies, scores 0–1 were combined to the group of no fibrosis and scores 2–4 to the group of mild fibrosis.

The inflammation score was the sum of g+i+t+ti from the biopsy report according to Banff classification (Loupy et al., 2017; Haas et al., 2018) in study III. G corresponded to glomerulitis, i and t to inflammation and tubulitis in unscarred renal cortical parenchyma, and ti to total inflamed cortical parenchyma including scarred sections. Ptc and intimal arteritis (v) were not added to the sum due to lack of ptc and v. Thus, the maximum score was 12. Because of minor inflammatory changes in biopsies, inflammation was graded as no inflammation or mild inflammation (0–1 = no inflammation, 2–6 = mild inflammation).

In *study IV*, a modified Banff´s fibrosis score (Becker et al., 2015) was calculated as the sum of gs+ci+ct+cv from the biopsy report. The classification of the parameters of kidney biopsy was based on the Banff classification (Roufosse et al., 2018). Maximum fibrosis score was 12. Due to minor sclerotic changes in kidney biopsies, scores 0–2 were combined to the group of no fibrosis and scores 3–8 to the group of mild to moderate fibrosis.

For evaluation of inflammatory changes in study IV, we assessed an inflammation score, which was calculated as the sum i+t+ti+g+i-IFTA from the biopsy report according to Banff classification (Roufosse et al., 2018). The abbreviated form i-IFTA corresponded to inflammation in the areas of IFTA. Due to lack of ptc and v, these parameters were not added to the sum. Hence, the maximum inflammation score was 15. Because of minor inflammatory changes in biopsies, inflammation scores 0–2 were combined to the group of no inflammation and scores 3–7 to the group of mild inflammation.

4.3.4 Other studies

Ambulatory 24 h blood pressure (O'Brien et al., 2013) was measured with a Schiller-BR-102 PLUS device (Medifin, Finland). The AAC-score was calculated from a lateral lumbar radiography (Kauppila et al., 1997).

4.3.5 Biochemical analyses

Plasma creatinine (P-crea) was measured enzymatically /Roche/cobas 8000 c 702. Quantification of renal function was based on the eGFR equation from the Chronic Kidney Disease Epidemiology Collaboration (CKD-EPI) study (Levey et al., 2009). Serum human leucocyte antigen donor specific antibodies and serum panel reactive antibodies were analysed by Luminex (Luminex Corp, USA) and HLA FusionTM (One Lambda, USA). Blood hemoglobin (B-Hb) was analysed by Sysmex XN, plasma fasting glucose (f-P-Gluc) enzymatically (Hexokinase)/Roche/cobas 8000 c 702, plasma fasting cholesterol (f-P-Chol) enzymatically (CHOD-PAP)/Roche/cobas 8000 c 702, plasma fasting high density lipoprotein (HDL) and LDL cholesterol enzymatically (Direct)/Roche/cobas 8000 c 702, plasma fasting triglycerides enzymatically (GPO-PAP)/Roche/cobas 8000 c 702, urine sodium (U-Na) by indirect ISE/cobas 8000 ISE, plasma troponin T (P-TnT) with ECLIA/Roche/cobas 8000 c 602, plasma N-terminal pro B-type natriuretic peptide (P-Pro-BNP) with ECLIA/Roche/cobas 8000c 801, and urine protein (U-Prot) with benzethonium chloride/Roche/cobas 8000 c 702.

4.3.6 Statistical analyses

All statistical analyses were performed with the SAS System version 9.4 for Windows (SAS Institute Inc., Cary, NC, USA). The significance level was set at $p = 0.05$ (two-tailed), and 95% confidence intervals were calculated.

Study I

Results were expressed as mean values and the range of the standard deviation. Pearson's correlation coefficients were calculated for determination of associations between numerical variables. The normality of the values of the variables was assessed by Shapiro-Wilk's test. Student's paired t-test was used to compare normally distributed variables. The Kruskall-Wallis test was used if variables were non-normally distributed.

Study II

Results were expressed as mean values and the range of the standard deviation. Comparisons between healthy controls and patients with a kidney transplant for continuous parameters were performed with the Kruskal-Wallis test.

Study III

Results were presented as median values with interquartile range. Comparisons between healthy control subjects and patients with a kidney transplant were performed for categorical variables with Fisher's exact test (gender) and for variables following a normal distribution with one-way analysis of variance and for continuous variables that were non-normally distributed with Wilcoxon's rank sum test. Pearson's correlation coefficients were calculated for determination of associations between numerical variables.

Study IV

Continuous variables were summarised and expressed as their median and interquartile range. Categorical variables were presented as counts. Continuous variables were compared between patients with a kidney transplant and healthy controls with one-way analysis of variance or Wilcoxon's rank sum test for non-normal distributions. Changes between two time points within one group were studied with the paired t-test or Wilcoxon's signed rank test.

Association between categorical variables were examined with Fisher's exact test. Associations between two continuous variables were evaluated with Pearson's correlation coefficient.

5 Results

5.1 Renal blood flow reserve in healthy persons and patients with atherosclerotic renovascular disease measured with [^{15}O]H_2O positron emission tomography (I)

5.1.1 Renal flow and flow reserve in study subjects

RFR of the healthy subjects was 22 (32)%. RFR of the stenosed kidneys of patients with unilateral RAS was 15 (22)% and that of contralateral kidneys 21 (26)%. RFR of patients with bilateral RAS was 27 (43)%. In all stenosed kidneys of non-diabetics, RFR was 14 (19)%, and in all stenosed kidneys of diabetics, RFR was 24 (41)%. There was no statistically significant difference in RFR values between any subgroup of patients with ARVD or between the healthy controls and patients with ARVD. Nor did diabetes affect statistically significantly the RFR value. Absolute renal cortical flow values are presented in **Table 6**.

Table 6. RFR and renal cortical flow values in healthy controls and patients with ARVD

	N	Basal flow (ml·g$^{(-1)}$·min$^{(-1)}$)	Stress flow (ml·g$^{(-1)}$·min$^{(-1)}$)	RFR (%)
Healthy controls	8	1.8 (0.3)	2.2 (0.6)	22 (32)
RAS unilateral, contralateral kidneys	7	1.8 (0.7)	2.1 (0.6)	21 (27)
RAS unilateral, stenosed kidneys	7	1.5 (0.7)	1.7 (0.7)	15 (22)
RAS bilateral	9	1.4 (0.3)	1.7 (0.4)	27 (43)
Diabetics, stenosed kidneys	13	1.3 (0.4)	1.6 (0.5)	24 (41)
Non-diabetics, stenosed kidneys	9	1.6 (0.5)	1.8 (0.5)	14 (20)

Values are expressed as mean (SD). N, number of patients per subgroups of healthy and bilateral RAS, number of kidneys in other groups; RFR, renal flow reserve, calculated as [(renal cortical stress flow - renal cortical basal flow)/renal cortical basal flow]x100%; RAS, renal artery stenosis. Modified from Päivärinta et al., 2018 (I).

There was a statistically significant negative correlation between both renal cortical basal flow and renal cortical stress flow and RAS grade in the stenosed kidneys of patients with unilateral RAS (r = -0.8, p = 0.04; r = -0.8, p = 0.02, respectively)(**Figure 8**). In patients with bilateral RAS, the degree of stenosis did not correlate with renal cortical basal flow nor renal cortical stress flow (p=NS), **Figure 9**.

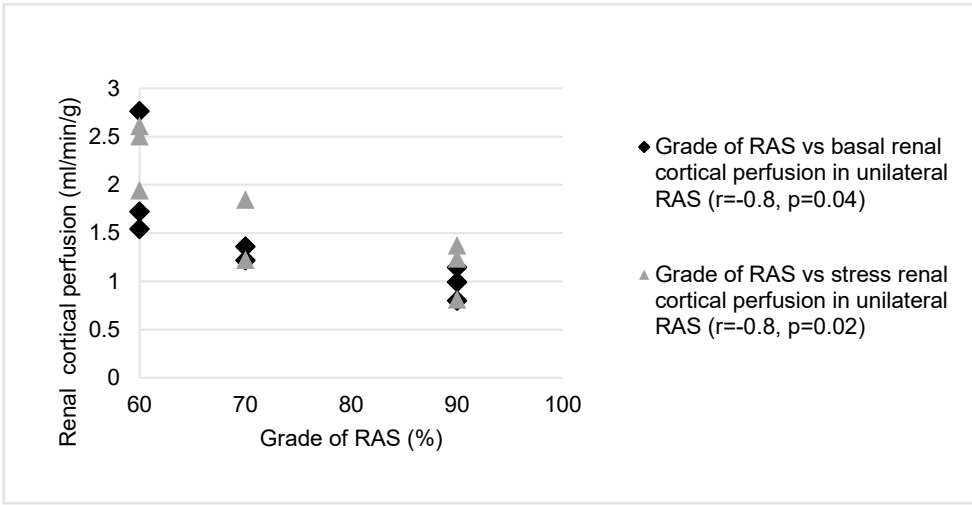

Figure 8. Grade of RAS versus renal cortical perfusion in patients with unilateral RAS. Modified from Päivärinta et al., 2018 (I).

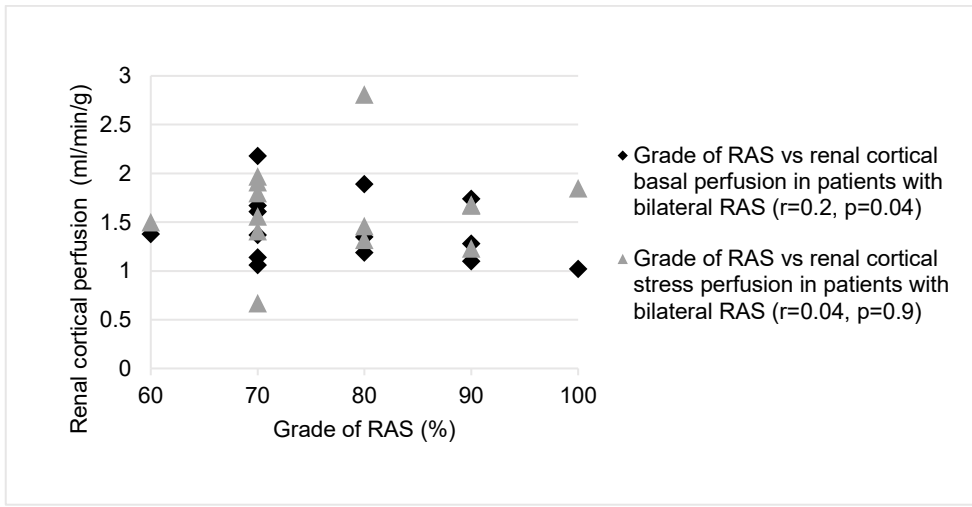

Figure 9. Grade of RAS versus renal cortical perfusion in patients with bilateral RAS. Modified from Päivärinta et al., 2018 (I).

In all stenosed renal arteries of non-diabetics, the stenosis grade correlated statistically significantly with renal cortical basal and stress flow ($r = -0.7$, $p = 0.03$; $r = -0.8$, $p = 0.007$). In all stenosed renal arteries of diabetics, the stenosis grade did not correlate with renal cortical basal flow nor renal cortical stress flow (p= NS in both).

5.1.2 Effect of enalapril on hemodynamics

In patients with bilateral RAS, enalapril caused a statistically significant reduction in MAP (MAP before and after enalapril 131 (15) mmHg and 120 (14) mmHg, respectively, $p = 0.04$). In patients with unilateral RAS, MAP was 115 (11) mmHg before enalapril and 117 (10) mmHg after enalapril ($p = 0.8$). In healthy controls, MAP was 96 (6) mmHg before and 97 (7) mmHg after enalapril ($p = 0.21$).

5.2 Myocardial perfusion reserve of kidney transplant patients is well preserved (II)

5.2.1 Myocardial perfusion in study subjects

Basal MP and RPP were statistically significantly higher in patients with a kidney transplant than in healthy controls ($p = 0.0044$ and $p = 0.0015$, respectively). The difference of basal MP between the groups disappeared after correction of basal MP for RPP (p= 0.31). There was no statistically significant difference in stress MP between the groups ($p = 0.53$). MPR in patients with a kidney transplant was lower than in controls, and the difference was statistically significant ($p = 0.0029$). After correction for RPP, the difference in MPR between the groups disappeared ($p = 0.8$). There were no regional differences in MP in any subjects. The myocardial perfusion values are presented in the **Table 7**.

There was no statistically significant correlation between transplant or dialysis vintage or B-Hb and basal or stress MP or MPR (p = NS in all comparisons). Basal MP correlated with eGFR when all 29 subjects of both groups were combined ($r = -0.43$, $p = 0.019$). However, the correlation disappeared after correction for RPP ($r = -0.08$, $p = 0.69$).

Table 7. Myocardial perfusion results

	Patients with Tx N = 19	**Controls N = 10**
Basal MP (ml·g$^{(-1)}$·min$^{(-1)}$)	1.3 (0.4)*	1.0 (0.2)
RPP	10053 (2878)*	6723 (1112)
Basal MP$_{corr}$ (ml·g$^{(-1)}$·min$^{(-1)}$)	0.9 (0.2)	1.0 (0.3)
Stress MP (ml·g$^{(-1)}$·min$^{(-1)}$)	3.8 (1.0)	4.0 (0.9)
MPR	3.0 (0.9)*	4.2 (1.0)
MPR$_{corr}$	4.3 (1.6)	4.1 (1.1)
CVRbasal (mmHg·ml$^{(-1)}$·g$^{(-1)}$· min$^{(-1)}$)	83 (19)	93 (21)
CVRstress (mmHg·ml$^{(-1)}$·g$^{(-1)}$·min$^{(-1)}$)	27 (9)	22 (8)

Values are mean (SD). Tx, kidney transplant; RPP, rate pressure product; basal MP$_{corr}$, corrected basal MP, MP/(individual RPP)x(RPP average of the healthy); MPR, myocardial perfusion reserve; MPR$_{corr}$, corrected myocardial perfusion reserve, stress MP/basal MP$_{corr}$; CVR, coronary vascular resistance. *p < 0.05 controls versus patients with a kidney transplant. Modified from Päivärinta et al., 2020 (II).

5.2.2 Hemodynamic measurements during imaging of myocardial perfusion

Systolic and diastolic blood pressure, MAP, and heart rate at rest were higher in the patients with a kidney transplant than in healthy controls ($p = 0.0023$, $p = 0.023$, $p = 0.0044$, and $p = 0.0083$, respectively). Systolic blood pressure and MAP at stress were higher in patients with a kidney transplant than in controls ($p = 0.03$ and $p = 0.04$, respectively). Hemodynamic measurements during PET imaging are presented in **Table 8**.

5.2.3 Other results

AAC was used to estimate the individual risk of atherosclerosis before transplantation in 17/19 patients. The AAC-score was 0 in 13 patients, 3 in one, 5 in one, 6 in one, and 8 in one patient. Two of the patients did not have their AAC score measured at all. Echocardiography was performed for 18/19 patients and there was an increased LVMI in 8/18 patients [mean LVMI 92 (26)]. All patients had a normal EF [mean EF 66 (5)%]. The time between PET imaging and AAC scoring and echocardiography varied from 1 to 7 years.

Table 8. Hemodynamic measurements during cardiac PET imaging

		Patients with Tx (N = 19)	Controls (N = 10)
Rest	BP systolic (mmHg)	151 (21)*	123 (16)
	BP diastolic (mmHg)	82 (16)*	70 (9)
	MAP (mmHg)	106 (16)*	88 (11)
	HR (beats/min)	66 (12)*	55 (4)
Stress	BP systolic (mmHg)	138 (17)*	120 (18)
	BP diastolic (mmHg)	71 (8)	65 (9)
	MAP (mmHg)	93 (9)*	84 (11)
	HR (beats/min)	89 (13)	86 (14)

Values are mean (SD). Tx, kidney transplant; BP, blood pressure; MAP, mean arterial pressure; HR, heart rate. *p < 0.05 controls versus patients with a kidney transplant. Modified from Päivärinta et al., 2020 (II).

5.3 Renal vascular resistance is increased in patients with a kidney transplant (III)

5.3.1 Renal cortical perfusion in study subjects

There was no statistically significant difference in renal cortical perfusion values between the healthy controls and patients with a kidney transplant (p = 0.099). RVR was higher in patients with a kidney transplant than in healthy controls (p = 0.01). Renal cortical perfusion values are presented in **Table 9**.

There was a correlation between renal cortical perfusion and eGFR in the healthy subjects (r = 0.78, p = 0.0072) but not in patients with a kidney transplant (r = 0.26, p = 0.28).

There was a statistically significant negative correlation between renal cortical perfusion and 24 h ambulatory systolic blood pressure and between renal cortical perfusion and 24 h ambulatory pulse pressure in patients with a kidney transplant (r = -0.56, p = 0.016; r = -0.56, p = 0.016, respectively).

The Doppler RI of patients with a kidney transplant correlated with renal cortical perfusion, RVR, age, pulse pressure on the PET-study day, and 24 hour ambulatory systolic blood pressure (r = -0.51, p = 0.026; r = 0.59, p = 0.008; r = 0.46, p = 0.049; r = 0.66, p = 0.0023; r = 0.58, p = 0.012, respectively). There was no correlation between Doppler RI and eGFR (r = -0.005, p = 0.98).

Hemodynamic parameters are shown in **Table 10**. Patients with a kidney transplant had a higher median systolic blood pressure and MAP than healthy control subjects (p = 0.0004; p = 0.0019, respectively).

Table 9. Renal cortical perfusion values in study subjects

	Patients with a kidney transplant N = 19	Controls N = 10
Renal perfusion (ml·g$^{(-1)}$·min$^{(-1)}$)	2.2 (2.0–3.0)	2.7 (2.4–4.0)
RVR (mmHg·ml$^{(-1)}$·g$^{(-1)}$·min$^{(-1)}$)	47.0 (36.7–51.4)*	32.4 (24.6–39.6)

Values are median (Q1-Q3). *P < 0.05 controls versus patients with a kidney transplant. N, number of patients; RVR, renal vascular resistance. Modified from Päivärinta et al., 2019 (III).

Table 10. Hemodynamic parameters

Blood pressure on the study day (mmHg)	Patients with a kidney Tx N = 19	Controls N = 10
Diastolic	70 (76–85)	75 (70–79)
Systolic	153 (137–160)*	126 (123–133)
MAP	105 (99–107)*	93 (88–96)
Heart rate (beats/min)	63 (50–76)	56 (50–60)
24 h ambulatory blood pressure (mmHg)		
Diastolic	81 (75–86)	
Systolic	144 (136–148)	
MAP	102 (96–108)	
Heart rate (beats/min)	68 (56–72)	

Values are median (Q1-Q3). MAP, mean arterial pressure; Tx, transplant. *p < 0.05 controls versus patients with a kidney transplant. Modified from Päivärinta et al., 2019 (III).

5.3.2 Renal cortical perfusion and histology in patients with a kidney transplant

A biopsy of the renal transplant was available in 17/19 patients. Sclerosed glomeruli were seen in 5 biopsies. The highest proportion of sclerosed glomeruli was 30%. None of the biopsies included arterial hyalinosis, arterial intimal thickening, intimal arteritis, ptc or double contour of glomerular basement membrane. SV40, CMV, and C4d were all negative. More histological data is shown in **Table 11**.

There were 10 kidney biopsies with no fibrosis and 7 biopsies with mild fibrosis. There was no correlation between cortical fibrosis and perfusion of kidney transplants (p = 0.56). However, Doppler RI of kidney transplants was higher in the group of mild fibrosis than in the group of no fibrosis (p = 0.03). A comparison of renal cortical perfusion, 24 h ambulatory MAP, transplant age, renal Doppler RI, and eGFR between the groups of no fibrosis and mild fibrosis is presented in **Table 12**.

There were 9 biopsies with no inflammation and 8 biopsies with mild inflammation. Kidney transplants with mild inflammatory changes were older than

those with no inflammatory changes (57 and 22 months, respectively, p = 0.003). No statistically significant difference was found in eGFR, renal perfusion, RVR, 24 h MAP, or Doppler RI between the groups (p > 0.05 in all).

Table 11. Histological findings of kidney transplant biopsies according to the Banff classification

Banff score	g	i	t	ti	ci	ct
0	13	9	15	8	12	12
1	1	6	1	7	5	5
2	1	1	1	1	0	0
3	2	1	0	1	0	0

Numbers in the table are kidneys. g, glomerulitis; i, interstitial inflammation in the non-scarred areas of renal cortex; t, tubulitis in the non-scarred areas of renal cortex; ti, total inflammation; ci, interstitial fibrosis; ct, tubular atrophy

Table 12. Renal cortical fibrosis and perfusion parameters

	eGFR (ml/min)	Renal perfusion ($ml \cdot g^{(-1)} \cdot min^{(-1)}$)	Renal vascular resistance ($mmHg \cdot ml^{(-1)} \cdot g^{(-1)} \cdot min^{(-1)}$)	RI	24 hour MAP (mmHg)	Tx age (months)
No fibrosis (N = 10)	55 (43–69)	2.3 (2.0–3.0)	40.9 (36.7–51.4)	0.66 (0.61–0.72)	98 (94–102)	44 (22–63)
Mild fibrosis (N = 7)	54 (47–71)	2.1 (1.8–2.4)	49.8 (44.2–58.4)	0.73 (0.70–0.76)*	106 (99–110)	27 (17–48)

Values are median (Q1–Q3). RI, renal artery resistance index measured by Doppler sonography; MAP, mean arterial pressure; Tx, kidney transplant. *p < 0.05, kidney transplants with mild fibrosis vs no fibrosis. Modified from Päivärinta et al., 2019 (III).

5.4 Renal vascular resistance decreases during the first year after kidney transplantation: a follow up study with [^{15}O]H_2O PET (IV)

5.4.1 Renal cortical perfusion values in study subjects

Renal cortical perfusion values of the study subjects are presented in **Table 13**.

Table 13. Renal cortical perfusion values of the study subjects

	Patients with a kidney transplant (N = 13)	**Controls (N = 10)**
Renal perfusion (ml·g$^{(-1)}$·min$^{(-1)}$)		
PET I	1.8 (1.6–2.0)*	2.7 (2.4–4.0)
PET II	2.2 (2.0–2.5)*	
RVR (mmHg·ml$^{(-1)}$·g$^{(-1)}$·min$^{(-1)}$)		
PET I	59.8 (46.5–64.6)*	32.4 (26.3–38.3)
PET II	44.7 (39.8–49.4)*	

Values are median (Q1–Q3). RVR, renal vascular resistance. *p < 0.05 patients with a kidney transplant vs controls. Modified from Päivärinta et al.(IV).

There was a statistically significant difference in renal cortical perfusion and RVR between the healthy controls and the patients with a kidney transplant both at 3 and at 12 months after transplantation ($p = 0.0002$, $p = 0.003$, $p = 0.0002$ and $p = 0.0004$ respectively).

The renal cortical perfusion in patients with a kidney transplant increased from 3 to 12 months after transplantation, but not statistically significantly so ($p = 0.054$). The decrease of RVR of patients with a kidney transplant between 3 and 12 months after transplantation was statistically significant ($p = 0.04$), **Figure 10**.

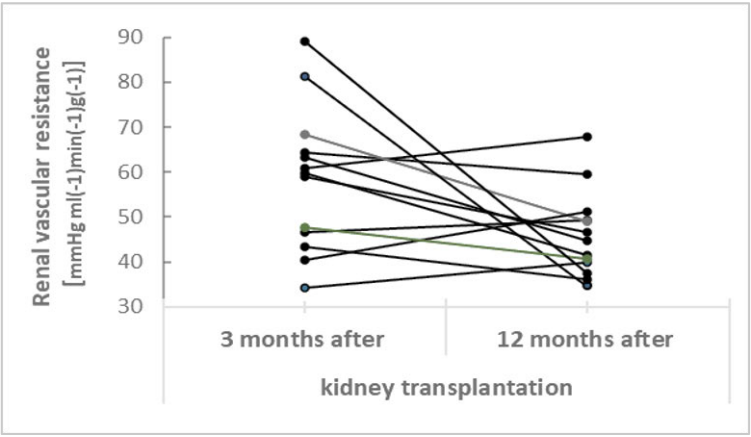

Figure 10. RVR of kidney transplant recipients at 3 and 12 monhts after transplantation. Modified from Päivärinta et al. (IV).

5.4.2 Hemodynamics

Hemodynamic data of the study subjects are presented in **Table 14**.

There was a statistically significant difference in systolic blood pressure, MAP, and heart rate between the healthy controls and patients with a kidney transplant both at 3 months ($p = 0.02$, $p = 0.02$, and $p = 0.03$, respectively) and 12 months after kidney transplantation ($p = 0.02$, $p = 0.03$, and $p = 0.004$, respectively). Blood pressures did not differ between 3 and 12 months after transplantation in patients with a kidney transplant ($p > 0.05$ in all).

5.4.3 Renal cortical perfusion and laboratory parameters

There was a statistically significant difference in P-Crea and eGFR between the healthy controls and patients with a kidney transplant both at 3 months ($p < 0.0001$ and $p < 0.0001$, respectively) and at 12 months after kidney transplantation ($p = 0.001$, $p = 0.009$, respectively) (**Table 15**). There was also a statistically significant difference among patients with a kidney transplant in terms of eGFR and P-Crea at 3 months compared to 12 months ($p = 0.0008$, $p = 0.0006$, respectively) (**Table 15**).

There was a statistically significant correlation between renal cortical perfusion and eGFR at 12 months after transplantation ($r = 0.57$, $p = 0.04$) but not between renal cortical perfusion and P-Crea ($p = 0.26$). Renal cortical perfusion at 3 months did not correlate with eGFR at 12 months after transplantation ($p = 0.36$). There was a statistically significant correlation between eGFR at 3 months and renal cortical perfusion and eGFR at 12 months after transplantation ($r = 0.65$, $p = 0.017$; $r = 0.94$, $p < 0.0001$).

Table 14. Hemodynamics of study subjects

	Patients with a kidney transplant (N = 13)	Controls (N = 10)
Hemodynamics on the day of PET I		
Blood pressure (mmHg)		
Systolic	140 (126–158)*	126 (123–133)
Diastolic	81 (77–85)	75 (70–79)
MAP	100 (95–109)*	93 (88–96)
Heart rate (beats/min)	67 (62–71)*	56 (50–60)
Hemodynamics on the day of PET II		
Blood pressure (mmHg)		
Systolic	139 (131–145)*	
Diastolic	78 (75–84)	
MAP	98 (93–107)*	
Heart rate (beats/min)	69 (60–73)*	

Values are expressed as median (Q1─Q3). MAP, mean arterial pressure. *p < 0.05 patients with a kidney transplant versus controls. Modified from Päivärinta et al. (IV).

Table 15. Renal function in patients and in healthy controls

	Patients with Tx 3 months	Patients with Tx 12 months	Healthy controls
eGFR (ml/min)	43 (33–53)*	55 (43–61)*†	82 (79–87)
P-Crea (µmol/l)	143 (119–161)*	114 (96–123)*†	73 (72–86)

Values are expressed as median (Q1–Q3). eGFR, estimated glomerular filtration rate; Crea, creatinine; Tx, kidney transplant. *p < 0.05 compared to the healthy controls; †p < 0.05 compared to values at 3 months. Modified from Päivärinta et al. (IV).

5.4.4 Renal cortical perfusion and histology in patients with a kidney transplant

Global sclerosis of glomeruli was seen in 8 biopsies. The highest proportion of globally sclerosed glomeruli out of all glomeruli was 43% in 1 biopsy. In 7 other biopsies with sclerosed glomeruli the average proportion of globally sclerosed glomeruli was 14%. There was neither C4d nor SV40 positivity in kidney biopsies.

Transplant glomerulopathy (cg) was present in 1 biopsy and arterial hyalinosis in 1 biopsy. There was no intimal arteritis or ptc in biopsies.

More precise information of kidney biopsies is presented in **Table 16**.

Table 16. Histological findings of kidney transplant biopsies according to the Banff classification (Roufosse et al., 2018).

Banff score	i	ti	t	i-IFTA	g	ct	ci	cv
0	11	9	11	7	8	2	6	4
1	1	2	2	3	2	10	5	2
2	1	1	0	1	2	0	1	3
3	0	1	0	2	1	1	1	0

Numbers in the table are kidneys. Under heading cv 4 biopsies are missing due to lack of large arteries. i, interstitial inflammation in non-scarred renal cortical areas; t, tubulitis in non-scarred renal cortical areas; i-IFTA, inflammation in the areas of Interstitial Fibrosis and Tubular Atrophy; ti, total inflammation; g, glomerulitis; ct, tubular atrophy; ci, interstitial fibrosis; cv, vascular fibrous intimal thickening. Modified from Päivärinta et al. (IV).

Renal cortical perfusion and histological findings in the kidney biopsies of patients with a kidney transplant

There was no statistically significant difference in renal cortical perfusion at 3 and 12 months between the patients with no fibrosis and with mild to moderate fibrosis in kidney allograft biopsies ($p = 0.08$ and $p = 0.29$, respectively), **Table 17**.

There was a statistically significant difference in P-Crea between the groups of no fibrosis and mild to moderate fibrosis at 12 months but not at 3 months after transplantation ($p = 0.025$, $p = 0.15$, respectively), **Table 17**. eGFR did not differ significantly between the groups with no fibrosis and with mild to moderate fibrosis in kidney transplant biopsy 3 and 12 months after transplantation ($p = 0.4$ and $p = 0.2$, respectively), **Table 17**.

Table 17. Renal fibrosis, perfusion and eGFR in patients with a kidney transplant.

	Fibrosis score 0–2	Fibrosis score 3–8
N	3	10
Renal perfusion at 3 months (ml $g^{(-1)}$ $min^{(-1)}$)	2.3 (1.8–2.9)	1.8 (1.5–2.1)
Renal perfusion at 12 months (ml $g^{(-1)}$ $min^{(-1)}$)	2.5 (2.0–3.0)	2.2 (2.0–2.5)
eGFR at 3 months (ml/min)	58 (29–86)	46 (30–61)
eGFR at 12 months (ml/min)	76 (45–107)	55 (37–72)
P-Crea at 3 months (µmol/l)	111 (65–156)	147 (122–172)
P-Crea at 12 months (µmol/l)	81 (47–115)	126 (108–145)*

Values means (95% CI). N, number of biopsies; P-Crea, plasma creatinine.*$p < 0.05$ compared to group with fibrosis score 0–2. Modified from Päivärinta et al. (IV).

6 Discussion

6.1 Renal flow reserve in patients with atherosclerotic renovascular disease and renal perfusion in patients with a kidney transplant (I, III and IV)

6.1.1 Methodological considerations of renal PET imaging and renal cortical perfusion

The PET-technique provides a method for measuring non-invasively, quantitatively, and regionally one-kidney perfusion without the need for contrast agent. Inaba et al. were the first to quantify renal perfusion in humans by means of PET using $[^{15}O]H_2O$ (Inaba et al., 1989). Renal cortical perfusion with $[^{15}O]H_2O$ PET correlates with eGFR (Rebelos et al., 2019) and the method has been validated in an experimental porcine study where the microsphere method was used for reference (Juillard et al., 2000).

The values for renal cortical perfusion as measured with $[^{15}O]H_2O$ PET have been highly variable in healthy subjects and have ranged from 1.6 $ml \cdot g^{(-1)} \cdot min^{(-1)}$ to 4.7 $ml \cdot g^{(-1)} \cdot min^{(-1)}$ (Nitzsche et al., 1993; Middlekauff et al., 2001; Alpert et al., 2002; Kudomi et al., 2009; Damkjær et al., 2010; Damkjær et al., 2012; Koivuviita et al., 2012; Rebelos et al., 2019; Assersen et al., 2019). Methodological differences partly explain this high variability. Renal cortical perfusion can be derived from k1 ($[^{15}O]H_2O$ uptake rate) or from k2 (clearance rate of $[^{15}O]H_2O$) corrected with p_{phys}). In the study of Kudomi et al., renal cortical perfusion based on k1 and k2 x p_{phys} were compared, and k1 clearly underestimated renal cortical perfusion due to the partial volume effect (Kudomi et al., 2009). In that study, the average renal cortical perfusion value in healthy subjects based on k1 was 1.6 $ml \cdot g^{(-1)} \cdot min^{(-1)}$ and 3.6 $ml \cdot g^{(-1)} \cdot min^{(-1)}$ based on k2 (Kudomi et al., 2009).

The only studies which have used k2 for estimating renal cortical perfusion in healthy subjects are the study of Kudomi et al. (2009) and the study of Koivuviita et al., who reported a renal cortical perfusion value of 1.8 $ml \cdot g^{(-1)} \cdot min^{(-1)}$ (Koivuviita et al., 2012). Thus, the range of renal cortical perfusion values in healthy subjects based on k2 is 1.8–3.6 $ml \cdot g^{(-1)} \cdot min^{(-1)}$ and on k1 1.6–4.7 $ml \cdot g^{(-1)} \cdot min^{(-1)}$. We used k2 in our

study and arrived at an average renal cortical perfusion value in healthy subjects of 2.7 $ml \cdot g^{(-1)} \cdot min^{(-1)}$ which is in line with previous reports.

In addition to k1 and k2, there are some other methodological issues which explain the variable values of renal cortical perfusion obtained by the PET technique. The border between the cortex and medulla is impossible to define exactly without contrast-enhanced CT or MRI. This leads easily to inclusion of some medullary parenchyme into cortical ROIs. Damkjaer et al. introduced a new technique to differentiate between renal cortex and medulla: tissue layers with a thickness of one voxel are eliminated stepwise from the external surface of the volume of interest (voxel peeling) until there is no decrease in blood flow and the medulla is reached (Damkjær et al., 2010; Damkjær et al., 2012). Nevertheless, in most studies on renal cortical perfusion there is no exact definition of the border between cortex and medulla. Our study PET-imaging was preceded by attenuation CT, which does not establish the border between cortex and medulla.

PET provides only moderate spatial resolution, and this circumstance is associated with a harmful partial volume effect that causes overestimation or underestimation of perfusion. Further, the fast dynamics and reversible uptake of the $[^{15}O]H_2O$ tracer is technically error-prone due to the relatively low temporal resolution of PET (Green & Hutchins, 2011).

The variability of renal cortical perfusion values seems not to be a problem of $[^{15}O]H_2O$ PET imaging only. Reported renal cortical perfusion values in healthy subjects has varied from 1.4 $ml \cdot g^{(-1)} \cdot min^{(-1)}$ to 4.3 $ml \cdot g^{(-1)} \cdot min^{(-1)}$ with ASL-MRI (Odudu et al., 2018; Buchanan et al., 2019). It is also noteworthy that renal cortical perfusion is influenced by several external factors which increase sympathetic activity of autonomic nervous system, *e.g.*, handgrip exercise and mental stress (Haddock et al., 2018).

6.1.2 Renal flow reserve in patients with atherosclerotic renovascular disease (I)

Large studies of patients with ARVD and moderate to severe CKD did not predict any advantage of renal artery stenting (Wheatley et al., 2009; Bax et al., 2009; Cooper et al., 2014). Importantly, however, the degree of RAS was only anatomically evaluated. There might be a subgroup of patients with ARVD whose kidney impairment is, in fact, caused by the hemodynamic effect of the stenosis and who could have improved renal function following revascularisation. Patients with potentially salvageable “hibernating” renal parenchyme and reversible renal dysfunction should be identified (Chrysochou et al., 2012). A pilot study by Chrysochou et al. demonstrated that increased BOLD-MRI-derived kidney deoxyhemoglobin coupled with isotopic single kidney GFR predicts a positive renal

functional response to revascularisation in patients with RAS and moderate CKD (Chrysochou et al., 2012). Increased deoxyhemoglobin in stenosed kidneys is probably derived from kidney tissue with a reduced oxygen supply and reversible dysfunction.

Our study is the first one to evaluate RFR quantitatively with PET in patients with ARVD. RFR might serve as a surrogate marker of "hibernating" renal parenchyme and be a predictor of the response to dilatation of RAS. RFR could reflect the vascular capacity of the kidney as MPR does of the cardiac microvasculature. However, it is important to note that the physiological behaviour of heart and kidney is different and physiological tests may have different clinical value. In addition, RFR is small compared to MPR. The renographic study of Peters et al., which is the only study in literature on the correlation between RFR and clinical outcome after RAS stenting, could not find any correlation between RFR and response to RAS stenting (Peters et al., 1990). The evidence of the the predictive value of FFR_{REN} and the translesional gradient of the clinical outcome after RAS stenting is also scarce and conflicting.

It is noteworthy, that despite the fact that patients with the same condition or healthy controls have been studied and the same vasoactive substance and imaging technique have been used, there is still high variability in RFR values between studies and patients. In our study, the average RFR value of healthy control subjects was 22% with a standard deviation (SD) of 32%. In patients with bilateral RAS, RFR was 27% and in patients with unilateral RAS, RFR was 15% in the stenosed kidneys and 21% in the contralateral kidneys. SD was 43%, 22% and 27%, respectively. In the renographic study of Peters et al., the ACE-inhibitor stimulated RFR of the stenosed kidneys of patients with unilateral RAS was 24% with a SD of 23% and of the non-stenosed kidneys 18% with a SD of 23% (Peters et al., 1990). Juillard et al. reported a RFR of 26% with a SD of 20% in patients with CKD stage III by $[^{15}O]H_2O$ PET with ACE-inhibitor stimulation (Juillard et al., 2002). Manoharan et al. used the intra-arterial Doppler guide-wire technique to study RFR in connection with intrarenal dopamine stimulation of healthy subjects and reported a value of 94% with a SD of 54% (Manoharan et al., 2006).

The small size of RFR makes its measurement challenging which partly explains the variability of RFR values. In addition, differences in the ability of the study subjects to handle salt intake are associated with varying RFR values in association of ACE-inhibition. In patients with essential hypertension, a high sodium diet does not increase renal blood flow in 40–50% of patients. In these "nonmodulators" ACE-inhibition reduces blood pressure and increases renal blood flow despite suppression of the RAAS in subjects who have a high salt intake diet (Hollenberg et al., 1981; Fisher et al., 1999). Variable activity of the local renin system explains partly the variation of hemodynamic responses to RAAS inhibition.

6.1.3 Renal cortical perfusion in patients with a kidney transplant (III, IV)

Studies III and IV

In study III, renal cortical perfusion was 2.2 $ml \cdot g^{(-1)} \cdot min^{(-1)}$ and the median eGFR 55 ml/min in patients who had undergone renal transplantation, on average, 33 months previously. In study IV, renal cortical perfusion of patients with a kidney transplant was 1.8 $ml \cdot g^{(-1)} \cdot min^{(-1)}$ (eGFR 43 ml/min) and 2.2 $ml \cdot g^{(-1)} \cdot min^{(-1)}$ (eGFR 55 ml/min) 3 and 12 months after transplantation, respectively. Renal cortical perfusion of the healthy controls was 2.7 $ml \cdot g^{(-1)} \cdot min^{(-1)}$ (III, IV). There was a statistically significant difference in renal cortical perfusion between patients who had undergone kidney transplantation and healthy controls in study IV; in study III there was a trend favouring a statistically significant difference in perfusion between the groups.

$[^{15}O]H_2O$-PET studies of patients with CKD stage 3–5 have reported renal cortical perfusion values between 1.3 $ml \cdot g^{(-1)} \cdot min^{(-1)}$ and 2.2 $ml \cdot g^{(-1)} \cdot min^{(-1)}$ (Alpert et al., 2002; Juillard et al., 2002; Koivuviita et al., 2012). Two of the studies (Alpert et al., 2002; Koivuviita et al., 2012) reported also renal cortical perfusion values of healthy control subjects which were higher than those of patients with CKD within the studies. Our results were in line with these earlier studies. Of note: there are no earlier studies on renal cortical perfusion in kidney transplant patients with $[^{15}O]H_2O$-PET to compare with.

The RVR of transplant recipients was increased compared to healthy controls in both studies (III, IV). All patients had hypertension which increases RVR, unless renal cortical perfusion increases in the same manner. CNI drugs have been associated with increased renal vasoconstriction through an imbalance between vasoconstrictive agents, *e.g.*, endothelin, and vasodilative agents, *e.g.*, prostaglandins and NO (Naesens et al., 2009). Sympathetic overactivation, which is highly prevalent in patients with CKD and is associated with renal cortical vasoconstriction (Haddock et al., 2018), may persist after kidney transplantation (Hausberg et al., 2002). Although a transplanted kidney is totally denervated, regeneration of sympathetic nerves has been demonstrated in transplanted kidneys in animal and human studies (Shannon et al., 1998; Booth et al., 2015). Finally, microcirculatory changes in transplanted kidneys, *e.g.*, vascular rarefaction and endothelial dysfunction as well as renal fibrosis, may increase RVR in patients with a kidney transplant.

There was a statistically significant correlation between renal cortical perfusion and eGFR in the healthy control subjects as well as in patients with a kidney transplant at 12 months after transplantation in study IV. In study III, there was no statistically significant correlation between renal cortical perfusion and eGFR in

patients with a kidney transplant. Earlier [^{15}O]H_2O-PET studies have reported a statistically significant correlation between renal cortical perfusion and eGFR in subjects with CKD as well as in subjects without CKD (Inaba et al., 1989; Rebelos et al., 2019). A renal ASL MRI study has shown that the cortical perfusion of a kidney allograft correlates moderately with eGFR (Odudu et al., 2018). One reason for the lack of correlation between renal cortical perfusion and eGFR in patients with a kidney transplant in study III may relate to variable contribution to renal perfusion from the native kidneys.

There was no correlation between renal allograft fibrosis and cortical perfusion, which was probably related to the fact that the fibrosis in the studied kidney allografts was only mild and to the small sample size. An association between renal cortical perfusion and fibrosis has been demonstrated by Doppler echo, contrast enhanced MRI and ASL (Nankivell et al., 2002; Schwenger et al., 2006; Pereira et al., 2010; Wang et al. 2019) in patients with a kidney allograft, and further PET-studies may well arrive at a similar result.

In study III, renal Doppler RI was higher in patients with mild allograft fibrosis than in patients with no allograft fibrosis. There was also a statistically significant correlation between renal Doppler RI and renal cortical perfusion, but not between renal cortical perfusion and fibrosis in patients with a kidney transplant. In study IV, neither renal cortical perfusion nor renal fibrosis were associated with renal RI. Studies of renal Doppler RI in patients with a kidney transplant have arrived at conflicting results. Radermacher et al. demonstrated a statistically significant correlation between renal fibrosis and Doppler RI in patients with a kidney transplant (Radermacher et al., 2003), while Naesens et al. did not (Naesens et al., 2013).

Study IV

RVR declined and eGFR rose between 3 and 12 months after renal transplantation. This phenomenon might be associated with the frequent adverse events (CMV infections and rejections) early after transplantation, which would reduce cortical allograft perfusion at 3 months. There is evidence that acute rejection decreases renal cortical perfusion (Jiménez et al., 2016). In addition, CMV infection is associated with endothelial dysfunction in patients with a kidney transplant (Kas Deelen et al., 2000). Furthermore, the CNI doses were tapered off after the transplantation, and relatively high doses soon after transplantation may affect eGFR and renal cortical perfusion at that time.

Renal function at 3 months predicted renal cortical perfusion and eGFR at 12 months after transplantation. Early post transplant renal function is associated with allograft outcome in several studies (First, 2003). However, renal cortical perfusion, which is closely related to eGFR, did not predict renal perfusion or eGFR at 12

months in patients with a kidney transplant in our study. The importance of early renal cortical perfusion for evaluation of the prognosis of the kidney transplant was emphasised in the study of Steegh et al., in which peritubular capillaries decreased mainly during the first 3 months after kidney transplantation, and this was associated with fibrosis and GFR at 1 year after transplantation (Steegh et al.,2011). Likewise, renal cortical perfusion by ASL and by contrast-enhanced Doppler sonography has been shown to predict kidney allograft function (Yu et al., 2021).

6.2 Myocardial perfusion reserve in kidney transplant patients is well preserved (II)

MPR, a surrogate marker for coronary microvascular supply and function, and stress MP, are reduced in conditions predisposing to atherosclerosis, *e.g.*, DM, hypertension, and hypercholesterolemia, which are associated with endothelial dysfunction (Brunner et al., 2005; Camici et al., 2015). In patients with CKD, several factors influence MP, including endothelial dysfunction of coronaries, a reduced cross-sectional area of the coronary microcirculation, increased sympathetic tone of coronary arterioles, and reduced smooth muscle relaxation of the coronaries (Radhakrishnan et al., 2019). Data on MPR in patients with CKD is conflicting (Radhakrishnan et al., 2019), and in patients with a kidney transplant, only Doppler echocardiographic MPR-studies have been published.

In our study, basal MP was higher at a value of 1.3 $ml \cdot g^{(-1)} \cdot min^{(-1)}$ in patients with a kidney transplant with CKD stage 2–3 compared to 1.0 $ml \cdot g^{(-1)} \cdot min^{(-1)}$ in healthy subjects. Stress MP did not differ between the groups. Basal MP and MPR of patients with a kidney transplant were equal to that of the healthy subjects after correction for cardiac workload. Both blood pressure and heart rate were increased in patients with a kidney transplant compared to healthy controls, probably because of sympathetic overactivation in transplant recipients. Although some studies have shown that kidney transplantation mitigates overall sympathetic dysfunction (Agarwal et al., 1991; Yildiz et al., 1998; Rubinger et al., 2009), others have not (Hausberg et al., 2002). In addition, immunosuppressive medication *per se* has been associated with increased sympathetic activation.

As in our study, a PET-study by Charytan et al. demonstrated normal MPR in patients with CKD stage 1–3 compared to healthy control subjects (Charytan et al., 2010). Similarly, Chade et al., in an intracoronary Doppler study, found normal MPR in patients with CKD 3 after correction for age, gender, hypertension, and DM (Chade et al., 2006). However, decreased MPR has been demonstrated both in patients with early stages of CKD (Charytan et al., 2018) and in patients with CKD stage 5D (Tok et al., 2005; Niizuma et al., 2008). Increased basal MP (Ragosta et al., 2004; Niizuma et al., 2008; Koivuviita et al., 2009; Fukushima et al., 2012) and

decreased stress MP (Tok et al., 2005; Bezante et al., 2009; Nelson et al., 2019) have been reported in patients with different stages of CKD.

The discrepancies in the findings of these studies are partly related to differences in methodology and partly to expression of the results. Many studies have neither corrected MP and MPR for cardiac workload nor reported basal and stress MP separately. In addition, many studies have not performed coronary angiography to exclude epicardial CAD, which reduces stress MP, nor has the presence or absence of LVH been considered – a variable which is associated with the value of stress MP (Olsen et al., 2004).

Transthoracic Doppler echocardiography has been used to study patients with kidney transplant and CKD stage 2 and reduced values of stress CFV and CFVR have been reported (Caliskan et al., 2008; Bozbas et al., 2008; Turiel et al., 2008). In all these studies, there was a statistically significant correlation between CFVR and dialysis vintage (Turiel et al., 2008; Bozbas et al., 2008; Caliskan et al., 2008). Our study did not find a correlation between dialysis vintage and MPR, which may be due to the short dialysis vintage of our patients. The average dialysis vintage before transplantation was 39–64 months in the Doppler studies (Turiel et al., 2008; Bozbas et al., 2008; Caliskan et al., 2008) but only 21 months in our study. The short dialysis vintage before transplantation in our patients may also explain why the stress MP values of the healthy control subjects and patients with a kidney transplant did not differ significantly.

Pretransplant dialysis vintage, *i.e.*, the waiting time on dialysis, is a strong risk factor for CV death after kidney transplantation (Meier-Kriesche et al., 2004; Helanterä et al., 2014). On the other hand, a small MPR is associated with a worse CV outcome compared to a normal MPR in patients with and without CKD (Murthy et al., 2012; Taqueti & Di Carli, 2018). Thus, reducing the dialysis vintage before transplantation might improve MPR and, ultimatelty, the prognosis of patients undergoing renal transplantation.

Since there are no prospective studies, it is impossible to state whether kidney transplantation improves MPR. In prospective studies exploiting FMD and venous plethysmography, endothelial function has been shown to improve after kidney transplantation (Passauer et al., 2003; Oflaz et al., 2006). Quite recently, Bajaj et al. demonstrated an association between coronary microvascular dysfunction and cardiac function in a longitudinal observational study with 352 patients without overt CAD. One third of the patients had CKD stage 3 or higher (Bajaj et al., 2020). MPR, but not eGFR, was associated with cardiac systolic global longitudinal strain and diastolic function as well as with risk of CV events. Thus, microvascular dysfunction may explain the effect of CKD on abnormal cardiac function and adverse cardiac events in patients without overt CAD (Bajaj et al., 2020). Since kidney

transplantation is associated with improved global longitudinal strain, one could assume that also MPR improves (Hewing et al., 2016).

6.3 Limitations of the studies

Sample size was relatively small in all studies, which may have impacted the results. In study I, the enrolled number of patients with ARVD suitable for RAS revascularisation was lower than initially expected. The patients in studies II and III were recruited between 1/2011 and 2/2017, during which time 90 patients from our clinic underwent kidney transplantation. Patients with a kidney transplant but without clinical atherosclerotic disease – a main inclusion criterion in our study – were rarer than originally expected. In study IV, there were 7 patients who did not complete the study. One patient lost the allograft early after transplantation, 4 patients did not receive an allograft during the follow-up time, and 2 patients declined kidney biopsy.

Study design. In study II, no coronary angiography to exclude obstructive CAD was performed. If present, CAD might have affected the value of stress MP. However, there were no regional perfusion differences in the myocardium typical for CAD in the patients. The time interval between echocardiography and cardiac PET imaging of kidney allograft recipients in study II was long, and this makes reliable comparisons between cardiac perfusion and echocardiographic findings impossible.

Methodology. In studies III and IV, some kidney transplant biopsies were not representative in view of the Banff criteria, especially arteries were partly lacking. Still, the number of vessels should not influence the fibrotic and inflammatory scores that were of interest in the present setting. Finally, the border between cortex and medulla cannot be defined exactly without contrast-enhanced CT or MRI, and addition of medullary parenchyme into cortical ROIs is probable. To ameliorate the partial-volume effect we calculated the renal cortical perfusion not instead from the uptake rate of $[^{15}O]H_2O$ but from the the clearance rate.

7 Summary/Conclusions

I [^{15}O]H_2O PET shows that the perfusion reserve is significantly smaller in the kidneys than the heart. Renal flow reserve is highly variable.

II [^{15}O]H_2O-PET shows that the resting myocardial perfusion is increased due to increased cardiac workload and the stress myocardial perfusion is preserved in patients with a kidney transplant with CKD stage 3. Myocardial perfusion reserve in patients with a kidney transplant is the same as in the healthy controls after correction by cardiac workload.

III [^{15}O]H_2O PET is a feasible method to measure renal cortical perfusion in patients with a kidney transplant. Renal vascular resistance in kidney transplant recipients with CKD stage 3 is increased compared with that of healthy control subjects. The renal Doppler resistance index correlates with the degree of renal fibrosis and with renal cortical perfusion in patients with a kidney allograft. There is no correlation between the renal cortical perfusion and the histology of the kidney allograft.

IV Renal cortical perfusion at 3 months does not predict renal fibrosis at 12 months in kidney transplant recipients. Renal cortical perfusion in patients with a kidney transplant with CKD stage 3 is worse than in healthy control subjects during the first year after transplantation. Renal vascular resistance decreases during the first year after transplantation.

- The small renal flow reserve makes its value questionable for predicting the response to dilatation of renal artery stenosis.
- The myocardial perfusion reserve is well preserved in patients with a kidney transplant with CKD stage 3. The increase of cardiac workload is probably linked to sympathetic overactivation in kidney transplant recipients.
- In kidney transplant recipients, renal cortical perfusion is decreased, which is likely related to renal microvascular changes and endothelial dysfunction. Evaluation of renal cortical perfusion of patients with a kidney allograft may help to identify kidney grafts, which need active measures to preserve allograft function.

8 Acknowledgements

This study was carried out at the Kidney Centre, Turku University Hospital, and the Turku PET Centre, and was conducted within the Finnish Centre of Excellence in Cardiovascular and Metabolic Diseases, supported by the Academy of Finland, the University of Turku, the Turku University Central Hospital, and the Åbo Akademi University. The study was financially supported by the Academy of Finland (BEAT DKD EU project), Finska Läkaresällskapet (the Finnish Medical Society) and the Perklén Foundation, the Finnish Cultural Foundation, the Finnish Society of Nephrology and the Turku University Hospital Foundation.

I am grateful to my supervisors Docent Kaj Metsärinne and Docent Niina Koivuviita for their mentorship and support, which helped me along every step of the way. You always had time to give advice how to proceed with my research. You taught me academic writing. Niina, you were leading the way. You also made my thesis possible by your arrangements of working schedules in a way that I could pursue this research. Kajus, thank you for giving me the possibility to do research and for encouraging me.

I thank Professor Juhani Knuuti, director of Turku PET Centre, for providing an outstanding environment for research and for introducing me the fundamentals of cardiac PET imaging. I express my gratitude to Professor Pirjo Nuutila for her assistance and advice. I am grateful to Professor Markus Juonala for granting me permission to conduct this work at the Institute of Clinical Medicine, the University of Turku. Professor Marja Hedman and Docent Ilkka Helanterä are acknowledged for their valuable comments on my thesis. Docent Robert Paul is acknowledged for his language review of this thesis. I am also grateful to Professor Ilkka Pörsti for accepting the invitation to act as my opponent in the dissertation defense. I thank Docent Mikko Pietilä for his contribution in the supervisory committee of this thesis.

I express my gratitude to all my collaborators and co-authors for their important role in this thesis. I especially acknowledge Docent Anne Räisänen-Sokolowski in Helsinki University Hospital for her expertise and assistance with the analyses of kidney biopsies. She gave me irreplaceable help in supporting my understanding of the pathology of the kidney transplant. I am also deeply grateful to MSc Vesa Oikonen for helping me from the very beginning with the PET analysis and the

modelling of complicated renal perfusion. Without his work and assistance, this thesis would not have been completed by now. I further express my gratitude to Professor Hidehiro Iida, who shared his knowledge in PET methodology. I owe my warmest thanks to MSc Eliisa Löyttyniemi, who performed the statistical analyses extremely fast.

D.Sc Jarmo Teuho, MSc Tuula Tolvanen, MSc Kaisa Liukko and MD Ilkka Manner are warmly acknowledged for their contributions to the original publications. I am grateful to Sauli Piirola, who taught me the fundamentals of Carimas. Chunley Han is also knowledged for helping with Carimas. I thank Marko Tättäläinen and Rami Mikkola who helped me with computer problems. Radiochemists, laboratory technicians, physicists, radiologists, study nurses and other staff of the Turku PET Centre are acknowledged for their important work.

I am grateful to the colleagues and other staff for companionship in the Turku University Hospital and the Tyks Salo Hospital. I owe my thanks especially to colleagues for friendship and for creating an inspiring atmosphere in the Kidney Centre. I thank Louise Aaltonen, Markus Hakamäki, Jussi Haverinen, Tapio Hellman, Roosa Lankinen, Outi Leinonen, Jonna Virtanen, and Jonas Öhman for assisting me in recruiting patients for my study. I thank Risto Tertti and Maija Heiro for inspiring to specialise in nephrology. I warmly thank the personnel of the Kidney Centre, especially Ulla Pietilä and Mirja Saarinen, who have helped me in organising practical issues.

I thank the patients and volunteers for their participation. Without them this study would not have been possible. I further extend my gratitude to Eija Päivärinta, who recruited all volunteers.

I sincerely thank my friends Mia and Milja for their friendship and support through all these years. I thank Aapo and Sofi, the children of my friends. It has been wonderful to see them grow.

I express my gratitude to my parents, Pekka and Norma Neva, who always believed in me and who gave me the strength to go forward. Their unconditional love has been the fundament of my life. I also thank my sister Pirjo, who was so important for me when I was a child.

I owe my deepest gratitude to my lovely children Sylvi and Sampo and my dear husband Jukka, who are the most important people in my life. Jukka, you have made my scientific work possible. Without your support and love, this thesis would never have been completed. Sylvi and Sampo, thank you for your patience with mom's research.

Salo, September 2021
Johanna Päivärinta

9 References

Abendschein, A. D., Fewell, J. E., Carlson, C. & Rapaport, E., 1982. Myocardial blood flow during acute isovolumic anemia and treadmill exercise in dogs. *Journal of Applied Physiology,* 53(1), p.203-206. <https://doi.org/10.1152/jappl.1982.53.1.203 >

Agarwal, A., Anand, I. S., Sakhuja, V. & Chugh, K. S., 1991. Effect of dialysis and renal transplantation on autonomic dysfunction in chronic renal failure. *Kidney International,* 40(3), p.489-495. <https://doi.org/10.1038/ki.1991.236>

Alpert, N. M., Rabito, C. A., Correia, D. J., Babich, J. W., Littman, B. H., Tompkins, R. G., Rubin, N. T., Rubin, R. H. & Fischman, A. J. , 2002. Mapping of local renal blood flow with PET and H(2)(15)O. *Journal of Nuclear Medicine,* 43(4), p.470-475. <http://www.ncbi.nlm.nih.gov/pubmed/11937589>

Amann, K., Breitbach, M., Ritz, E. & Mall, G., 1998. Myocyte/capillary mismatch in the heart of uremic patients. *Journal of the American Society of Nephrology,* 9(6), p.1018-1022. <https://doi.org/10.1681/ASN.V961018 >

Anderson, T. J., Uehata, A., Gerhard, M. D., Meredith, I. T., Knab, S., Delagrange, D., Lieberman, E. H., Ganz, P., Creager, M. A., Yeung, A. C. & Selwyn, A. P., 1995. Close relation of endothelial function in the human coronary and peripheral circulations. *Journal of the American College of Cardiology,* 26(5), p.1235-1241. <http://dx.doi.org/10.1016/0735-1097(95)00327-4>

Assersen, K. B., Høilund-Carlsen, P. F., Olsen, M. H., Greve, S. V., Gam-Hadberg, J. C., Braad, P., Damkjaer, M. & Bie, P., 2019. The exaggerated natriuresis of essential hypertension occurs independently of changes in renal medullary blood flow. *Acta Physiologica,* 226(3), p.e13266 <https://doi.org/10.1111/apha.13266>

Aukland, K. , 1980. Methods for measuring renal blood flow: Total flow and regional distribution. *Annual Review of Physiology,* 42(1), p.543-555. <https://doi.org/10.1146/annurev.ph.42.030180.002551>

Baigent, C., Landray, M. J, Reith, C., Emberson, J., Wheeler D. C., Tomson, C., Wanner, C., Krane, V., Cass, A., Craig, J., Neal, B., Jiang, L., Hooi, L., Levin, A., Agodoa, L., Gaziano, M., Kasiske, B., Walker, R., Massy, Z., Feldt-Rasmussen, B., Krairittichai, U., Ophascharoensuk, V., Fellström, B., Holdaas, H., Tesar, V., Wiecek, A., Grobbee, D., de Zeeuw, D., Grönhagen-Riska, C., Dasgupta, T., Lewis, D., Herrington, W., Mafham, M., Majoni, W., Wallendszus, K., Grimm, R., Pedersen, T., Tobert, J., Armitage, J., Baxter, A., Bray, C., Chen, Y., Chen, Z., Hill, M., Knott, C., Parish, S., Simpson, D., Sleight, P., Young, A. & Collins, R., 2011. The effects of lowering LDL cholesterol with simvastatin plus ezetimibe in patients with chronic kidney disease (Study of Heart and Renal Protection): A randomised placebo-controlled trial. (SHARP). *The Lancet,* 377(9784), p.2181-2192. <https://doi.org/10.1016/s0140-6736(11)60739-3>

Bajaj, N., Singh, A., Zhou, W., Gupta, A., Fujikura, K., Byrne, C., Harms, H., Osborne, M., Bravo, P., Andrikopolou, E., Divakaran, S., Bibbo, C., Hainer, J., Skali, H., Taqueti, V., Steigner, M., Dorbala, S., Charytan, D., Prabhu, S., Blankstein, R., Deo, R., Solomon, S. & Di Carli, M., 2020. Coronary microvascular dysfunction, left ventricular remodeling, and clinical outcomes in patients with chronic kidney impairment. *Circulation,* 141(1), p.21-33. <https://doi.org/10.1161/circulationaha.119.043916>

Barrett, C., Navakatikyan, M. & Malpas, S., 2001. Long-term control of renal blood flow: what is the role of the renal nerves? *American Journal of Physiology-Regulatory Integrative and Comparative Physiology,* 280, p. R1534–R1545. <https://doi.org/10.1152/ajpregu.2001.280.5.r1534>

Bax, L, Woittiez, A-J. J., Kouwenberg, H. J., Mali, W., Buskens, E., Beek, F., Braam, B., Huysmans, F., Schultze, L. J., Kool, M., Rutten, C., Aarts, J., Rabelink, T. J., Plouin, P-F., Raynaud, A., van Montfrans, G. A., Reekers, J. A., van den Meiracker, A. H., Pattynama, P. M., van de Ven, P. J., Vroegindeweij, D., Kroon, A. A., de Haan, M., Postma, C. T. & Beutler, J. J., 2009. Stent placement in patients with atherosclerotic renal artery stenosis and impaired renal function. *Annals of Internal Medicine,* 150(12), p.840. <https://doi.org/10.7326/0003-4819-150-12-200906160-00119>

Baylis, C., 2008. Nitric oxide deficiency in chronic kidney disease. *American Journal of Physiology - Renal Physiology,* 294(1), p.1-9. <https://doi.org/10.1152/ajprenal.00424.2007>

Becker, L. E., Weritz, B., Yi, X., Gross-Weissmann, M., Waldherr, R., Zeier, M. & Sommerer, C., 2015. Evolution of allograft fibrosis and function in kidney transplant recipients: A retrospective analysis of stable patients under CNI and mTORi. *Transplant International,* 28(5), p.553-564. <https://doi.org/10.1111/tri.12529>

Beregi, J., Mounier-Vehier, C., Devos, P., Gautier, C., Libersa, C., McFadden, E. P. & Carré, A., 2000. Doppler flow wire evaluation of renal blood flow reserve in hypertensive patients with normal renal arteries. *CardioVascular and Interventional Radiology,* 23(5), p.340-346. <https://doi.org/10.1007/s002700010083>

Bezante, G. P., Viazzi, F., Leoncini, G., Ratto, E., Conti, N., Balbi, M., Agosti, S., Deferrari, L., Deferrari, G. & Pontremoli, R., 2009. Coronary flow reserve is impaired in hypertensive patients with subclinical renal damage. *American Journal of Hypertension,* 22(2), p.191-196. <http://dx.doi.org/10.1038/ajh.2008.351>

Bohle, A., Mackensen-Haen, S. & Wehrmann, M., 1996. Significance of postglomerular capillaries in the pathogenesis of chronic renal failure. *Kidney and Blood Pressure Research,* 19(3-4), p.191-195. <https://doi.org/10.1159/000174072>

Boor, P. & Floege, J., 2015. Renal allograft fibrosis: Biology and therapeutic targets. *American Journal of Transplantation*,15(4), p.863-886.<https://doi.org/10.1111/ajt.13180>

Booth, L., Nishi, E., Yao, S., Ramchandra, R., Lambert, G., Schlaich, M. & May, C., 2015. Reinnervation of renal afferent and efferent nerves at 5.5 and 11 months after catheter-based radiofrequency renal denervation in sheep. *Hypertension,* 65(2), p.393-400. <https://doi.org/10.1161/hypertensionaha.114.04176>

Bottomley, M. J. & Harden, P. N., 2013. Update on the long-term complications of renal transplantation. *British Medical Bulletin,* 106(1), p.117-134. <https://doi.org/10.1093/bmb/ldt012>

Bozbas, H., Pirat, B., Demirtas, S., Simşek, V., Yildirir, A., Sade, E., Sayin, B., Sezer, S., Karakayali, H. & Muderrisoglu, H., 2008. Evaluation of coronary microvascular function in patients with end-stage renal disease, and renal allograft recipients. *Atherosclerosis,* 202(2), p.498-504. <https://doi.org/10.1016/j.atherosclerosis.2008.04.043>

Brunner, H., Cockcroft, J. R., Deanfield, J., Donald, A., Ferrannini, E., Halcox, J., Kiowski, W., Lüscher, T. F., Mancia, G., Natali, A., Oliver, J. J., Pessina, A. C., Rizzoni, D., Rossi, G. P., Salvetti, A., Spieker, L. E., Taddei, S. & Webb, D. J., 2005. Endothelial function and dysfunction. part II: Association with cardiovascular risk factors and diseases. A statement by the working group on endothelins and endothelial factors of the European society of hypertension. *Journal of Hypertension,* 23(2), p.233-246. <https://doi.org/10.1097/00004872-200502000-00001>

Buchanan, C. E., Mahmoud, H., Cox, E. F., McCulloch, T., Prestwich, B. L., Taal, M. W., Selby, N. M. & Francis, S. T., 2019. Quantitative assessment of renal structural and functional changes in chronic kidney disease using multi-parametric magnetic resonance imaging. *Nephrology Dialysis Transplantation,* 35(6), p.955-964. <https://doi.org/10.1093/ndt/gfz129>

Buus, N. H., Bottcher, M., Hermansen, F., Sander, M., Nielsen, T. T. & Mulvany, M. J., 2001. Influence of nitric oxide synthase and adrenergic inhibition on adenosine-induced myocardial hyperemia. *Circulation,* 104(19), p.2305-2310. <https://doi.org/10.1161/hc4401.098293>

Caliskan, Y., Oflaz, H., Demirturk, M., Yazici, H., Turkmen, A., Çimen, A., Elitok, A. & Yildiz, A., 2008. Coronary flow reserve dysfunction in hemodialysis and kidney transplant patients. *Clinical Transplantation,* 22(6), p.785-793. <https://doi.org/10.1111/j.1399-0012.2008.00879.x>

Camici, P. G., d'Amati, G. & Rimoldi, O., 2015. Coronary microvascular dysfunction: Mechanisms and functional assessment. *Nature Reviews. Cardiology,* 12(1), p.48-62. <https://doi.org/10.1038/nrcardio.2014.160>

Cervenka, L., Horáek, V., Vanecková, I., Hubáek, J., Oliverio, M., Coffman, T. M. & Navar, L. G., 2002. Essential role of AT1A receptor in the development of 2K1C hypertension. *Hypertension*, 40(5), p. 735-741. <https://doi.org/10.1161/01.HYP.0000036452.28493.74>

Chade, A. R., Brosh, D., Higano, S. T., Lennon, R. J., Lerman, L. O. & Lerman, A., 2006. Mild renal insufficiency is associated with reduced coronary flow in patients with non-obstructive coronary artery disease. *Kidney International,* 69(2), p.266-271. <http://dx.doi.org/10.1038/sj.ki.5000031>

Chade, A., 2017. Small vessels, big role: Renal microcirculation and progression of renal injury. *Hypertension,* 69(4), p.551-563. <https://doi.org/10.1161/hypertensionaha.116.08319>

Chade, A., 2018. Understanding and managing atherosclerotic renovascular disease: Still a work in progress. *F1000Research,* 7, p.1862-1870. <http://dx.doi.org/10.12688/f1000research.16369.1>

Charytan, D. M., Shelbert, H. R. & Di Carli, M. F., 2010. Coronary microvascular function in early chronic kidney disease. *Circulation Cardiovascular Imaging,* 3(6), p.663-671. <https://doi.org/10.1161/circimaging.110.957761>

Charytan, D. M., Skali, H., Shah, N. R., Veeranna, V., Cheezum, M. K., Taqueti, V. R., Kato, T., Bibbo, C. R., Hainer, J., Dorbala, S., Blankstein, R. & Di Carli, M. F., 2018. Coronary flow reserve is predictive of the risk of cardiovascular death regardless of chronic kidney disease stage. *Kidney International,* 93(2), p.501-509. <https://doi.org/10.1016/j.kint.2017.07.025>

Chrysochou, C., Foley, R. N., Young, J. F., Khavandi, K., Cheung, C. M. & Kalra, P. A., 2012. Dispelling the myth: The use of renin-angiotensin blockade in atheromatous renovascular disease. *Nephrology Dialysis Transplantation,* 27(4), p.1403-1409. <https://doi.org/10.1093/ndt/gfr496>

Chrysochou, C., Mendichovszky, I. A., Buckley, D. L., Cheung, C. M., Jackson, A. & Kalra, P. A., 2012. BOLD imaging: A potential predictive biomarker of renal functional outcome following revascularization in atheromatous renovascular disease. *Nephrology Dialysis Transplantation,* 27(3), p.1013-1019. <https://doi.org/10.1093/ndt/gfr392>

Cianciolo, G., Capelli, I., Angelini, M. L., Valentini, C., Baraldi, O., Scolari, M. P. & Stefoni, S., 2014. Importance of vascular calcification in kidney transplant recipients. *American Journal of Nephrology,* 39(5), p.418-426. <https://doi.org/10.1159/000362492>

Coemans, M., Süsal, C., Döhler, B., Anglicheau, D., Giral, M., Bestard, O., Legendre, C., Emonds, M., Kuypers, D., Molenberghs, G., Verbeke, G. & Naesens, M., 2018. Analyses of the short- and long-term graft survival after kidney transplantation in Europe between 1986 and 2015. *Kidney International,* 94, p-964-973. <https://doi.org/10.1016/j.kint.2018.05.018>

Cooper, C. J., Murphy, T. P., Cutlip, D. E., Jamerson, K., Henrich, W., Reid, D. M., Cohen, D. J., Matsumoto, A. H., Steffes, M., Jaff, M. R., Prince, M. R., Lewis, E. F., Tuttle, K. R., Shapiro, J. I., Rundback, J. H., Massaro, J. M., D'Agostino, S., Ralph, B. & Dworkin, L. D., 2014. Stenting and medical therapy for atherosclerotic renal-artery stenosis. *The New England Journal of Medicine,* 370(1), p.13-22. <https://doi.org/10.1056/nejmoa1310753>

Czernin, J., Müller, P., Chan, S., Brunken, R. C., Porenta, G., Krivokapich, J., Chen, K., Chan, A., Phelps, M. E. & Schelbert, H. R., 1993. Influence of age and hemodynamics on

myocardial blood flow and flow reserve. *Circulation,* 88(1), p.62-69. <https://doi.org/10.1161/01.cir.88.1.62>

Damkjær, M., Vafaee, M., Møller, M. L., Braad, P. E., Petersen, H., Høilund-Carlsen, P. F. & Bie, P., 2010. Renal cortical and medullary blood flow responses to altered NO availability in humans. *American Journal of Physiology - Regulatory, Integrative and Comparative Physiology,* 299(6), p.1449-1455. <https://doi.org/10.1152/ajpregu.00440.2010>

Damkjær, M., Vafaee, M., Braad, P. E., Petersen, H., Høilund-Carlsen, P. F. & Bie, P., 2012. Renal cortical and medullary blood flow during modest saline loading in humans. *Acta Physiologica,* 205(4), p.472-483. <https://doi.org/10.1111/j.1748-1716.2012.02436.x>

Danad, I., Uusitalo, V., Kero, T., Saraste, A., Raijmakers, P. G., Lammertsma, A. A., Heymans, M. W., Kajander, S. A., Pietilä, M., James, S., Sorensen, J., Knaapen, P. & Knuuti, J., 2014. Quantitative assessment of myocardial perfusion in the detection of significant coronary artery disease: Cutoff values and diagnostic accuracy of quantitative [^{15}O]H_2O PET imaging. *Journal of the American College of Cardiology,* 64(14), p.1464-1475. <https://doi.org/10.1016/j.jacc.2014.05.069>

De Bruyne, B., Manoharan, G., Pijls, N. H. J., Verhamme, K., Madaric, J., Bartunek, J., Vanderheyden, M. & Heyndrickx, G. R., 2006. Assessment of renal artery stenosis severity by pressure gradient measurements. *Journal of the American College of Cardiology,* 48(9), p.1851-1855. <http://dx.doi.org/10.1016/j.jacc.2006.05.074>

Deanfield, J. E., Halcox, J. P. & Rabelink, T. J., 2007. Endothelial function and dysfunction: Testing and clinical relevance. *Circulation,* 115(10), p.1285-1295. <https://doi.org/10.1161/CIRCULATIONAHA.106.652859>

DeForrest, J. M., Knappenberger, R. C., Antonaccio, M. J., Ferrone, R. A. & Creekmore, J. S., 1982. Angiotensin II is a necessary component for the development of hypertension in the two kidney, one clip rat. *The American Journal of Cardiology,* 49(6), p.1515-1517. <http://dx.doi.org/10.1016/0002-9149(82)90373-3>

Devereux, R. B. & Reichek, N., 1977. Echocardiographic determination of left ventricular mass in man. Anatomic validation of the method. *Circulation (New York, N.Y.),* 55(4), p.613-618. <https://doi.org/10.1161/01.cir.55.4.613>

DiBona, G. F., 1987. Renal innervation and denervation: Lessons from renal transplantation reconsidered. *Artificial Organs,* 11(6), p.457-462. <https://doi.org/10.1111/j.1525-1594.1987.tb02710.x>

DiBona, G. F. & Sawin, L. L., 2004. Effect of renal denervation on dynamic autoregulation of renal blood flow. *American Journal of Physiology,* 286(6), p.F1209-1218. <https://doi.org/10.1152/ajprenal.00010.2004>

Djamali, A., Sadowski, E. A., Muehrer, R. J., Reese, S., Smavatkul, C., Vidyasagar, A., Fain, S. B., Lipscomb, R. C., Hullett, D. H., Samaniego-Picota, M., Grist, T. M. & Becker, B. N., 2007. BOLD-MRI assessment of intrarenal oxygenation and oxidative stress in patients with chronic kidney allograft dysfunction. *American Journal of Physiology. Renal Physiology,* 292(2), p.F513-F522. <https://doi.org/10.1152/ajprenal.00222.2006>

Duncker, D. J., Koller, A., Merkus, D. & Canty, J. M., 2014. Regulation of coronary blood flow in health and ischemic heart disease. *Progress in Cardiovascular Diseases,* 57(5), p.409-422. <https://doi.org/10.1016/j.pcad.2014.12.002>

Eirin, A., Textor, S. & Lerman, L., 2019. Novel therapeutic strategies for renovascular disease. *Current Opinion in Nephrology and Hypertension,* 28(4), p.383-389. <https://doi.org/10.1097/mnh.0000000000000513>

El Maghraby, T. A. F., van Eck-Smit, B. L. F., de Fijter, J. W. & Pauwels, E. K. J., 1998. Quantitative scintigraphic parameters for the assessment of renal transplant patients. *European Journal of Radiology,* 28(3), p.256-269. <https://doi.org/10.1016/S0720-048X(97)00179-4>

El-Zoghby, Z. M., Stegall, M. D., Lager, D. J., Kremers, W. K., Amer, H., Gloor, J. M. & Cosio, F. G., 2009. Identifying specific causes of kidney allograft loss. *American Journal of Transplantation,* 9(3), p.527-535. <https://doi.org/10.1111/j.1600-6143.2008.02519.x>

Evans, R. G., 2008. Intrarenal oxygenation: Unique challenges and the biophysical basis of homeostasis. *American Journal of Physiology,* 295(5), p.F1259-1270. <https://doi.org/10.1152/ajprenal.90230.2008>.

Feher, A. & Sinusas, A. J., 2017. Quantitative assessment of coronary microvascular function: Dynamic single-photon emission computed tomography, positron emission tomography, ultrasound, computed tomography, and magnetic resonance imaging. *Circulation. Cardiovascular Imaging,* 10(8):e006427.<https://doi.org/10.1161/circimaging.117.006427>

Fellstrom, B. C., Jardine, A. G., Schmieder, R. E., Holdaas, H., Bannister, K., Beutler, J., Chae, D., Chevaile, A., Cobbe, S. M., Gronhagen-Riska, C., De Lima, J. J., Lins, R., Mayer, G., McMahon, A. W., Parving, H., Remuzzi, G., Samuelsson, O., Sonkodi, S., Sci., D., Suleymanlar, G., Tsakiris, D., Tesar, V., Todorov, V., Wiecek, A., Wuthrich, R. P., Gottlow, M., Johnsson, E.& Zannad, F. (AURORA Study Group), 2009. Rosuvastatin and cardiovascular events in patients undergoing hemodialysis. *The New England Journal of Medicine,* 360(14), p.1395-1407. <https://doi.org/10.1056/nejmoa0810177>

Fenchel, M., Martirosian, P., Langanke, J., Giersch, J., Miller, S., Stauder, N. I., Kramer, U., Claussen, C. D. & Schick, F., 2006. Perfusion MR imaging with FAIR true FISP spin labeling in patients with and without renal artery stenosis: Initial experience. *Radiology,* 238(3), p.1013-1021. <https://doi.org/10.1148/radiol.2382041623>

Fine, L. G. & Norman, J. T., 2008. Chronic hypoxia as a mechanism of progression of chronic kidney diseases: From hypothesis to novel therapeutics. *Kidney International,* 74(7), p.867-872. <https://doi.org/10.1038/ki.2008.350>

First, M. R., 2003. Renal function as a predictor of long-term graft survival in renal transplant patients. *Nephrology Dialysis Transplantation,* 18 Suppl 1(90001), p.i3-6. <https://doi.org/10.1093/ndt/gfg1027>

Fisher, N. D., Price, D. A., Litchfield, W. R., Williams, G. H. & Hollenberg, N. K., 1999. Renal response to captopril reflects state of local renin system in healthy humans. *Kidney International,* 56(2), p.635-641. <http://dx.doi.org/10.1046/j.1523-1755.1999.00579.x>

Flickinger, A. L., Lerman, L. O., Sheedy, P. F. & Turner, S. T., 1996. The relationship between renal cortical volume and predisposition to hypertension. *American Journal of Hypertension,* 9(8), p.779-786. <http://dx.doi.org/10.1016/0895-7061(96)00097-0>

Foley, R. N., Parfrey, P. S. & Sarnak, M. J., 1998. Clinical epidemiology of cardiovascular disease in chronic renal disease. *American Journal of Kidney Diseases,* 32(5), p.S112-S119. <https://doi.org/10.1053/ajkd.1998.v32.pm9820470>

Fujii, H., Takiuchi, S., Kawano, Y. & Fukagawa, M., 2008. Putative role of asymmetric dimethylarginine in microvascular disease of kidney and heart in hypertensive patients. *American Journal of Hypertension,* 21(6), p.650-656. <http://dx.doi.org/10.1038/ajh.2008.29>

Fukushima, K., Javadi, M. S., Higuchi, T., Bravo, P. E., Chien, D., Lautamäki, R., Merrill, J., Nekolla, S. G. & Bengel, F. M., 2012. Impaired global myocardial flow dynamics despite normal left ventricular function and regional perfusion in chronic kidney disease: A quantitative analysis of clinical 82Rb PET/CT studies. *Journal of Nuclear Medicine,* 53(6), p.887-893. <https://doi.org/10.2967/jnumed.111.099325>

Furchgott, R. F. & Zawadzki, J. V., 1980. The obligatory role of endothelial cells in the relaxation of arterial smooth muscle by acetylcholine. *Nature,* 288(5789), p.373-376. <http://dx.doi.org/10.1038/288373a0>

Gansevoort, R. T., Correa-Rotter, R., Hemmelgarn, B. R., Jafar, T. H., Heerspink, H. J. L., Mann, J. F., Matsushita, K. & Wen, C. P., 2013. Chronic kidney disease and cardiovascular risk: Epidemiology, mechanisms, and prevention. *The Lancet,* 382(9889), p.339-352. <https://doi.org/10.1016/S0140-6736(13)60595-4>

Gavras, H., Brunner, H. R., Vaughan, E. D., Jr & Laragh, J. H., 1973. Angiotensin-sodium interaction in blood pressure maintenance of renal hypertensive and normotensive rats. *Science,* 180(4093), p.1369-1372. <http://www.sciencemag.org/cgi/content/abstract/180/4093/1369>

Gloviczki, M., Glockner, J., Lerman, L., McKusick, M., Misra, S., Grande, J. & Textor, S., 2010. Preserved oxygenation despite reduced blood flow in poststenotic kidneys in human atherosclerotic renal artery stenosis. *Hypertension,* 55(4), p.961-966. <http://dx.doi.org/10.1161/HYPERTENSIONAHA.109.145227>

Gloviczki, M., Glockner, J., Crane, J., McKusick, M., Misra, S., Grande, J., Lerman, L. & Textor, S., 2011. Blood Oxygen Level–Dependent magnetic resonance imaging identifies cortical hypoxia in severe renovascular disease. *Hypertension*, 58(6), p.1066-1072. <http://dx.doi.org/10.1161/HYPERTENSIONAHA.111.171405>

Go, A. S., Chertow, G. M., Fan, D., McCulloch, C. E. & Hsu, C., 2004. Chronic kidney disease and the risks of death, cardiovascular events, and hospitalization. *The New England Journal of Medicine,* 351(13), p.1296-1305. <https://doi.org/10.1056/nejmoa041031>

Gould, K. L., Johnson, N. P., Bateman, T. M., Beanlands, R. S., Bengel, F. M., Bober, R., Camici, P. G., Cerqueira, M. D., Chow, B. J. W., Di Carli, M. F., Dorbala, S., Gewirtz, H., Gropler, R. J., Kaufmann, P. A., Knaapen, P., Knuuti, J., Merhige, M. E., Rentrop, K. P., Ruddy, T. D., Schelbert, H. R., Schindler, T. H., Schwaiger, M., Sdringola, S., Vitarello, J., Williams, K., Gordon, D., Dilsizian, V. & Narula, J., 2013. Anatomic versus physiologic assessment of coronary artery disease: Role of coronary flow reserve, fractional flow reserve, and positron emission tomography imaging in revascularization decision-making. *Journal of the American College of Cardiology,* 62(18), p.1639-53. <https://doi.org/10.1016/j.jacc.2013.07.076>

Grassi, G., Quarti-Trevano, F., Seravalle, G., Arenare, F., Volpe, M., Furiani, S., Dell'Oro, R. & Mancia, G., 2011. Early sympathetic activation in the initial clinical stages of chronic renal failure. *Hypertension,* 57(4), p.846-851. <https://doi.org/10.1161/hypertensionaha.110.164780>

Green, M. & Hutchins, G., 2011. Positron emission tomography (PET) assessment of renal perfusion. *Seminars in Nephrology,* 31(3), p.291-299. <https://doi.org/10.1016/j.semnephrol.2011.05.008>

Grenier, N., Cornelis, F., Le Bras, Y., Rigou, G., Boutault, J. R. & Bouzgarrou, M., 2013. Perfusion imaging in renal diseases. *Diagnostic and Interventional Imaging,* 94(12), p.1313-1322. <https://doi.org/10.1016/j.diii.2013.08.018>

Haas, M., Loupy, A., Lefaucheur, C., Roufosse, C., Glotz, D., Seron, D., Nankivell, B. J., Halloran, P. F., Colvin, R. B., Akalin, E., Alachkar, N., Bagnasco, S., Bouatou, Y., Becker, J. U., Cornell, L. D., Huyen, J. P. D., Gibson, I. W., Kraus, E. S., Mannon, R. B., Naesens, M., Nickeleit, V., Nickerson, P., Segev, D. L., Singh, H. K., Stegall, M., Randhawa, P., Racusen, L., Solez, K. & Mengel, M., 2018. The banff 2017 kidney meeting report: Revised diagnostic criteria for chronic active T cell–mediated rejection, antibody-mediated rejection, and prospects for integrative endpoints for next-generation clinical trials. *American Journal of Transplantation,* 18(2), p.293-307. <https://doi.org/10.1111/ajt.14625>

Haddock, B. T., Francis, S. T., Larsson, H. B. W. & Andersen, U. B., 2018. Assessment of perfusion and oxygenation of the human renal cortex and medulla by quantitative MRI during handgrip exercise. *Journal of the American Society of Nephrology,* 29(10), p.2510-2517. <https://doi.org/10.1681/asn.2018030272>

Hakeem, A., Bhatti, S., Karmali, K. N., Dillie, K., Cook, J. R., Xu, J., Samad, Z. & Chang, S. M., 2010. Renal function and risk stratification of diabetic and nondiabetic patients undergoing evaluation for coronary artery disease. *Journal of the American College of Cardiology: Cardiovascular Imaging,* 3(7), p.734-745. <https://doi.org/10.1161/01.CIR.0000034043.16664.96>

Hansen, K. J., Edwards, M. S., Craven, T. E., Cherr, G. S., Jackson, S. A., Appel, R. G., Burke, G. L. & Dean, R. H., 2002. Prevalence of renovascular disease in the elderly: A population-based study. *Journal of Vascular Surgery,* 36(3), p.443-451. <http://dx.doi.org/10.1067/mva.2002.127351>

Hausberg, M., Kosch, M., Harmelink, P., Barenbrock, M., Hohage, H., Kisters, K., Dietl, K. H. & Rahn, K. H., 2002. Sympathetic nerve activity in end-stage renal disease. *Circulation,* 106(15), p.1974-1979. <https://doi.org/10.1161/01.CIR.0000034043.16664.96>

Helanterä, I., Salmela, K., Kyllönen, L., Koskinen, P., Grönhagen-Riska, C. & Finne, P., 2014. Pretransplant dialysis duration and risk of death after kidney transplantation in the current era. *Transplantation,* 98(4), p.458-464. <https://doi.org/10.1097/tp.0000000000000085>

Hensen, L. C. R., Goossens, K., Delgado, V., Abou, R., Rotmans, J. I., Jukema, J. W. & Bax, J. J., 2018. Prevalence of left ventricular systolic dysfunction in pre-dialysis and dialysis patients with preserved left ventricular ejection fraction. *European Journal of Heart Failure,* 20(3), p.560-568. <https://doi.org/10.1002/ejhf.1077>

Herrmann, S. M. & Textor, S. C., 2019. Renovascular hypertension. *Endocrinology and Metabolism Clinics of North America,* 48(4), p.765-778. <http://dx.doi.org/10.1016/j.ecl.2019.08.007>

Hetzel, G. R., Plum, J., Fussholler, A., Voiculescu, A., Grunberg, W., & Grabensee, B., 2005. Effects of candesartan on glomerular hemodynamics and permselectivity in patients with favorable renal allograft function. *Transplantation*, 79(6), p. 710-715. <https://doi.org/10.1097/01.tp.0000155303.53547.20>

Heusch, P., Wittsack, H., Blondin, D., Ljimani, A., Nguyen-Quang, M., Martirosian, P., Zenginli, H., Bilk, P., Kröpil, P., Heusner, T. A., Antoch, G. & Lanzman, R. S., 2014. Functional evaluation of transplanted kidneys using arterial spin labeling MRI. *Journal of Magnetic Resonance Imaging,* 40(1), p.84-89. <https://doi.org/10.1002/jmri.24336>

Hewing, B., Dehn, A. M., Staeck, O., Knebel, F., Spethmann, S., Stangl, K., Baumann, G., Dreger, H., Budde, K. & Halleck, F., 2016. Improved left ventricular structure and function after successful kidney transplantation. *Kidney and Blood Pressure Research,* 41(5), p.701-709. <https://doi.org/10.1159/000450559>

Holdaas, H., Fellstrom, B., Cole, E., Nyberg, G., Olsson, A. G., Pedersen, T. R., Madsen, S., Gronhagen-Riska, C., Neumayer, H., Maes, B., Ambuhl, P., Hartmann, A., Staffler, B. & Jardine, A. G., 2005. Long-term cardiac outcomes in renal transplant recipients receiving fluvastatin: The ALERT extension study. *American Journal of Transplantation,* 5(12), p.2929-2936. <https://doi.org/10.1111/j.1600-6143.2005.01105.x>

Holdaas, H., Fellström, B., Jardine, A. G., Holme, I., Nyberg, G., Fauchald, P., Grönhagen-Riska, C., Madsen, S., Neumayer, H., Cole, E., Maes, B., Ambühl, P., Olsson, A. G., Hartmann, A., Solbu, D. O. & Pedersen, T. R., 2003. Effect of fluvastatin on cardiac outcomes in renal transplant recipients: A multicentre, randomised, placebo-controlled trial. *The Lancet (London, England),* 361(9374), p.2024-2031.<https://doi.org/10.1016/s0140-6736(03)13638-0>

Hollenberg, N. K., Meggs, L. G., Williams, G. H., Katz, J., Garnic, J. D. & Harrington, D. P., 1981. Sodium intake and renal responses to captopril in normal man and in essential hypertension. *Kidney International,* 20(2), p.240-245. <http://dx.doi.org/10.1038/ki.1981.126>

Hollenberg, N. K., Sandor, T., Holtzman, E., Meyerovitz, M. F. & Harrington, D. P., 1989. Renal vasomotion in essential hypertension: Influence of vasodilators. *Hypertension,* 14(1), p.9-13. <https://doi.org/10.1161/01.HYP.14.1.9>

Iida, H., Kanno, I., Takahashi, A., Miura, S., Murakami, M., Takahashi, K., Ono, Y., Shishido, F., Inugami, A. & Tomura, N., 1988. Measurement of absolute myocardial blood flow with [^{15}O] H_2O and dynamic positron-emission tomography. Strategy for quantification in relation to the partial-volume effect. *Circulation,* 78(1), p.104-115. <https://doi.org/10.1161/01.cir.78.1.104>

Iida, H., Rhodes, C. G., de Silva, R., Araujo, L. I., Bloomfield, P. M., Lammertsma, A. A. & Jones, T., 1992. Use of the left ventricular time-activity curve as a noninvasive input function in dynamic oxygen-15-water positron emission tomography. *The Journal of Nuclear Medicine,* 33(9), p.1669-1677. <http://jnm.snmjournals.org/cgi/content/abstract/33/9/1669>

Inaba, T., Yamashita, M., Kawase, Y., Nakahashi, H. & Watanabe, H., 1989. Quantitative measurement of renal plasma flow by positron emission tomography with oxygen-15 water. *The Tohoku Journal of Experimental Medicine,* 159(4), p.283-289. <https://doi.org/10.1620/tjem.159.283>

Ishii, M., Ikeda, T., Takagi, M., Sugimoto, T., Atarashi, K., Igari, T., Uehara, Y., Matsuoka, H., Hirata, Y., Kimura, K., Takeda, T. & Murao, S., 1983. Elevated plasma catecholamines in hypertensives with primary glomerular diseases. *Hypertension,* 5(4), p.545-551. <https://doi.org/10.1161/01.hyp.5.4.545>

Ishii, Y., Sawada, T., Kubota, K., Fuchinoue, S., Teraoka, S. & Shimizu, A., 2005. Injury and progressive loss of peritubular capillaries in the development of chronic allograft nephropathy. *Kidney International,* 67(1), p.321-332. <https://doi.org/10.1111/j.1523-1755.2005.00085.x>

Jardine, A. G., Gaston, R. S., Fellstrom, B. C. & Holdaas, H., 2011. Prevention of cardiovascular disease in adult recipients of kidney transplants. *The Lancet,* 378(9800), p.1419-1427. <http://dx.doi.org/10.1016/S0140-6736(11)61334-2>

Jiménez, C., López, M. O., Ros, A., Aguilar, A., Menendez, D., Rivas, B., Santana, M. J., Vaca, M. A., Escuin, F., Madero, R. & Selgas, R., 2016. The natural history of kidney graft cortical microcirculation determined by real-time contrast-enhanced sonography (RT-CES). *PloS One,* 11(3), p.e0150384. <https://doi.org/10.1371/journal.pone.0150384>

Johnson, R. J. & Feehally, J., 2003. Comprehensive 2nd edition Clinical Nephrology. Copyright Elsevier (2003).

Juillard, L., Janier, M. F., Fouque, D., Cinotti, L., Maakel, N., Le Bars, D., Barthez, P. Y., Pozet, N. & Laville, M., 2002. Dynamic renal blood flow measurement by positron emission tomography in patients with CRF. *American Journal of Kidney Diseases,* 40(5), p.947-954. <https://doi.org/10.1053/ajkd.2002.36325>

Juillard, L., Janier, M. F., Fouque, D., Lionnet, M., Le Bars, D., Cinotti, L., Barthez, P., Gharib, C. & Laville, M., 2000. Renal blood flow measurement by positron emission tomography using 15O-labeled water. *Kidney International,* 57(6), p.2511-2518. <http://dx.doi.org/10.1046/j.1523-1755.2000.00110.x>

Kądziela, J., Januszewicz, A., Prejbisz, A., Michałowska, I., Januszewicz, M., Florczak, E., Kalińczuk, Ł, Norwa-Otto, B., Warchoł, E. & Witkowski, A., 2013. Prognostic value of renal fractional flow reserve in blood pressure response after renal artery stenting (PREFER study). *Cardiology Journal,* 20(4), p.418-422. <https://doi.org/10.5603/cj.2013.0101>

Kang, D., Kanellis, J., Hugo, C., Truong, L., Anderson, S., Kerjaschki, D., Schreiner, G. F. & Johnson, R. J., 2002. Role of the microvascular endothelium in progressive renal disease. *Journal of the American Society of Nephrology,* 13(3), p.806-816. <https://doi.org/10.1681/asn.v133806>

Karthikeyan, V., Karpinski, J., Nair, R. C. & Knoll, G., 2004. The burden of chronic kidney disease in renal transplant recipients. *American Journal of Transplantation,* 4(2), p.262-269. <https://doi.org/10.1046/j.1600-6143.2003.00315.x>

Kas-Deelen, A. M., Harmsen, M. C., De Maar, E. F., Oost-Kort, W. W., Tervaert, J. W. C., Van Der Meer, J., Van Son, W. J. & The, T. H., 2000. Acute rejection before cytomegalovirus infection enhances von Willebrand factor and soluble VCAM-1 in blood. *Kidney International,* 58(6), p.2533-2542. <http://dx.doi.org/10.1046/j.1523-1755.2000.00438.x>

Kauppila, L. I., Polak, J. F., Cupples, L. A., Hannan, M. T., Kiel, D. P. & Wilson, P. W. F., 1997. New indices to classify location, severity and progression of calcific lesions in the abdominal aorta: A 25-year follow-up study. *Atherosclerosis,* 132(2), p.245-250. <https://doi.org/10.1016/S0021-9150(97)00106-8>

Koivuviita, N., Tertti, R., Luotolahti, M., Raitakari, O., Vahlberg, T., Nuutila, P., Knuuti, J. & Metsärinne, K., 2011. The effect of revascularization of atherosclerotic renal artery stenosis on coronary flow reserve and peripheral endothelial function. *Nephron Clinical Practice,* 118(3), p.c241-c248. <https://doi.org/10.1159/000321643>

Koivuviita, N., Liukko, K., Kudomi, N., Oikonen, V., Tertti, R., Manner, I., Vahlberg, T., Nuutila, P. & Metsärinne, K., 2012. The effect of revascularization of renal artery stenosis on renal perfusion in patients with atherosclerotic renovascular disease. *Nephrology Dialysis Transplantation,* 27(10), p.3843-3848. <https://doi.org/10.1093/ndt/gfs301>

Koivuviita, N., Tertti, R., Järvisalo, M., Pietilä, M., Hannukainen, J., Sundell, J., Nuutila, P., Knuuti, J. & Metsärinne, K., 2009. Increased basal myocardial perfusion in patients with chronic kidney disease without symptomatic coronary artery disease. *Nephrology Dialysis Transplantation,* 24(9), p.2773-2779. <https://doi.org/10.1093/ndt/gfp175>

Kudomi, N., Koivuviita, N., Liukko, K., Oikonen, V., Tolvanen, T., Iida, H., Tertti, R., Metsärinne, K., Iozzo, P. & Nuutila, P., 2009. Parametric renal blood flow imaging using [^{15}O]H_2O and PET. *European Journal of Nuclear Medicine and Molecular Imaging,* 36(4), p.683-691. <https://doi.org/10.1007/s00259-008-0994-8>

Lamb, K. E., Lodhi, S. & Meier-Kriesche, H., 2011. Long-Term renal allograft survival in the United States: A critical reappraisal. *American Journal of Transplantation,* 11(3), p.450-462. <https://doi.org/10.1111/j.1600-6143.2010.03283.x>

Lang, R. M., Badano, L. P., Mor-Avi, V., Afilalo, J., Armstrong, A., Ernande, L., Flachskampf, F. A., Foster, E., Goldstein, S. A., Kuznetsova, T., Lancellotti, P., Muraru, D., Picard, M. H., Rietzschel, E. R., Rudski, L., Spencer, K. T., Tsang, W. & Voigt, J., 2015. Recommendations for cardiac chamber quantification by echocardiography in adults: An update from the American society of echocardiography and the European association of cardiovascular imaging. *European Heart Journal Cardiovascular Imaging,* 16(3), p.233-271. <https://doi.org/10.1093/ehjci/jev014>

Levey, A., Stevens, L. A., Schmid, C. H., Zhang, Y., Castro, A. F., Feldman, H. I., Kusek, J., Eggers, P, Van Lente, F., Greene, T. & Coresh, J., 2009. CKD-EPI (Chronic Kidney Disease Epidemiology Collaboration). A new equation to estimate glomerular filtration rate. *Annals of Internal Medicine,* 150(9), p.604-612. <https://doi.org/10.7326/0003-4819-150-9-200905050-00006>

Loupy, A., Haas, M., Solez, K., Racusen, L., Glotz, D., Seron, D., Nankivell, B. J., Colvin, R. B., Afrouzian, M., Akalin, E., Alachkar, N., Bagnasco, S., Becker, J. U., Cornell, L., Drachenberg, C., Dragun, D., Kort, H., Gibson, I. W., Kraus, E. S., Lefaucheur, C., Legendre, C., Liapis, H., Muthukumar, T., Nickeleit, V., Orandi, B., Park, W., Rabant, M., Randhawa, P., Reed, E. F., Roufosse, C., Seshan, S. V., Sis, B., Singh, H. K., Schinstock, C., Tambur, A., Zeevi, A. & Mengel, M., 2017. The Banff 2015 kidney meeting report: Current challenges in rejection classification and prospects for adopting molecular pathology. *American Journal of Transplantation,* 17(1), p.28-41. <https://doi.org/10.1111/ajt.14107>

Loupy, A., Aubert, O., Orandi, B., Naesens, M., Bouatou, Y., Raynaud, M., Divard, G., Jackson, A., Viglietti, D., Giral, M., Kamar, N., Thaunat, O., Morelon, E., Delahousse, M., Kuypers, D., Hertig, A., Rondeau, E., Bailly, E., Eskandary, F., Böhmig, G., Gupta, G., Glotz, D., Legendre, C., Montgomery, R., Stegall, M., Empana, J., Jouven, X., Segev, D. & Lefaucheur, C., 2019. Prediction system for risk of allograft loss in patients receiving kidney transplants: international derivation and validation study. *British Medical Journal,* 366: 14923. <https://doi.org/10.1136/bmj.l4923>

Ludmer, P. L., Selwyn, A. P., Shook, T. L., Wayne, R. R., Mudge, G. H., Alexander, R. W. & Ganz, P., 1986. Paradoxical vasoconstriction induced by acetylcholine in atherosclerotic coronary arteries. *The New England Journal of Medicine,* 315(17), p.1046-1051. <http://dx.doi.org/10.1056/NEJM198610233151702>

Mann, S. J., Pickering, T. G., Sos, T. A., Uzzo, R. G., Sarkar, S., Friend, K., Rackson, M. E. & Laragh, J. H., 1991. Captopril renography in the diagnosis of renal artery stenosis: Accuracy and limitations. *The American Journal of Medicine,* 90(1), p.30-40. <http://dx.doi.org/10.1016/0002-9343(91)90503-P>

Manoharan, G., Pijls, N. H. J., Lameire, N., Verhamme, K., Heyndrickx, G. R., Barbato, E., Wijns, W., Madaric, J., Tielbeele, X., Bartunek, J. & De Bruyne, B., 2006. Assessment of renal flow and flow

reserve in humans. *Journal of the American College of Cardiology,* 47(3), p.620-625. <http://dx.doi.org/10.1016/j.jacc.2005.08.071>

Matas, A, Smith, J, Skeans, M, Thompson, B., Gustafsson, S., Stewart, D., Cherikh, W., Wainright, J., Boyle, G., Snyder, J., Israni, A. & Kasiske, B., 2015. OPTN/SRTR 2013 Annual Data Report: Kidney. *American Journal of Transplantation,* 15(S2), p.1-34. < https://doi.org/10.1111/ajt.13195>

Meier-Kriesche, H., Baliga, R. & Kaplan, B., 2003. Decreased renal function is a strong risk factor for cardiovascular death after renal transplantation. *Transplantation,* 75(8), p.1291-1295. <https://doi.org/10.1097/01.tp.0000061602.03327.e2>

Meier-Kriesche, H., Port, F. K., Ojo, A. O., Rudich, S. M., Hanson, J. A., Cibrik, D. M., Leichtman, A. B. & Kaplan, B., 2000. Effect of waiting time on renal transplant outcome. *Kidney International,* 58(3), p.1311-1317. <https://doi.org/10.1046/j.1523-1755.2000.00287.x>

Meier-Kriesche, H., Schold, J. D., Srinivas, T. R., Reed, A. & Kaplan, B., 2004. Kidney transplantation halts cardiovascular disease progression in patients with end-stage renal disease. *American Journal of Transplantation,* 4(10), p.1662-1668. <https://doi.org/10.1111/j.1600-6143.2004.00573>

Middlekauff, H., Nitzsche, E. U., Hoh, C, Hamilton, M. A., Fonarow, G. C., Hage, A. & Moriguchi, J. D., 2001. Exaggerated muscle mechanoreflex control of reflex renal vasoconstriction in heart failure. *Journal of Applied Physiology,* 90(5), p.1714-1719. <https://doi.org/10.1152/jappl.2001.90.5.1714>

Miles, K., Hayball, M. & Dixon, A., 1994. Functional imaging of changes in human intrarenal perfusion using quantitative dynamic computed tomography. *Investigative Radiology,* 29(10), p.911-914. <https://doi.org/10.1097/00004424-199410000-00008>

Mitchell, J. A., Subramanian, R., White, C. J., Soukas, P. A., Almagor, Y., Stewart, R. E. & Rosenfield, K., 2007. Predicting blood pressure improvement in hypertensive patients after renal artery stent placement. *Catheterization and Cardiovascular Interventions,* 69(5), p.685-689. <https://doi.org/10.1002/ccd.21095>

Miyamori, I., Yasuhara, S., Takeda, Y., Koshida, H., Ikeda, M., Nagai, K., Okamoto, H., Morise, T., Takeda, R. & Aburano, T., 1986. Effects of converting enzyme inhibition on split renal function in renovascular hypertension. *Hypertension,* 8(5), p.415-421. <https://doi.org/10.1161/01.HYP.8.5.15>

Morita, K., Seki, T., Nonomura, K., Koyanagi, T., Yoshioka, M. & Saito, H., 1999. Changes in renal blood flow in response to sympathomimetics in the rat transplanted and denervated kidney. *International Journal of Urology,* 6(1), p.24-32. <https://doi.org/10.1046/j.1442-2042.1999.06117.x>

Mounier-Vehier, C., Cocheteux, B., Haulon, S., Devos, P., Lions, C., Gautier, C., Carre, A. & Beregi, J., 2004. Changes in renal blood flow reserve after angioplasty of renal artery stenosis in hypertensive patients. *Kidney International,* 65(1), p.245-250. <http://dx.doi.org/10.1111/j.1523-1755.2004.00374.x>

Mourad, G., Ribstein, J. & Mimran, A. , 1993. Converting-enzyme inhibitor versus calcium antagonist in cyclosporine-treated renal transplants. *Kidney International,* 43(2), p.419-425. <http://dx.doi.org/10.1038/ki.1993.61>

Murthy, V., Naya, M., Foster, C. R., Hainer, B., Gaber, M., Alm, D, Sharmila, M., Charytan, D., Blankstein, R. & Di Carli, M., 2012. Coronary vascular dysfunction and prognosis in patients with chronic kidney disease. *Journal of American College of Cardiology: Cardiovascular Imaging,* 5(10), p.1025-1034. <https://doi.org/10.1016/j.jcmg.2012.06.007>

Naesens, M., Kuypers, D. R. J., De Vusser, K., Vanrenterghem, Y., Evenepoel, P., Claes, K., Bammens, B., Meijers, B. & Lerut, E., 2013. Chronic histological damage in early indication biopsies is an independent risk factor for late renal allograft failure. *American Journal of Transplantation,* 13(1), p.86-99. <https://doi.org/10.1111/j.1600-6143.2012.04304.x>

Naesens, M., Heylen, L., Lerut, E., Claes, K., De Wever, L., Claus, F., Oyen, R., Kuypers, D., Evenepoel, P., Bammens, B., Sprangers, B., Meijers, B., Pirenne, J., Monbaliu, D., de Jonge, H., Metalidis, C., De Vusser, K. & Vanrenterghem, Y., 2013. Intrarenal resistive index after renal transplantation. *The New England Journal of Medicine,* 369(19), p.1797-1806. <https://doi.org/10.1056/nejmc1315502>

Naesens, M, Kuypers D. & Sarwal W., 2009. Calcineurin inhibitor nephrotoxicity. *Clinical Journal of American Society of Nephrology,* 4(2), p.481-508. <https://doi.org/10.2215/cjn.04800908>

Nanayakkara, P. W. & Gaillard, C., 2010. Vascular disease and chronic renal failure: New insights. *The Netherlands Journal of Medicine,* 68(1), p.5-14. <https://www.ncbi.nlm.nih.gov/pubmed/20103816>

Nankivell, B. J., Chapman, J. R. & Gruenewald, S. M., 2002. Detection of chronic allograft nephropathy by quantitative Doppler imaging. *Transplantation,* 74(1), p.90-96. <https://doi.org/10.1097/00007890-200207150-00016>

Nankivell, B. J. & Kuypers, D. R., 2011. Diagnosis and prevention of chronic kidney allograft loss. *The Lancet,* 378(9800), p.1428-1437. <https://doi.org/10.1016/s0140-6736(11)60699-5>

Nankivell, B. J., Borrows, R. J., Fung, C. L., O'Connell, P. J., Allen, R. D. M. & Chapman, J. R., 2003. The natural history of chronic allograft nephropathy. *The New England Journal of Medicine,* 349(24), p.2326-2333. <https://doi.org/10.1056/nejmoa020009>

Nelson, A., Dundon, B., Worthley, S., Richardson, J., Puri, R., Wong, D., Coates, P., Faull, R. & Worthley, M., 2019. End-stage renal failure is associated with impaired coronary microvascular function. *Coronary Artery Disease,* 30(7), p.520-527. <https://doi.org/10.1097/mca.0000000000000727>

Nesterov, S. V., Han, C., Mäki, M., Kajander, S., Naum, A. G., Helenius, H., Lisinen, I., Ukkonen, H., Pietilä, M., Joutsiniemi, E. & Knuuti, J., 2009. Myocardial perfusion quantitation with ^{15}O-labelled water PET: high reproducibility of the new cardiac analysis software (Carimas^{TM}). *European Journal of Nuclear Medicine and Molecular Imaging*, 36(10), p.1594-1602. <https://doi.org/10.1007/s00259-009-1143-8>

Niizuma, S., Takiuchi, S., Okada, S., Horio, T., Kamide, K., Nakata, H., Yoshihara, F., Nakamura, S., Kawano, Y., Nakahama, H., Iwanaga, Y. & Nakatani, S., 2008. Decreased coronary flow reserve in haemodialysis patients. *Nephrology Dialysis Transplantation,* 23(7), p.2324-2328. <https://doi.org/10.1093/ndt/gfm954>

Nitzsche, E. U., Choi, Y., Killion, D., Hoh, C. K., Hawkins, R. A., Rosenthal, J. T., Buxton, D. B., Huang, S. C., Phelps, M. E. & Schelbert, H. R., 1993. Quantification and parametric imaging of renal cortical blood flow in vivo based on Patlak graphical analysis. *Kidney International,* 44(5), p.985-996. <https://doi.org/10.1038/ki.1993.340>

Normand, G., Lemoine, S., Le Bars, D., Merida, I., Irace, Z., Troalen, T., Costes, N. & Juillard, L., 2019. PET [11C]acetate is also a perfusion tracer for kidney evaluation purposes. *Nuclear Medicine and Biology,* 76-77, p.10-14. <http://dx.doi.org/10.1016/j.nucmedbio.2019.08.004>

O'Brien, E., Parati, G. & Stergiou, G., 2013. Ambulatory blood pressure measurement: What is the international consensus? *Hypertension (Dallas, Tex.:1979),* 62(6), p.988-994. <https://doi.org/10.1161/hypertensionaha.113.02148>

Odudu, A., Nery, F., Harteveld, A. A., Evans, R. G., Pendse, D., Buchanan, C. E., Francis, S. T. & Fernández-Seara, M. A. , 2018. Arterial spin labelling MRI to measure renal perfusion: A systematic review and statement paper. *Nephrology Dialysis Transplantation,* 33(suppl.2), p.ii15-ii21. <https://doi.org/10.1093/ndt/gfy180>

Oflaz, H., Turkmen, A., Turgut, F., Pamukcu, B., Umman, S., Ucar, A., Akyol, Y., Uzun, S., Kazancioglu, R., Kurt, R. & Sever, M. S., 2006. Changes in endothelial function before and after renal transplantation. *Transplant International,* 19(4), p.333-337. <https://doi.org/10.1111/j.1432-2277.2006.00288.x>

Olsen, M. H., Wachtell, K., Meyer, C., Hove, J. D., Palmieri, V., Dige-Petersen, H., Rokkedal, J., Hesse, B. & Ibsen, H., 2004. Association between vascular dysfunction and reduced myocardial flow reserve in patients with hypertension: A LIFE substudy. *Journal of Human Hypertension,* 18(6), p.445-452. <http://dx.doi.org/10.1038/sj.jhh.1001716>

Parnham, S., Gleadle, J. M., Leong, D., Grover, S., Bradbrook, C., Woodman, R. J., De Pasquale, C. G. & Selvanayagam, J. B., 2015. Myocardial perfusion is impaired in asymptomatic renal and liver transplant recipients: A cardiovascular magnetic resonance study. *Journal of Cardiovascular Magnetic Resonance: Official Journal of the Society for Cardiovascular Magnetic Resonance,* 17(1), p.56-65. <https://doi.org/10.1186/s12968-015-0166-5>

Passauer, J., Büssemaker, E., Lassig, G. & Gross, P., 2003. Kidney transplantation improves endothelium-dependent vasodilation in patients with endstage renal disease. *Transplantation,* 75(11), p.1907-1910. <https://doi.org/10.1097/01.tp.0000065739.19681.93>

Pereira, R. S., Gonul, I. I., McLaughlin, K., Yilmaz, S. & Mahallati, H., 2010. Assessment of chronic renal allograft nephropathy using contrast-enhanced MRI: A pilot study. *American Journal of Roentgenology,*194 (5), p. W407-W413.<https://doi.org/10.2214/ajr.09.2912>

Peters, A. M., Brown, J., Crossman, D., Brady, A. J., Hemingway, A. P., Roddie, M. E. & Allison, D. J., 1990. Noninvasive measurement of renal blood flow with technetium-99m-DTPA in the evaluation of patients with suspected renovascular hypertension. *The Journal of Nuclear Medicine,* 31(12), p.1980-1985. <http://jnm.snmjournals.org/cgi/content/abstract/31/12/1980>

Pilmore, H., Dent, H., Chang, S., McDonald, S. P. & Chadban, S. J., 2010. Reduction in cardiovascular death after kidney transplantation. *Transplantation,* 89(7), p.851-857. <https://doi.org/10.1097/tp.0b013e3181caeead>

Prince, M., Tafur, J. D. & White, C. J., 2019. When and how should we revascularize patients with atherosclerotic renal artery stenosis? *Journal of American College of Cardiology: Cardiovascular Interventions,* 12(6), p.505-517. <http://dx.doi.org/10.1016/j.jcin.2018.10.023>

Pruijm, M., Mendichovszky, I. A., Liss, P., van der Niepen, P., Textor, S. C., Lerman, L. O., Krediet, C. T. P., Caroli, A., Burnier, M. & Prasad, P. V., 2018. Renal blood oxygenation level-dependent magnetic resonance imaging to measure renal tissue oxygenation: A statement paper and systematic review. *Nephrology Dialysis Transplantation,* 33(2), p.ii22-ii28. <https://doi.org/10.1093/ndt/gfy243>

Racusen, L. C., Solez, K., Colvin, R. B., Bonsib, S. M., Castro, M. C., Cavallo, T., Croker, B. P., Demetris, A. J., Drachenberg, C. B., Fogo, A. B., Furness, P., Gaber, L. W., Gibson, I. W., Glotz, D., Goldberg, J. C., Grande, J., Halloran, P. F., Hansen, H. E., Hartley, B., Hayry, P. J., Hill, C. M., Hoffman, E. O., Hunsicker, L. G., Lindblad, A. S., Marcussen, N., Mihatsch, M. J., Nadasdy, T., Nickerson, P., Olsen, T. S., Papadimitriou, J. C., Randhawa, P. S., Rayner, D. C., Roberts, I., Rose, S., Rush, D., Salinas-Madrigal, L., Salomon, D. R., Sund, S., Taskinen, E., Trpkov, K. & Yamaguchi, Y., 1999. The Banff 97 working classification of renal allograft pathology. *Kidney International,* 55(2), p.713-723. <http://dx.doi.org/10.1046/j.1523-1755.1999.00299.x>

Radermacher, J., Mengel, M., Ellis, S., Stuht, S., Hiss, M., Schwarz, A., Eisenberger, U., Burg, M., Luft, F. C., Gwinner, W. & Haller, H. , 2003. The renal arterial resistance index and renal allograft survival. *The New England Journal of Medicine,* 349(2), p.115-124. <https://doi.org/10.1136/heartjnl-2019-315138>

Radhakrishnan, A., Pickup, L. C., Price, A. M., Law, J. P., Edwards, N. C., Steeds, R. P., Ferro, C. J. & Townend, J. N., 2019. Coronary microvascular dysfunction: A key step in the development of uraemic cardiomyopathy? *Heart,* 105(17), p.1302-1309. <http://dx.doi.org/10.1136/heartjnl-2019-315138>

Ragosta, M., Samady, H., Isaacs, R. B., Gimple, L. W., Sarembock, I. J. & Powers, E. R., 2004. Coronary flow reserve abnormalities in patients with diabetes mellitus who have end-stage renal disease and normal epicardial coronary arteries. *American Heart Journal,* 147(6), p.1017-1023. <https://doi.org/10.1016/j.ahj.2003.07.029>

Rangaswami, J., Mathew, R., Parasuraman, R., Tantisattamo, E., Lubetzky, M., Rao, S., Yaqub, M., Birdwell, K., Bennett, W., Dalal, P., Kapoor, R., Lerma, E., Lerman, M., McCormick, N., Bangalore, S., McCullough, P. & Dadhania, D., 2019. Cardiovascular disease in the kidney transplant recipient: Epidemiology, diagnosis and management strategies. Oxford University Press (OUP). *Nephrology Dialysis Transplantation*, 34, p. 760-773. <https://doi.org/10.1093/ndt/gfz053>

Rebelos, E., Dadson, P., Oikonen, V., Iida, H., Hannukainen, J. C., Iozzo, P., Ferrannini, E. & Nuutila, P., 2019. Renal hemodynamics and fatty acid uptake: Effects of obesity and weight loss. *American Journal of Physiology: Endocrinology and Metabolism,* 317(5), p.E871-E878. <https://doi.org/10.1152/ajpendo.00135.2019>

Roufosse, C., Simmonds, N., Clahsen-van Groningen, M., Haas, M., Henriksen, K. J., Horsfield, C., Loupy, A., Mengel, M., Perkowska-Ptasińska, A., Rabant, M., Racusen, L. C., Solez, K. & Becker, J. U., 2018. A 2018 reference guide to the Banff classification of renal allograft pathology. *Transplantation,* 102(11), p.1795-1814. <https://doi.org/10.1097/tp.0000000000002366>

Rubinger, D., Backenroth, R. & Sapoznikov, D., 2009. Restoration of baroreflex function in patients with end-stage renal disease after renal transplantation. *Nephrology Dialysis Transplantation,* 24(4), p.1305-1313. <https://doi.org/10.1093/ndt/gfn732>

Saad, A., Dietz, A. B., Herrmann, S. M. S., Hickson, L. J., Glockner, J. F., McKusick, M. A., Misra, S., Bjarnason, H., Armstrong, A. S., Gastineau, D. A., Lerman, L. O. & Textor, S. C., 2017. Autologous mesenchymal stem cells increase cortical perfusion in renovascular disease. *Journal of the American Society of Nephrology,* 28(9), p.2777-2785. <https://doi.org/10.1681/asn.2017020151>

Salmela, K. T. & Kyllönen, L. E. J., 2004. Two decades of experience with cyclosporine in renal transplantation in Helsinki. *Transplantation Proceedings,* 36(2), p.S94-S98. <http://dx.doi.org/10.1016/j.transproceed.2004.01.036>

Sata, Y., Head, G., Denton, K., May, C. & Schlaich, M., 2018. Role of the sympathetic nervous system and its modulation in renal hypertension. *Frontiers in Medicine, Nephrology (Lausanne),* 5: 82. <https://doi.org/10.3389/fmed.2018.00082>.

Schlaich, M. P., Socratous, F., Hennebry, S., Eikelis, N., Lambert, E. A., Straznicky, N., Esler, M. D. & Lambert, G. W., 2009. Sympathetic activation in chronic renal failure. *Journal of the American Society of Nephrology,* 20(5), p.933-939. <https://doi.org/10.1681/ASN.2008040402>

Schneider, A. G., Goodwin, M. D. & Bellomo, R., 2013. Measurement of kidney perfusion in critically ill patients. *Critical Care (London, England),* 17(2), p.220. <https://doi.org/10.1186/cc12529>

Schneider, A. G., Hofmann, L., Wuerzner, G., Glatz, N., Maillard, M., Meuwly, J., Eggimann, P., Burnier, M. & Vogt, B., 2012. Renal perfusion evaluation with contrast-enhanced ultrasonography. *Nephrology Dialysis Transplantation,* 27(2), p.674-681. <https://doi.org/10.1093/ndt/gfr345>

Scholbach, T., Girelli, E., & Scholbach, J., 2005. Dynamic tissue perfusion measurement: A novel tool in follow-up of renal transplants. *Transplantation*, 2005, 79(12):1711-1716. <https://doi.org/10.1097/01.tp.0000164145.89275.02>

Scholbach, T., Wang, H., Yang, A., Loong, C. & Wu, T., 2013. Correlation of histopathologic and dynamic tissue perfusion measurement findings in transplanted kidneys. *BMC Nephrology,* 14(1), p.143. <https://doi.org/10.1186/1471-2369-14-143>

Schwenger, V., Korosoglou, G., Hinkel, U., Morath, C., Hansen, A., Sommerer, C., Dikow, R., Hardt, S., Schmidt, J., Kucherer, H., Katus, H. A. & Zeier, M., 2006. Real-time contrast-enhanced sonography of renal transplant recipients predicts chronic allograft nephropathy. *American Journal of Transplantation,* 6(3), p.609-615. <https://doi.org/10.1111/j.1600-6143.2005.01224.x>

Sdringola, S., Johnson, N. P., Kirkeeide, R., Cid, E., Gould, K. & Lance, M. D., 2011. Impact of unexpected factors on quantitative myocardial perfusion and coronary flow reserve in young,

asymptomatic volunteers. *Journal of American Collage of Cardiology: Cardiovascular Imaging,* 4(4), p.402-412. <https://doi.org/10.1016/j.jcmg.2011.02.008>

Sellarés, J., de Freitas, D. G., Mengel, M., Reeve, J., Einecke, G., Sis, B., Hidalgo, L. G., Famulski, K., Matas, A. & Halloran, P. F., 2012. Understanding the causes of kidney transplant failure: The dominant role of antibody-mediated rejection and nonadherence. *American Journal of Transplantation,* 12(2), p.388-399. <https://doi.org/10.1111/j.1600-6143.2011.03840.x>

Servais, A., Meas-Yedid, V., Noël, L. H., Martinez, F., Panterne, C., Kreis, H., Zuber, J., Timsit, M. O., Legendre, C., Olivo-Marin, J. C. & Thervet, E., 2011. Interstitial fibrosis evolution on early sequential screening renal allograft biopsies using quantitative image analysis. *American Journal of Transplantation,* 11(7), p.1456-1463. <https://doi.org/10.1111/j.1600-6143.2011.03594.x>

Shah, N. R., Charytan, D. M., Murthy, V. L., Skali Lami, H., Veeranna, V., Cheezum, M. K., Taqueti, V. R., Kato, T., Foster, C. R., Hainer, J., Gaber, M., Klein, J., Dorbala, S., Blankstein, R. & Di Carli, M. F., 2016. Prognostic value of coronary flow reserve in patients with dialysis-dependent ESRD. *Journal of the American Society of Nephrology,* 27(6), p.1823-1829. <https://doi.org/10.1681/asn.2015030301>

Shannon, J. L., Headland, R., MacIver, A. G., Ferryman, S. R., Barber, P. C. & Howie, A. J., 1998. Studies on the innervation of human renal allografts. *Journal of Pathology,* 186(1), p.109-115. <https://doi.org/10.1002/(sici)1096-9896(199809)186:1%3C109::aid-path134%3E3.0.co;2-n>

Steegh, F., Gelens, M. A., Nieman, F. H. M., van Hooff, J. P., Cleutjens, J. P. M., van Suylen, R. J., Daemen, M, van Heurn, E., Christiaans, M. H. L. & Peutz-Kootstra, C. J., 2011. Early loss of peritubular capillaries after kidney transplantation. *Journal of the American Society of Nephrology,* 22(6), p.1024-1029. <https://doi.org/10.1681/asn.2010050531>

Stegall, M. D., Gaston, R. S., Cosio, F. G. & Matas, A., 2015. Through a glass darkly: Seeking clarity in preventing late kidney transplant failure. *Journal of the American Society of Nephrology,* 26(1), p.20-29. <https://doi.org/10.1681/asn.2014040378>

Stenvinkel, P., Carrero, J. J., Axelsson, J., Lindholm, B., Heimbürger, O. & Massy, Z., 2008. Emerging biomarkers for evaluating cardiovascular risk in the chronic kidney disease patient: How do new pieces fit into the uremic puzzle? *Clinical Journal of the American Society of Nephrology*, 3(2), p. 505-521. <10.2215/CJN.03670807>

Tamaki, N., Alpert, N., Rabito, C., Barlai-Kovach, M., Correia, J. & Strauss, H., 1988. The effect of captopril on renal blood flow in renal artery stenosis assessed by positron tomography with rubidium-82. *Hypertension,* 11(3), p.217-222. <https://doi.org/10.1161/01.hyp.11.3.217>

Taqueti, V & Di Carli, M. F., 2018. Coronary microvascular disease pathogenic mechanisms and therapeutic options. *Journal of the American College of Cardiology,* 72(21), p.2625-2641. <https://doi.org/10.1016/j.jacc.2018.09.042>

Textor, S. C. & Lerman, L. O., 2019. The role of hypoxia in ischemic chronic kidney disease. *Seminars in Nephrology,* 39(6), p.589-598. <http://dx.doi.org/10.1016/j.semnephrol.2019.10.008>

Tok, D., Gullu, H., Erdogan, D., Topcu, S., Ciftci, O., Yildirim, I. & Muderrisoglu, H., 2005. Impaired coronary flow reserve in hemodialysis patients: A transthoracic Doppler echocardiographic study. *Nephron Clinical Practice,* 101(4), p.c200-c206. <https://doi.org/10.1159/000087579>

Toth, G. B., Varallyay, C. G., Horvath, A., Bashir, M. R., Choyke, P. L., Daldrup-Link, H. E., Dosa, E., Finn, J. P., Gahramanov, S., Harisinghani, M., Macdougall, I., Neuwelt, A., Vasanawala, S. S., Ambady, P., Barajas, R., Cetas, J. S., Ciporen, J., DeLoughery, T. J., Doolittle, N. D., Fu, R., Grinstead, J., Guimaraes, A. R., Hamilton, B. E., Li, X., McConnell, H. L., Muldoon, L. L., Nesbit, G., Netto, J. P., Petterson, D., Rooney, W. D., Schwartz, D., Szidonya, L. & Neuwelt, E. A., 2017. Current and potential imaging applications of ferumoxytol for magnetic resonance imaging. *Kidney International,* 92(1), p.47-66. <https://doi.org/10.1016/j.kint.2016.12.037>

Tublin, M. E., Bude, R. O. & Platt, J. F., 2003. The resistive index in renal Doppler sonography: Where do we stand? *American Journal of Roentgenology,* 180(4), p.885-892. <https://doi.org/10.2214/ajr.180.4.1800885>

Turiel, M., Sitia, S., Tomasoni, L., Cicala, S., Viganò, S. M., Menegotto, A., Martina, V., Bodini, B. D., Bacchiani, G., Ghio, L. & Cusi, D., 2008. Subclinical impairment of coronary flow velocity reserve assessed by transthoracic echocardiography in young renal transplant recipients. *Atherosclerosis,* 204(2), p.435-439. <https://doi.org/10.1016/j.atherosclerosis.2008.09.036>

Uren, N. G., Camici, P. G., Melin, J. A., Bol, A., de Bruyne, B., Radvan, J., Olivotto, I., Rosen, S. D., Impallomeni, M. & Wijns, W., 1995. Effect of aging on myocardial perfusion reserve. *The Journal of Nuclear Medicine,* 36(11), p.2032-2036. <https://jnm.snmjournals.org/content/36/11/2032.long>

Uren, N. G., Melin, J. A., De Bruyne, B., Wijns, W., Baudhuin, T. & Camici, P. G., 1994. Relation between myocardial blood flow and the severity of coronary-artery stenosis. *The New England Journal of Medicine,* 330(25), p.1782-1788. <http://content.nejm.org/cgi/content/abstract/330/25/1782>

Vallée, J., Lazeyras, F., Khan, H. G. & Terrier, F., 2000. Absolute renal blood flow quantification by dynamic MRI and Gd-DTPA. *European Radiology,* 10(8), p.1245-1252. <https://doi.org/10.1007/s003300000434>

Van Brussel, P. M., van de Hoef, Tim P, de Winter, R. J., Vogt, L. & van den Born, B., 2017. Hemodynamic measurements for the selection of patients with renal artery stenosis: A systematic review. *Journal of American College of Cardiology, Cardiovascular Interventions,* 10(10), p.973-985. <https://doi.org/10.1016/j.jcin.2017.02.046>

Van Loon, E., Bernards, J., Van Craenenbroeck, A. & Naesens, M., 2020a. The causes of kidney allograft failure: More than alloimmunity. A viewpoint article. *Transplantation,* 104(2), p.e46-e56. <https://doi.org/10.1097/tp.0000000000003012>

Van Loon, E., Senev, A., Lerut, E., Coemans, M., Callemeyn, J., Van Keer, J., Daniëls, L., Kuypers, D., Sprangers, B., Emonds, M. & Naesens, M., 2020b. Assessing the complex causes of kidney allograft loss. *Transplantation,* 104(12), p.2557-2566. <https://doi.org/10.1097/tp.0000000000003192>

Vanhove, T., Goldschmeding, R. & Kuypers, D., 2017. Kidney fibrosis: Origins and interventions. *Transplantation,* 101(4), p.713-726. < https://doi.org/10.1097/tp.0000000000001608>

Verbeke, F., Biesen, W., Honkanen, E., Wikström, B., Jensen, P. B., Krzesinski, J., Rasmussen, M., Vanholder, R. & Rensma, P. L. (CORD Study Investigators), 2011. Prognostic value of aortic stiffness and calcification for cardiovascular events and mortality in dialysis patients: Outcome of the calcification outcome in renal disease (CORD) study. *Clinical Journal of American Society of Nephrology*, 6(1), p. 153-159. <https://doi.org/10.2215/cjn.05120610>

Viganò, S. M., Turiel, M., Martina, V., Meregalli, E., Tomasoni, L., De Blasio, G., Delfino, L., Edefonti, A., Grillo, P., Procaccio, M., Cusi, D. & Ghio, L., 2007. Reduced coronary flow reserve in young adults with renal transplant. *Nephrology Dialysis Transplantation,* 22(8), p.2328-2333. <https://doi.org/10.1093/ndt/gfm110>

Villa, G., Ringgaard, S., Hermann, I., Noble, R., Brambilla, P., Khatir, D. S., Zöllner, F. G., Francis, S. T., Selby, N. M., Remuzzi, A. & Caroli, A., 2020. Phase-contrast magnetic resonance imaging to assess renal perfusion: A systematic review and statement paper. *Magnetic Resonance Materials in Physics, Biology and Medicine (New York, N.Y.),* 33(1), p.3-21. <https://doi.org/10.1007/s10334-019-00772-0>

Wang, L., Masson, P., Turner, R., Lord, S., Baines, L., Craig, J. & Webster, A., 2015. Prognostic value of cardiac tests in potential kidney transplant recipients. A systematic review. *Transplantation,* 99(4), p.731-745. <https://doi.org/10.1097/tp.0000000000000611>

Wang, W., Yu, Y., Wen, J., Zhang, M., Chen, J. & Cheng, D., 2019. Combination of functional magnetic resonance imaging and histopathologic analysis to evaluate interstitial fibrosis

in kidney allografts. *Clinical Journal of American Society of Nephrology (ASN)*. <https://doi.org/10.2215/cjn.00020119>

Wang, W., Yuanmeng, Y., Xue, L., Chen, J., Zhang, Y., Zhang, L. & Wen, J., 2020. Early detection of subclinical pathology in patients with stable kidney graft function by arterial spin labeling. *European Radiology*. <://doi.org/10.1007/s00330-020-07369-5>

Wanner, C., Krane, V., Marz, W., Olschewski, M., Mann, J. F. E., Ruf, G., & Ritz, E., 2005. German Diabetes and Dialysis Study . Atorvastatin in patients with type 2 diabetes mellitus undergoing hemodialysis. *The New England Journal of Medicine,* 353(3), p.238-248. <http://content.nejm.org/cgi/content/abstract/353/3/238>

Wenning, C., Vrachimis, A., Pavenstädt, H., Reuter, S., Schäfers, M. & Wenning, C., 2020. Coronary artery calcium burden, carotid atherosclerotic plaque burden, and myocardial blood flow in patients with end-stage renal disease: A non-invasive imaging study combining PET/CT and 3D ultrasound. *Journal of Nuclear Cardiology* <https://doi.org/10.1007/s12350-020-02080-w>

Wheatley, K, Ives, N, Gray, R, Kalra, P. A., Moss, J. G., Baigent, C., Carr, S., Chalmers, N., Eadington, D., Hamilton, G., Lipkin, G., Nicholson, A. & Scoble J., 2009. Revascularization versus medical therapy for renal artery stenosis. (ASTRAL) *The New England Journal of Medicine,* 361(20), p.1953-1962. <http://content.nejm.org/cgi/content/abstract/361/20/1953>

Winther, S., Bøttcher, M., Jørgensen, H., Bouchelouche, K., Gormsen, L., Oczachowska-Kulik, A., Holm, N., Bøtker, H., Ivarsen, P. & Svensson, M., 2016. Coronary calcium score may replace cardiovascular risk factors as primary risk stratification tool before kidney transplantation. *Transplantation,* 100(10), p.2177-2187. <https://doi.org/10.1097/tp.0000000000000992>

Winther, S., Svensson, M., Jørgensen, H. S., Rasmussen, L. D., Holm, N. R., Gormsen, L. C., Bouchelouche, K., Bøtker, H. E., Ivarsen, P. & Bøttcher, M., 2018. Prognostic value of risk factors, calcium score, coronary CTA, myocardial perfusion imaging, and invasive coronary angiography in kidney transplantation candidates. *Journal of American College of Cardiology: Cardiovascular Imaging,* 11(6), p.842-854. <http://dx.doi.org/10.1016/j.jcmg.2017.07.012>

Woolen, S., Shankar, P., Gagnier, J., MacEachern, M., Singer, L & Davenport, M., 2020. Risk of Nephrogenic Systemic Fibrosis in Patients With Stage 4 or 5 Chronic Kidney Disease Receiving a Group II Gadolinium-Based Contrast Agent. A Systematic Review and Meta-analysis. *Journal of the American Medical Association, Internal Medicine*, 180(2), p.223-230. <https://doi.org/10.1001/jamainternmed.2019.5284>

Yildiz, A., Sever, M. Ş, Demirel, Ş, Akkaya, V., Türk, S., Türkmen, A., Ecder, T. & Ark, E., 1998. Improvement of uremic autonomic dysfunction after renal transplantation: A heart rate variability study. *Nephron,* 80(1), p.57-60. <https://doi.org/10.1159/000045126>

Yilmaz, M. I., Saglam, M., Caglar, K., Cakir, E., Sonmez, A., Ozgurtas, T., Aydin, A., Eyileten, T., Ozcan, O., Acikel, C., Tasar, M., Genctoy, G., Erbil, K., Vural, A. & Zoccali, C., 2006. The determinants of endothelial dysfunction in CKD: Oxidative stress and asymmetric dimethylarginine. *American Journal of Kidney Diseases,* 47(1), p.42-50. <https://doi.org/10.1053/j.ajkd.2005.09.029>

Yilmaz, M. I., Stenvinkel, P., Sonmez, A., Saglam, M., Yaman, H., Kilic, S., Eyileten, T., Caglar, K., Oguz, Y., Vural, A., Çakar, M., Altun, B., Yenicesu, M. & Carrero, J. J., 2011. Vascular health, systemic inflammation and progressive reduction in kidney function; clinical determinants and impact on cardiovascular outcomes. *Nephrology Dialysis Transplantation,* 26(11), p.3537-3543. <https://doi.org/10.1093/ndt/gfr081>

Yilmaz, S., Isik, I., Afrouzian, M., Monroy, M., Sar, A., Benediktsson, H. & McLaughlin, K., 2007. Evaluating the accuracy of functional biomarkers for detecting histological changes in chronic allograft nephropathy. *Transplant International,* 20(7), p.608-615. <https://doi.org/10.1111/j.1432-2277.2007.00494.x>

Yu, Y., Wei, W., Wen, J., Zhang, Y., Lu, G. M. & Long, J. Z., 2021.Detection of renal allograft fibrosis with MRI: arterial spin labeling outperforms reduced fiel-of-view IVIM. *European Radiology*. <https://doi.org/10.1007/s00330-021-07818-9>

TURUN
YLIOPISTO
UNIVERSITY
OF TURKU

ISBN 978-951-29-8586-9 (PRINT)
ISBN 978-951-29-8587-6 (PDF)
ISSN 0355-9483 (Print)
ISSN 2343-3213 (Online)

Painosalama, Turku, Finland 2021